Importance of Endothelial Nitric Oxide Synthase after Experimental Subarachnoid Hemorrhage in Mice

Irina Johanna Lenz, geb. Westermayer

München 2020

Aus dem Institut für Schlaganfall- und Demenzforschung
Institut der Ludwig-Maximilians-Universität München
Direktor: Prof. Dr. med. Martin Dichgans

Importance of Endothelial Nitric Oxide Synthase after Experimental Subarachnoid Hemorrhage in Mice

Dissertation
zum Erwerb des Doktorgrades der Medizin
an der Medizinischen Fakultät der
Ludwig–Maximilians–Universität zu München

vorgelegt von
Irina Johanna Lenz, geb. Westermayer
aus Gilching
2020

Mit Genehmigung
der Medizinischen Fakultät
der Universität München

Berichterstatter:	Prof. Dr. Nikolaus Plesnila
Mitberichterstatter:	PD Dr. Martin Strowitzki
	Prof. Dr. Jörg-Christian Tonn
	Prof. Dr. Hans-Walter Pfister
Mitbetreuung durch die promovierte Mitarbeiterin:	PD Dr. Nicole Terpolilli
Dekan:	Prof. Dr. med. dent. Reinhard Hickel
Tag der mündlichen Prüfung:	20.02.2020

Summary

Subarachnoid hemorrhage (SAH) is a severe subtype of stroke with poor neurological outcome in patients despite improved surgical and medical management. It is mostly caused by aneurysm rupture and leads to dispersion of blood throughout the subarachnoid space. One main aspect of poor outcome in patients is the formation of vasospasms in big vessels within the first week after SAH. A part of the artery constricts and therefore decreases blood flow and brain perfusion. But even patients without these macrovasospasms can present with severe neurological damage. Consequently, pathologies were investigated within the early phase, the first 72 hours after subarachnoid hemorrhage, summarized as "early brain injury" (EBI). EBI is presenting with the formation of vasospasms in small arteries and arterioles, called microvasospasms, immediately after SAH as previously shown in humans and experimental animals. The mechanisms behind the formation of microvasospasms are not completely understood at this point, but they have been linked to acute endothelial nitric oxide depletion. Lack of vascular NO is caused both by NO scavenging by hemoglobin, as well as by a defect in the endothelial nitric oxide synthase, the main source of vascular NO in the brain. Nitric oxide is a strong vasodilator in the cerebral microcirculation and a lack of NO impairs vessel reactivity. Patients with loss-of-function polymorphisms of the eNOS gene have a higher risk of developing vasospasms after SAH. Further, eNOS has been shown to produce less NO after SAH, but the consequence of this finding on brain function and outcome remained unclear so far. Therefore the aim of the current study was to investigate the importance of eNOS after experimental subarachnoid hemorrhage by using eNOS deficient mice. The results of the current study demonstrate that eNOS knockout mice have more severe SAHs as indicated by higher intracranial pressure, lower cerebral blood flow, larger intracranial blood deposition, and more re-bleedings. These findings are in line with prolonged tail bleeding times in these animals. On the level of the cerebral microcirculation in vivo two-photon microscopy revealed a lower vessel density and a decreased perfused vessel volume in eNOS deficient mice, which worsened after SAH. These mice displayed also more microvasospasms than control animals. Finally, these phenotypes resulted in gene-dose dependent high mortality in homozygous (50%) and heterozygous (25%) eNOS deficient mice after SAH. These results clearly demonstrate the protective activity of endothelial NO after SAH and suggests endothelial NO signaling as a potential novel therapeutic target for SAH.

Kurzfassung

Die Subarachnoidalblutung (SAB) ist eine schwere Form des Schlaganfalls mit schlechter Prognose. Die häufigste Form stellt die aneurysmatische SAB dar. Dort platzt ein Aneurysma an der Schädelbasis und Blut strömt aus dem Gefäßlumen und verteilt sich im Subarachnoidalraum. Ein Hauptaspekt der schlechten Prognose nach SAB ist die Entwicklung von Vasospasmen in großen zerebralen Gefäßen in der ersten Woche nach der Blutung. Ein Abschnitt der betroffenen Arterie verengt sich und limitiert somit die Durchblutung und als Konsequenz die nutritive Versorgung des Gehirns. Doch selbst Patienten ohne diese Makrovasospasmen zeigen bereits früh nach SAB schwere neurologische Defizite. Diese frühe Phase nach SAB, d.h. die ersten 72 Stunden nach der Blutung, wurden unter dem Begriff „Early Brain Injury“ (EBI) zusammengefasst und genauer untersucht. EBI präsentiert sich mit der Ausbildung von Vasospasmen in den Gefäßen der zerebralen Mikrozirkulation, wie am Menschen und im Mausmodell gezeigt werden konnte. Die genauen Mechanismen hinter der Bildung dieses Mikrovasospasmen (MVS) sind noch nicht vollständig erforscht, aber sie konnten mit einem akuten Mangel an endothelialem Stickstoffmonoxid (NO) in Verbindung gebracht werden. Dieser endotheliale NO Mangel ist wohl durch die Inaktivierung von NO durch Hämoglobin auf der einen Seite und durch einen Defekt der endothelialen NO Synthase (eNOS) bedingt. NO ist ein starker Vasodilatator und ein Verlust führt zu gestörter Autoregulation der zerebralen Blutgefäße. Patienten mit loss-of-function Mutationen des eNOS Gens zeigen ein höheres Risiko für Aneurysmen, eine stärkere Tendenz zur Ruptur eben dieser und eine verstärkte Entwicklung von MVS nach SAB. Eine verringerte Funktion der eNOS nach SAB konnte bereits gezeigt werden, allerdings bleibt unklar inwieweit dies mit dem post-hämorrhagischen Hirnschaden in Zusammenhang steht. Ziel der aktuellen Studie war daher mit Hilfe von eNOS defizienten Mäuse die Bedeutung der endothelialen Stickstoffmonoxid Synthase nach experimenteller Subarachnoidalblutung zu untersuchen. eNOS defiziente Tiere zeigen eine schwerere SAB mit einem stärkeren Anstieg des intrakraniellen Drucks und einem stärkeren Abfall der zerebralen Durchblutung. Zugleich habe diese Tiere nach SAB größere Hämatome an der Schädelbasis. Des Weiteren haben eNOS knockout Mäuse eine verlängerte Blutungszeit und eine stark erhöhte Rate an spontanen Nachblutungen in den ersten 90 Minuten nach SAB. Unter dem Zwei-Photonen Mikroskop stellt sich eine Störung der Mikrozirkulation, hauptsächlich in verringerter Gefäßdichte und perfundiertem Gefäßvolumen sowie in erhöhter Anzahl an MVS dar. Bereits naive knockout Mäuse zeigen diese Defizite der Mikrozirkulation. In der Tat ähnelt das Bild dem der Wildtyp Tiere nach SAB. Nach SAB zeigen die eNOS defizienten Tiere eine noch stärkere Verschlechterung der Mikrozirkulation. All dies führte zu einer stark erhöhten Mortalität bei den Knockout Tieren. Daraus lässt sich schließen, dass endotheliales NO eine starke protektive Wirkung nach SAB entfaltet. Eine Widerherstellung der NO Signalkaskade könnte somit eine potenziell neues Therapieziel für Patienten mit SAB darstellen.

Conference proceedings

"CO_2 can Do?!? Effect of NO Inhalation on CO_2 Regulation after Subarachnoid hemorrhage in mice"

I.Westermayer
Statusseminar des Promotionsstudiums „Molekulare Medizin" und „Systembiologische Medizin" im Rahmen des Förderprogramm für Forschung und Lehre der LMU München
(Herrsching, 07. Mai 2016)

"Role of endothelial Nitric Oxide in Early Brain Injury after experimental subarachnoid hemorrhage in mice."

I.Westermayer, S. Katzdobler, N. Terpolilli, N. Plesnila
42. Jahrestagung der Sektion Intrakranieller Druck, Hirndurchblutung und Hydrozephalus der Deutschen Gesellschaft für Neurochirurgie
(Bern/CH, 04.- 05. November 2016)

"Nitric Oxide and the Cerebral Microcirculation After Experimental Subarachnoid Hemorrhage"

N. Terpolilli, **I.Westermayer**, N. Plesnila
Vasospasm 2017 - The 14th International Conference on Neurovascular Events after Subarachnoid Hemorrhage
(Huntington Beach, Los Angeles/USA, 30. September - 3. October 2017)

"Role of endothelial Nitric Oxide in Early Brain Injury after experimental subarachnoid hemorrhage in mice."

I.Westermayer, N. Terpolilli, N. Plesnila
Sektionstagung Vaskuläre Neurochirurgie der Deutschen Gesellschaft für Neurochirurgie
(Aachen, 02. - 03. March 2018)

Poster

"Role of endothelial Nitric Oxide in Early Brain Injury after experimental subarachnoid hemorrhage in mice."

I.Westermayer, S. Katzdobler, N. Terpolilli, N. Plesnila
Brain 2017 - 28th International Symposium on Cerebral Blood Flow, Metabolism and Function & 13th International Conference on Quantification of Brain Function with PET (Berlin, 01. - 04. April 2017)

Contents

1 Introduction

1.1 Subarachnoid hemorrhage

Depending on its pathophysiology stroke can be divided into two categories. There is ischemic stroke, where a vessel is occluded by thrombus formation or by an embolus, both of which subsequently lead to impairment or loss of perfusion. The second subtype is hemorrhagic stroke. This category includes intraparenchymal/intracerebral bleedings and subarachnoid hemorrhage (SAH). This thesis focusses on SAH.

1.1.1 Definition

The brain and spinal cord within the skull and the spinal canal are covered by three connective tissue layers, the meninges: from outward to inward these are the dura mater, the arachnoid mater, and the pia mater. The subarachnoid space can be found between the arachnoid and the pia layer. It is filled with cerebrospinal fluid (CSF) and contains arteries and veins that penetrate the parenchyma so as to provide adequate blood supply to the brain (see Fig. 1.1).

If bleeding occurs from these vessels into the subarachnoid space - either due to trauma or spontaneously - it is called subarachnoid hemorrhage (SAH) (see Fig. 1.2).

There are two types of subarachnoid hemorrhage. One is traumatic SAH which occurs in up to 60% of patients with severe traumatic brain injury[42], the other is spontaneous SAH which occurs in more than 85% of cases due to spontaneous rupture of aneurysms located on subarachnoid arteries [7, 60]. The latter type of SAH is the main focus of this dissertation.

1.1.2 Aneurysms

An aneurysm is a blood vessel deformation which forms due to an acquired or preexisting structural weakness of the vessel wall. Over time the transmural pressure gradient occurring during each heart beat may dilate the aneurysm over time thus thinning the vessel wall. This process may go on until the aneurysm ruptures spontaneously or following an increase in systemic blood pressure. Aneurysms are categorized according to their morphology as saccular or fusiform. The most common forms leading to SAH are saccular or “Berry” aneurysms (see Fig. 1.3a)). The other, non-saccular forms of aneurysms, e.g. fusiform, dolichoectatic, and dissecting aneurysms, (see Fig. 1.3b [203]) amount to less than 0.1% of all known cases [6, 170].

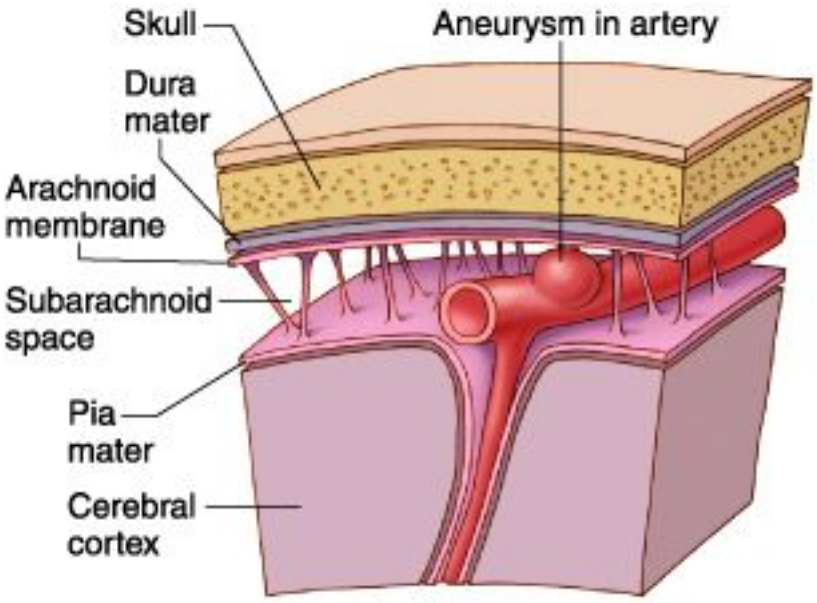

Figure 1.1: Anatomy of the subarachnoid space. There are three layers of tissue between the brain and the skull. From outside to inside the dura mater, the arachnoid mater and the pia mater. The subarachnoid space is located between the arachnoid mater and the pia mater. The blood vessels, that supply the brain parenchyma, are located in the subarachnoid space. `https://www.mdguidelines.com/mda/subarachnoid-hemorrhage-non-traumatic`

Most aneurysms are located at the skull base in the anterior part of the Circle of Willis (see Fig. 1.4), most commonly in the anterior communicating artery (35%), the internal carotid artery (30%), and the middle carotid artery (22%). 30% of patients have multiple aneurysms [91]. Aneurysm formation can be associated with genetic connective tissue disorders such as autosomal dominant polycystic kidney disease [159], Marfan syndrome, or Ehlers-Danlos syndrome, suggesting a genetic risk factor as well.

1.1.3 Incidence and prevalence of aneurysmal subarachnoid hemorrhage

Incidence and prevalence of aneurysmal subarachnoid hemorrhage The worldwide incidence of subarachnoid hemorrhage is estimated to be 9/100,000 - except for Finland and Japan, both of which have a much higher incidence of up to 15-17/100,000 [26]. Over all, the incidence of SAH remained stable over the past decades [116]. There is a slightly higher risk for women than men, the peak being around 50-60 years of age [26, 131, 167]. It is estimated that worldwide approximately 500,000 patients suffer a SAH each year, almost two-thirds of which are in low- and middle-income countries [78].

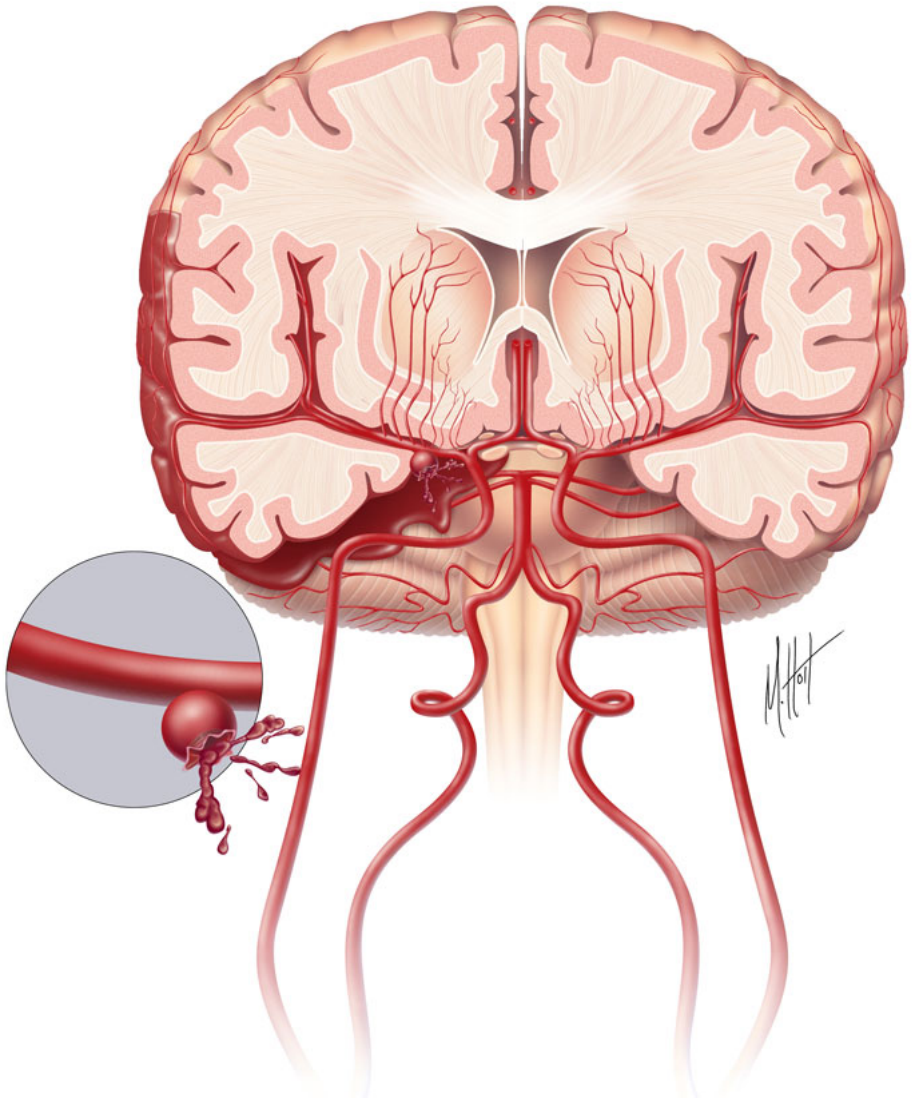

Figure 1.2: Illustration of an aneurysmatic subarachnoid hemorrhage. The saccular aneurysm located at the medial carotid artery burst and blood flows out of the vessel and disperses into the subarachnoid space. Courtesy of Mattew Holt, `https://www.bodyrender.com`.

1.1.4 Risk factors

There are modifiable risk factors for SAH, such as smoking, alcohol abuse, and arterial hypertension [43, 86]. Non-modifiable risk factors include sex, age and a family history of SAH [85, 96].

1.1.5 Clinical manifestations and diagnosis

SAH usually presents with a sudden onset of a very severe headache, also called "thunderclap headache", accompanied by nausea or vomiting [149]. The patient may show signs of meningeal irritation, sudden loss of consciousness, focal neurologic deficits or seizures [112]. Around 10% to 40% of patients report prodromal events (mostly sudden onset headaches of

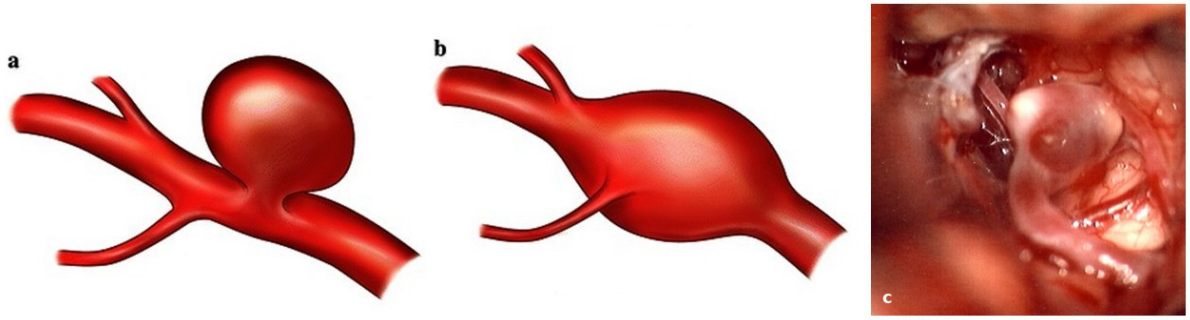

Figure 1.3: Illustration of the two main types of cranial aneurysms.(a) The saccular form, where the aneurysm has a neck and is formed like a berry. (b) The fusiform aneurysm which is an elongated dilation that follows the length of the blood vessel.(c) Intraoperative image showing an aneurysm. a,b: Withers et al. 2013, [203]; c: Courtesy of Dr. Terpolilli.

short duration) caused by minimal SAH, also known as "sentinel leaks". They may precede a major hemorrhage by several weeks [146]. As symptoms may be unspecific, minor leak SAH is often misdiagnosed [40, 196]. Missed sentinel leaks may lead to devastating consequences for the patient, since there is a significant risk of rebleedings. Initial misdiagnosis happens mainly in patients with minor SAH, but among those it has been associated with increased mortality and morbidity[101]. SAH is often associated with marked cardiovascular impairment [138] such as arrhythmias, cardiomyopathy, and autonomic dysfunction [49] thereby increasing its risk of being overlooked [12]. In a two-center study by Papanikolaou et al. in 2012, 62% of 37 patients presented with supranormal pulse-wave velocity and 14 patients (38%) presented with left ventricular systolic dysfunction [138]. Another study recently suspected that up to 10% of cases of sudden out-of-hospital cardio-pulmonary arrest are in fact caused by SAH [22, 105]. The best way to diagnose SAH is by cranial computed tomography (CT) scan [195], since on a native scan blood can easily be identified (see Fig. 1.5).

In order to identify the source of hemorrhage, CT angiography or transarterial angiography can be performed (see Fig. 1.6). Once visualized through angiography, the aneurysm morphology can be reconstructed in 3-D.

In up to 15% of spontaneous SAH cases no distinct bleeding source can be found on radiological imaging [60, 99, 192]. This may be due to a very small bleeding or due to delayed diagnosis since only relatively fresh blood can be diagnosed by CT scan [57]. In this case SAH can only be reliable identified by performing a lumbar puncture or MRI [191].

1.1.6 Classifications of subarachnoid hemorrhage

Historically, the first grading system for SAH is the Hunt and Hess classification, published in 1968 [79]. The scale is based on patient symptoms. Unfortunately the categories are not precisely defined and the scale therefore has low levels of reproducibility and validity [28]. In 1974 a new scale was introduced in the setting of acute brain injury: the Glasgow

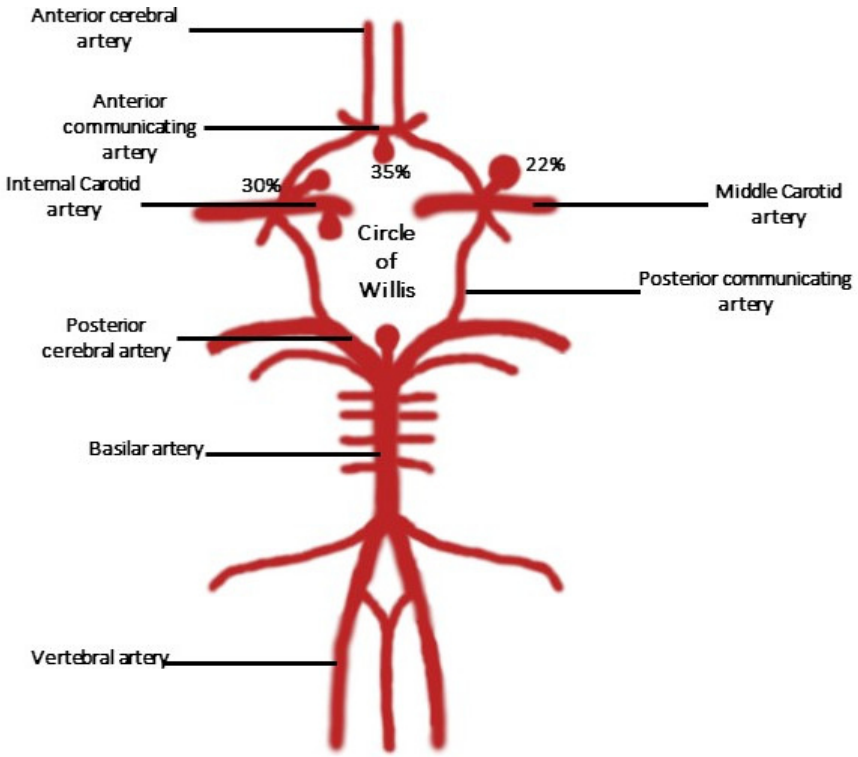

Figure 1.4: Anatomy circle of Willis and localization of aneurysms. The circle of Willis is formed by four main arteries. From the base of the scull comes the basilar artery. It is connected via the posterior cerebral artery to the middle cerebral artery. At that point it connects with the internal carotid artery. Last, an anterior commuting artery closes the circle. Saccular aneurysms are mainly located at the circle of Willis. 35% are located on the anterior communicating artery. Around 30% are found on the internal carotid artery and around 22% at the middle carotid artery. Only few are located at the posterior cerebral artery[91].

Coma Scale (GCS) [182]. It is an easy to use grading system of consciousness and coma, based on three categories: eye opening, motor and verbal response [82] (see Tab. 1.1).

Two other crucial scores for grading subarachnoid hemorrhage include the GCS score: The World Federation of Neurogical Surgeons scale (WFNS) of 1988 [205] and the Prognosis on Admission of Aneurysmal Subarachnoid hemorrhage scale (PAASH). There are numerous other grading scales for SAH used worldwide, e.g. like the Oshiro scale, [136]. A comparison of the three major scores is depicted in Tab. 1.2.

The Hunt and Hess scale has the lowest interobserver agreement at 0.48 (95% CI, 0.36 - 0.59) as compared to the World Federation of Neurogical Surgeons scale with an (agreement of 0.60, 95% CI, 0.48 - 0.73) and the Prognosis on Admission of Aneurysmal Subarachnoid hemorrhage scale (agreement 0.64. 95% CI, 0.49 - 0.79) [28]. The Fisher scale grades SAH according to CT findings into four hemorrhage patterns visible in the subarachnoid space as seen in Tab. 1.3. [50] The common aim of these scales is to allow a quick classification of patients upon arrival and to predict outcome and risk of complications.

Feature	Response	Score
Best eye response	Open spontaneously Open to verbal command Open to pain No eye opening	4 3 2 1
Best verbal response	Orientated Confused Inappropriate words Incomprehensible sounds No verbal response	5 4 3 2 1
Best motor response	Obeys commands Localizing Pain Withdrawal from pain Abnormal Flexion to pain Abnormal Extension to pain No motor response	6 5 4 3 2 1
		Total 3-15

Table 1.1: Glasgow coma scale. The glasgow coma scale is divided into three categories: 1) the best eye response, 2) the best verbal response and 3) the best motor response. Depending on the response of the patient, a score from 1 to 6 is associated. The three scores are then added up to form the final score which ranges between 3 (no response in all three categories) and 15 (best response in all three categories). Modified from: Jain, S., 2018 [82].

Grade	Hunt and Hess Scale	WFNS Scale	PAASH Scale
I	Asymptomatic, minimal headache and slight nuchal rigidity	GCS score 15	GSC score 15
II	Moderate to severe headache, nuchal rigidity, no neurological deficit other than cranial nerve palsy	GCS score 13-14 without focal deficit	GCS score 11-14
III	Drowsiness, confusion, or mild focal deficit	GCS score 13-14 with focal deficit	GCS score 8-10
IV	Stupor, moderae to severe hemiparesis, possibly early decerebrate rigidity, and vegetative disturbances	GCS score 7-12	GCS score 4-7
V	Deep coma, decerebrate rigidity, moribund appearance	GCS score 3-5	GCS score 3

Table 1.2: Comparison of Hunt and Hess, WFNS and PAASH classification of subarachnoid hemorrhage. All three grade patients from I (best) to V (worst). In the second row the Hunt and Hess classification takes into consideration symptoms of the patient and focal deficits. The WFNS Scale, seen in the fourth row depends on the Glasgow Coma Scale and focal deficits. The last row contains the PAASH scale. This one is only based on the Glasgow coma scale. Modified from: Degen et al. 2011, Tab. 1 [28].

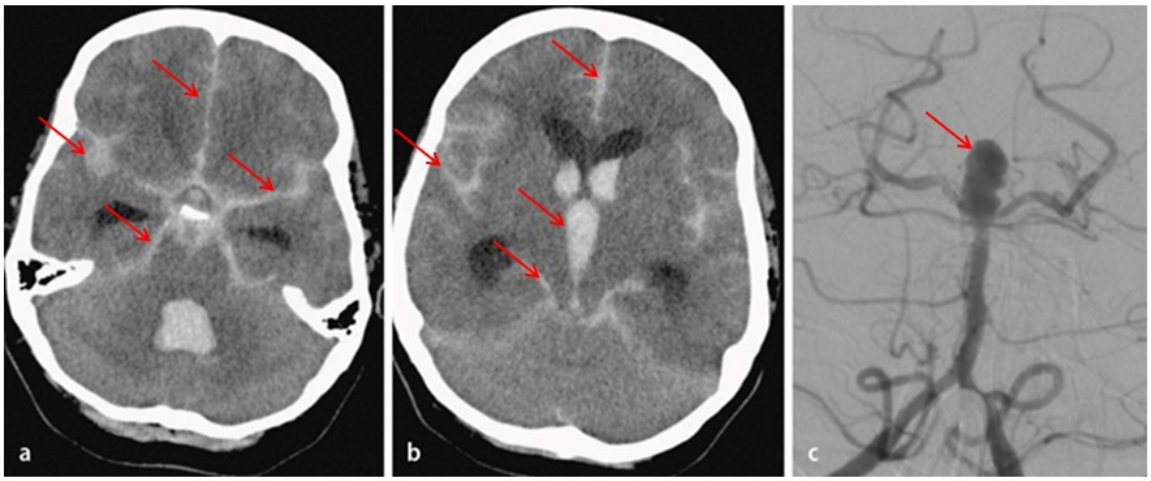

Figure 1.5: Cerebral CT scan with subarachnoid blood and angiogramm with big aneurysm at the circle of Willis.(a,b) On the cerebral CT scan fresh blood is visible as hyperdense (lighter) compared to the brain parenchyma. It is clearly visible in the interhemispheric space and the cisterns. (c) On the angiogram, the basilar cerebral artery is perfused and highlights the circle of Willis. At the bifurcation of the two is displayed a big saccular aneurysm. Curtesy of Dr. Terpolilli.

1.1.7 Therapy

SAH is a medical emergency and should immediately be treated in a well-equipped neurointensive care unit [127]. As there is tremendous risk of re-bleeding, which will be further discussed in Section 1.1.9, the primary therapeutic focus is to seal the bleeding site as soon as technically possible. Patients should be continuously monitored and regularly reassessed by experienced health care professionals [158]. General management should contain treatment of hyperglycemia [87, 103], hyperthermia [140, 199] and - if necessary - arterial hypertension. The latter must be carefully considered and adapted to the patients individual needs as a compromise must be found between the risk of re-bleeding facilitated by too high blood pressure and the risk of infarction with too low blood pressure [115, 202]. If present, cardiovascular complications need to be addressed appropriately to improve outcome [49]. Aneurysm occlusion can be achieved by open surgery and clipping or by an endovascular approach. Surgery consists in placing a vessel clip around the aneurysm base, thereby excluding it from normal blood circulation [20] (see Fig. 1.7). The endovascular approach consists in placing platinum coils into the aneurysm thereby inducing local blood clotting and aneurysm occlusion. Alternatively a stenting device may be placed (such as a Flow diverter stent) in order to prevent influx of blood into the aneurysm [65, 66] (see Fig. 1.8).

Studies disagree on which method leads to better outcome [111, 123, 177]. The decision should be made individually for each patient, taking into account factors like location of the aneurysm, accessibility, aneurysm size and the age of the patient. Outcome is comparable for both procedures [31, 162], but an individual selection of the optimal treatment modality results in optimal outcome [31].

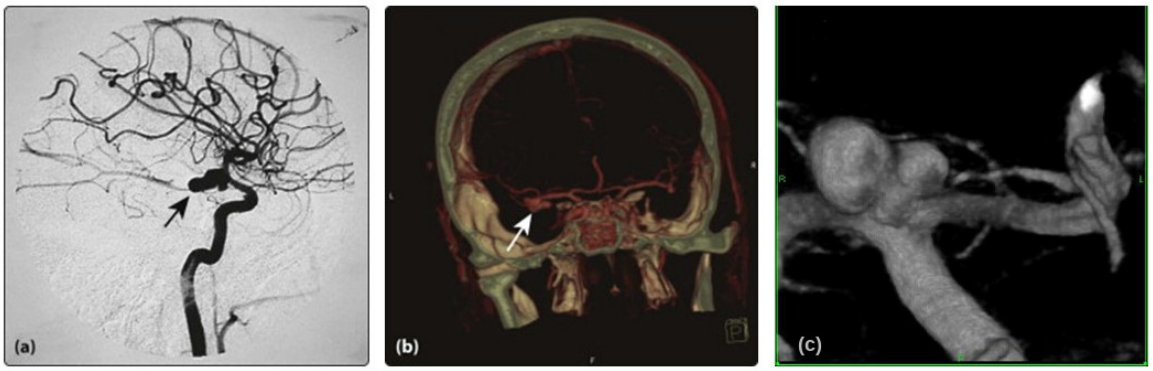

Figure 1.6: Display of saccular aneurysms in different sequences. (a) Digital subtraction angiogram displaying a large multiloculated aneurysm arising from the middle cerebral artery (b) CT angiogram depicting an aneurysm on the middle cerebral artery. (c) 3-D reconstruction of an aneurysm ant the bifurcation of the medial carotid artery and the circle of Willis done based on MRI data. A,b: modified from Fuller G. (2010) [58]; c: Curtesy of Dr. Terpolilli.

1.1.8 Outcome and impact for society

Although quality of medical intensive care and treatment of SAH have improved over the last decades, its outcome in general remains devastating. Acute fatality is >50% due to the initial hemorrhage or complications [163]. Around 15% of patients die during onset of hemorrhage and before even reaching medical care. Another 30% to 40% die within the first twenty-four hours after SAH [167, 171]. The 30-day in-hospital mortality for subarachnoid hemorrhage has been estimated to be approximately 40% (2016). Around 50% of surviving patients are left with permanent disabilities [36] (see Tab. 1.4).

Hemorrhagic strokes make up only 5% of all strokes [167], but are responsible for 40% of all stroke related deaths [7]. The mean age of death for patients with ischemic stroke is 81 years, for patients with intracerebral hemorrhage 73 years and for SAH patients 59 years [84, 131, 167]. Since many SAH patients are in the middle of their professional working life, the disorder results in a disproportionally high socioeconomic burden [84, 167]. The cost for the treatment of SAH exceeds five billion Euros per year in the European Union and the United States alone. Even though ischemic stroke is twenty times more frequent than SAH, the socioeconomic impact of the two diseases is almost the same [35, 150, 183].

1.1.9 Pathophysiology of subarachnoid hemorrhage

Within seconds after onset of SAH, as blood flows with arterial pressure into the limited subarachnoid space, intracranial pressure (ICP) raises massively [134]. In animal experiments, the immediate increase of ICP is around 80 mmHg. Many studies proved that as ICP increases during onset of SAH, the cerebral blood flow (CBF) drops drastically [11]. As the CBF decreases and at the same time the ICP increases the cerebral perfusion

Fisher grade	CT scan
I	No subarachnoid blood visible
II	Diffuse or vertical layer <1mm of blood in subarachnoid space
III	Localized clot and/or vertical layer >1 mm of blood in subarachnoid space
IV	Intracerebral or intraventricular hemorrhage with diffuse or no SAH

Table 1.3: Fischer classification of subarachnoid hemorrhage. The Fisher classification is based on blood visible on cranial CT scan. It ranks from Grade I, no visible blood in subarachnoid space and IV, intracerebral of intraventricular hemorrhage with diffuse or no SAH. Modified from: Fisher, 1980 [50].

pressure (CPP) is diminished [11, 133]. The CPP is defined as the middle arterial blood pressure (MAP) minus the intracranial pressure.

$$\mathrm{CPP} = \mathrm{MAP} - \mathrm{ICP}$$

If bleeding from the aneurysm continues, ICP rises further and CBF stops. These patients die on site due to cerebral circulatory arrest. If the bleeding ceases, ICP and CPP normalize or stabilize. Increased ICP after SAH is associated with the severity of early brain injury and patient mortality [207, 72]. The transient increase in intracranial pressure leads to global cerebral ischemia and brain edema. In this scenario the magnitude of edema correlates very well with the duration of global ischemia and the severity of the SAH. If brain edema is very pronounced, lethal cerebral herniation may occur [102]. Another complication which may cause herniation is the development of hydrocephalus [33]. After SAH, the presence of blood in the cerebrospinal fluid can impair the absorption of cerebrospinal fluid (hydrocephalus malresorptivus) or a direct blood clot may obstruct fluid draining passages (hydrocephalus occlusus) [63, 18]. As space inside the skull is limited, in both cases the fluid accumulates and leads to an increase in intracranial pressure and increases the risk of herniation. Once patients survive the initial SAH, the main and most threatening complication remains re-bleeding [47, 135]. Before 1983 it was believed that this mostly occurs later than 7 days after the initial hemorrhage [90]. However, today we know that rebleedings after SAH peak as early as within 6 hours after SAH onset [104, 173]. Hunt and Hess showed a very high incidence of recurrent hemorrhage in their study in 1968: many patients even bled more than once, and re-bleeding occurred after up to 3 months

Mortality of SAH	%
Total	51
Out-of-hospital death	10 - 15
Mortality first 24 hours	30
day mortality	40
1 - year mortality	40
2 - year mortality	50
Permanent disability	50 - 60

Table 1.4: Mortality of Subarachnoid hemorrhage. The total mortality of subarachnoid hemorrhage is 51% [163]. Between 10% and 15% are out-of-hospital deaths. 30% of patients die within the first 24 hours, 40% within the first month[167, 171]. The 1 year mortality is 40% and the 2 year mortality is 50%. Last, 50% to 60% of patients that survive subarachnoid bleeding retain permanent disability[36].

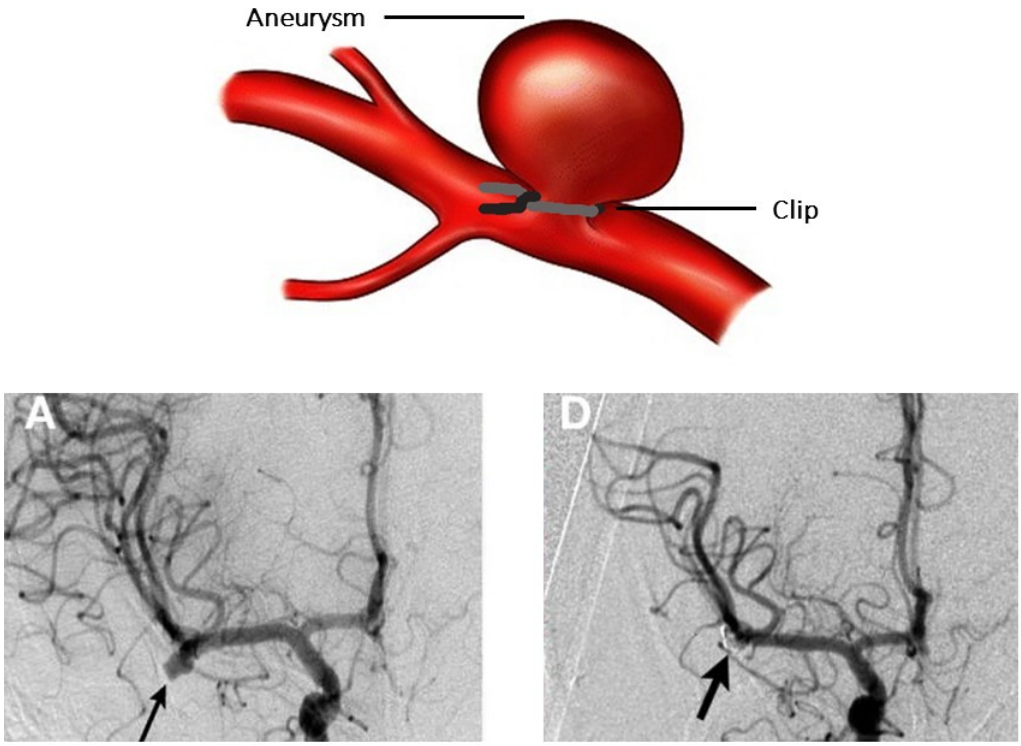

Figure 1.7: Clipping of MCA aneurysm. A 49-year-old woman presented with subarachnoid hemorrhage. (A) Cerebral angiography demonstrated a 6-mm right MCA bifurcation aneurysm. Like most MCA aneurysms, this lesion had a wide neck involving the origins of the insular (M2) MCA divisions. A single clip was applied across the aneurysm neck. (D) Postoperative angiography confirmed complete clipping (arrows) of the aneurysm. Modified from Seibert, B., 2011, [170].

after SAH [79]. Their work indicated that within the first two years after SAH almost 90% of patients (with and without treatment) suffered from at least one episode of re-bleeding. Almost half of these patients had more than one re-bleeding, 3% four or more events (see Tab. 1.5). This indicates the importance of recurrent hemorrhage as a complication of SAH.

Today, after the aneurysm has been treated successfully the risk of re-bleeding decreases significantly. Very few re-bleedings occur after elimination of the aneurysm. A study in 2018 showed an incidence of 2.3% after coil embolization [95].

1.2 Delayed cerebral ischemia

After the source of bleeding is secured, other aspects determine patient outcome. Five to seven days after SAH new infarcts may appear on CT scans [68] and focal neurological deficit may be observed[194]. These delayed changes are attributed to delayed cerebral ischemia (DCI), a condition associated with worse outcome. The exact mechanisms behind the formation of delayed cerebral ischemia are not clearly understood. For decades, DCI was believed to be caused by spasms of large intracranial vessels [25, 51].

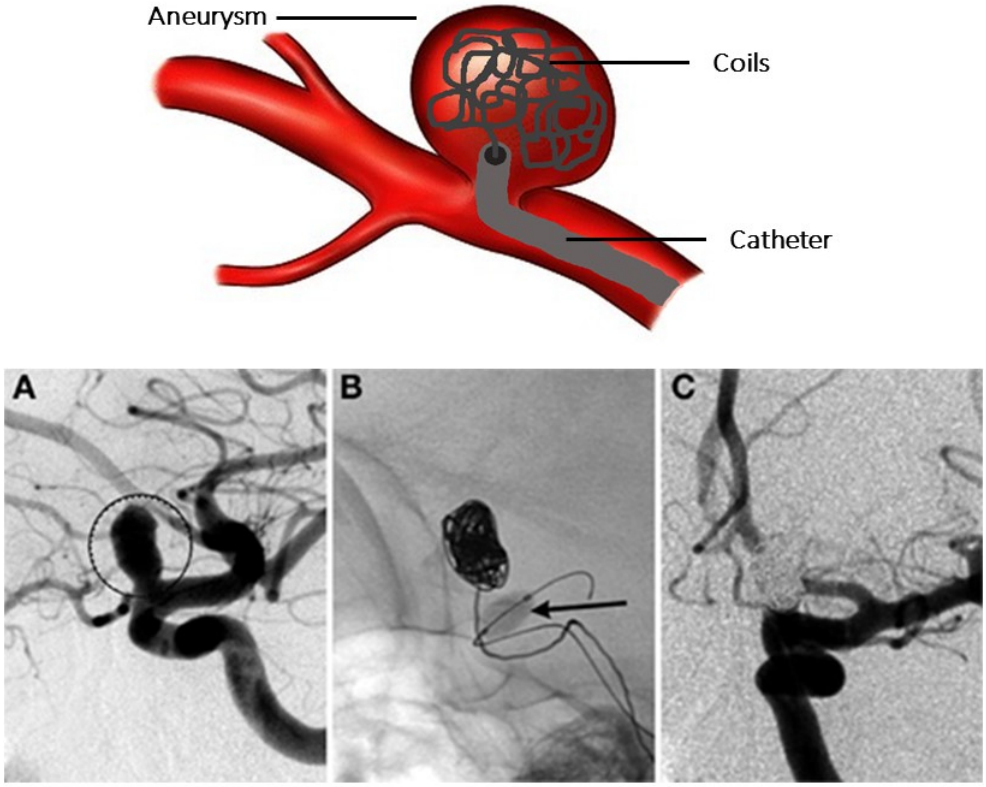

Figure 1.8: Balloon assisted coil embolization. A 74-year-old man with a strong family history of aneurysmal SAH was found to have a left ophthalmic aneurysm. (A) Lateral view of a left ICA injection shows a 7.5-mm left ophthalmic artery aneurysm (circled) with a 4.2-mm neck. The patient underwent balloon assisted coil embolization. (B) Lateral fluoroscopic view shows the inflated balloon (arrow) with coils being deployed through a microcatheter within the aneurysm. (C) AP view of the final left ICA injection shows no residual aneurysm. Modified from Seibert, B., 2011 [170].

1.2.1 Macrovasospasms

Cerebral macrovasospasms have been studied since their first description in 1951 [39]. Ecker and Riemenschneider found, that, in the presence of ruptured cerebral aneurysms, the caliber of the affected cerebral arteries was drastically reduced. They called this type of arterial narrowing "arterial spasms" [39]. As arteries constrict, they limit blood flow and therefore reduce perfusion to the brain parenchyma. Consequently, cerebral ischemia and poor outcome may occur. In 1978, Weir et al. showed that patients with more macrovasospasms have a higher mortality than those with less [201]. As indicated in Section 1.2, it has long been believed that the development of DCI was mainly caused by the formation of macrovasospasms. Interestingly, it has recently been shown that vasospasms and DCI do not always occur together. On the one hand, there are patients with vasospasms who do not show DCI and on the other hand there are those developing DCI without the detection of vasospasms [193]. In addition to those findings, a large multi-center clinical study, the CONSCIOUS trial, showed that despite successful treatment of vasospasms, there was no effect on long-term outcome [117, 190]. Therefore, it was suggested that delayed cerebral ischemia has to be a multifactorial phenomenon [151]. A clinical study in

%	Nr. of rebleedings
89	≥1
47	>1
30	2
14	3
3	≥4

Table 1.5: Number of rebleeings after subarachnoid hemorrhage in patients in 1986. Hunt and Hess counted the number of rebleedings in patients with and without treatment and for an observation period of 2 years.
Modified from: Hunt and Hess, Ars neurochirurgica, 1968, tab. 9 [79].

2015 found that delayed cerebral ischemia from macrovasospasms does not predict mortality after subarachnoid hemorrhage [102]. Late patient deterioration could have its origins much earlier than previously assumed [14].

1.3 Early brain injury

As a consequence of the sobering results from clinical studies addressing large artery spasms and late brain injury after SAH, more attention was given to the early phase, namely the first 72 hours after the bleeding. The pathophysiological changes in this time period are summarized as "early brain injury" (EBI; Fig. 1.9).

1.3.1 Pathophysiological changes

1.3.1.1 Microvascular constriction

Although previous research was more focused on the formation of delayed macrovasospasms it has since been shown that microvascular constrictions, called microvasospasms (MVS), occur and play an important role in the pathophysiology after SAH. As early as 1975 a study on Guinee pigs indicated that the contact of blood with cortical pial micro vessels leads to vascular contraction [71]. When the diameter of an artery decreases, volume flowrate decreases by the power of four as stated in the Hagen-Poiseuille Law of fluid kinetics. That means that vasoconstriction by 16% decreases blood volume flowrate by 50%. On the other hand, flowrate can be doubled by a dilatation of 19% of the initial diameter (see Fig. 1.10).

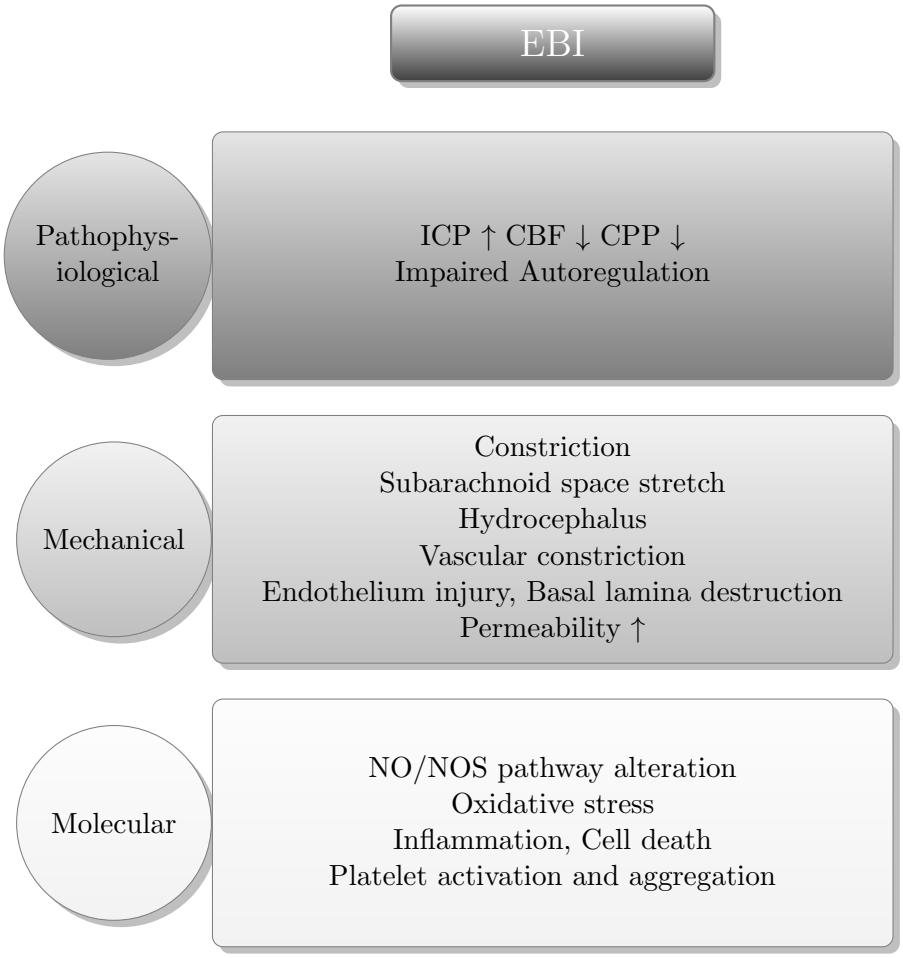

Figure 1.9: Summary of early brain injury. Early brain injury consists of three main mechanism. First, there are the physiological changes like increase in intracranial pressure, decrease in cerebral blood flow and decrease in cerebral perfusion pressure. On top of these there is impaired autoregulation. Second, there are mechanical changes during EBI. These contain constriction and subarachnoid space stretch, as well as development of hydrocephalus and vascular changes. These vascular changes are constrictions and spasms, endothelial injury, basal lamina disruption and increased permeability through the blood-brain-barrier. Third, there are molecular changes. These contain the important alterations in nitric oxide and nitric oxide synthase pathways, as well as oxidative stress, inflammation, cell death and platelet activation and aggregation.

Hence, in small arterioles even a small reduction in vessel diameter can have significant effects on blood flow and parenchymal perfusion, [141].

The acute narrowing of vessels occurs predominantly in arterioles and not in venules as shown by Friedrich et al. [55]. In their endovascular perforation mouse model of SAH, more than 70% of arterioles showed constrictions whereas venular calibers were not affected. Microvasospasms have been demonstrated as early as 5 minutes after SAH in rats [179]. Vessels can either constrict along their whole length or only be affected in some areas. The latter leads to pearl-string-like microvasospasms, which have been observed in humans [141, 189] and can be reproduced in mouse models [44, 55, 184] as seen in Fig. 1.11 [189].

Observations in humans suggest an elevated general microvascular tone of vessels in contact with subarachnoid blood [141]. These vessels also show a higher contractile response [141], as also shown experimentally in rabbits [27]. In addition, animal studies indicate

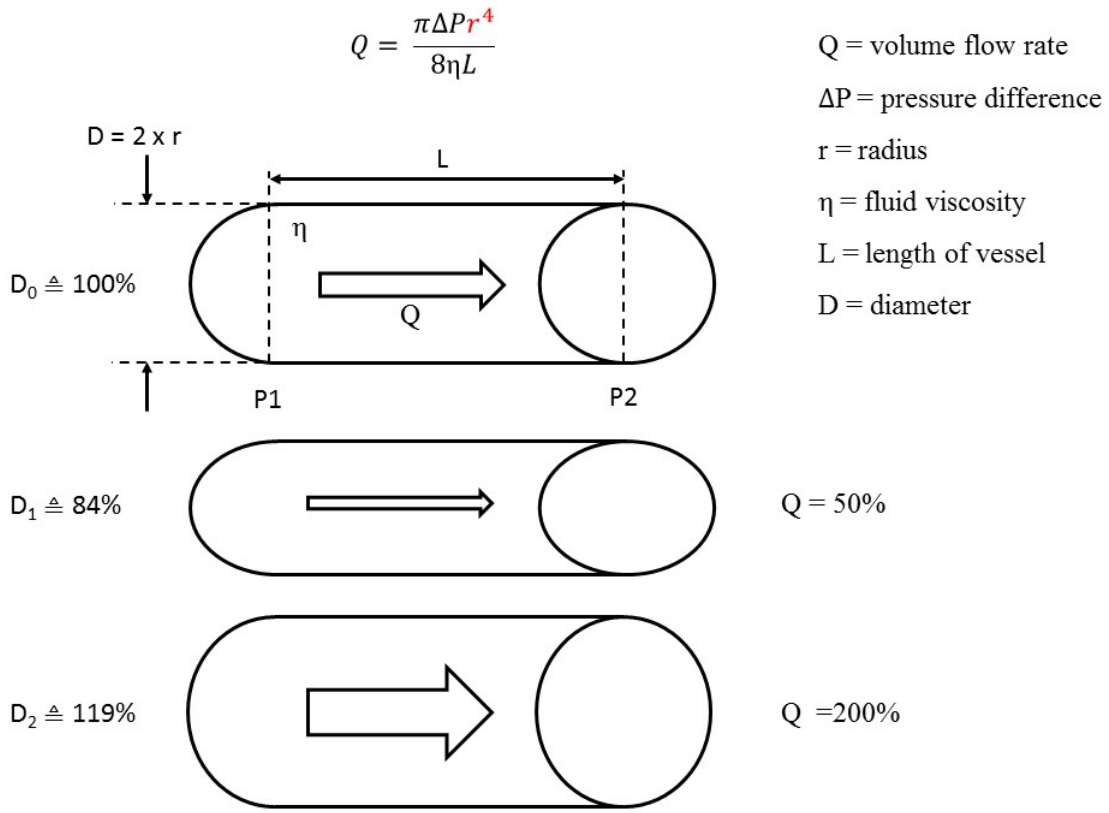

Figure 1.10: Hagen-Poisseulles Law of volume flow rate. Hagen-Poiseuilles Law of fluid kinetics applied to blood vessels states that volume flowrate is proportional to the vessel radius to the power of four. That means, that on one the one hand, vasoconstriction to 84% of initial value cuts blood volume flowrate to half of its initial value. On the other hand, the flowrate can be doubled by a dilatation to 119% of initial diameter.

that the mechanical stress (stretching of the subarachnoid space induced by hemorrhage), is directly transferred onto unruptured subarachnoid blood vessels and stimulates their constriction [8, 89, 167]. Recent studies indicate that the early formation of microvasospasms after SAH may be one of the major determinants of outcome after SAH and needs therefore to be targeted to allow for adequate brain perfusion [55, 183]. In addition to vascular constriction, arterioles demonstrate a strongly altered reactivity and especially a decreased response to vasodilation stimuli early after SAH [13].

1.3.1.2 Autoregulation

Under physiological conditions high carbon dioxide (CO_2) levels results in dilatation of cerebral arteries and subsequent increase of cerebral blood flow. In patients, CO_2 reactivity is impaired for up to 7 days after SAH [30]. Studies on mice and primates show that early after subarachnoid hemorrhage CO_2 reactivity is severely reduced [9, 54, 83, 88].

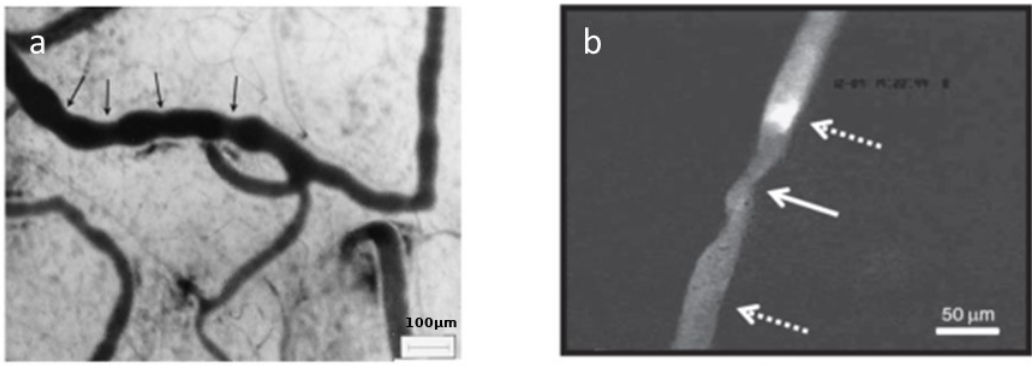

Figure 1.11: Early microvasospasms in patients and in mice (a) Image of early cerebral mircovasospasms in patients. The arrows indicate locations of pearl-string-like spasms. Uhl et al. Neurosurgery 2003 [189]. (b) microvasospasms in a murine SAH model 3 hours after SAH. Friedrich et al. 2012 [55].

1.3.1.3 Platelet activation and aggregation

Platelet activation within the first 48 hours after SAH has been observed in clinical settings [73, 168]. In animal models, activated and aggregated platelets were found within 2 hours after hemorrhage in big arteries and within 10 minutes after SAH in small intraparenchymal vessels [23, 56]. This leads to formation of micro emboli, a phenomenon suspected to be, at least partly, responsible for the so-called "no reflow" phenomenon which was first described by Adelbert Ames and colleagues in 1968 [5]. They stopped blood flow to the brain in a rabbit model for more than 5 minutes. They then observed that even when blood flow was reinitiated reperfusion did not occur in all areas of the brain. This phenomenon has later also been observed in humans [193], as well as in the SAH animal model [155].

1.3.1.4 Vascular alterations, permeability

Platelets release collagen-IV digestive enzymes when they are activated [56]. This leads to numerous vascular alterations like endothelial injury and destruction of the basal lamina [56]. If vessel wall permeability is increased and - thus - the blood-brain-barrier disrupted, the consequences are oxidative stress and cerebral edema [34].

1.4 Cerebral nitric oxide and nitric oxide synthases

1.4.1 Nitric oxide synthesis

Many of the above-mentioned changes have been linked to Nitric oxide. Nitric oxide (NO) is a gaseous signaling molecule critically involved in vessel dilatation and neuronal signaling. NO is synthetized from L-arginine in presence of the co-substrates molecular oxygen and reduced nicotinamide-adenine-dinucleotide phosphate (NADPH) by the three differentially localized NO-synthases (Fig. 1.12): The neuronal form, nNOS (NOS I), is mainly expressed in neuronal cells. It is involved in synaptic plasticity and blood pressure

regulation [52, 187, 206]. The inducible NO-Synthase, iNOS (NOS II) can be expressed in many different cell types and is reported to contribute to non-specific immune defense. In addition, iNOS plays an important role in inflammation and the pathophysiology of septic shock [52]. The endothelial isoform, eNOS (NOS III) is expressed in endothelial cells and promotes vessel dilatation. Therefore eNOS is involved in many pathological processes such as blood pressure regulation, vascular injury [106] and arteriosclerosis [52].

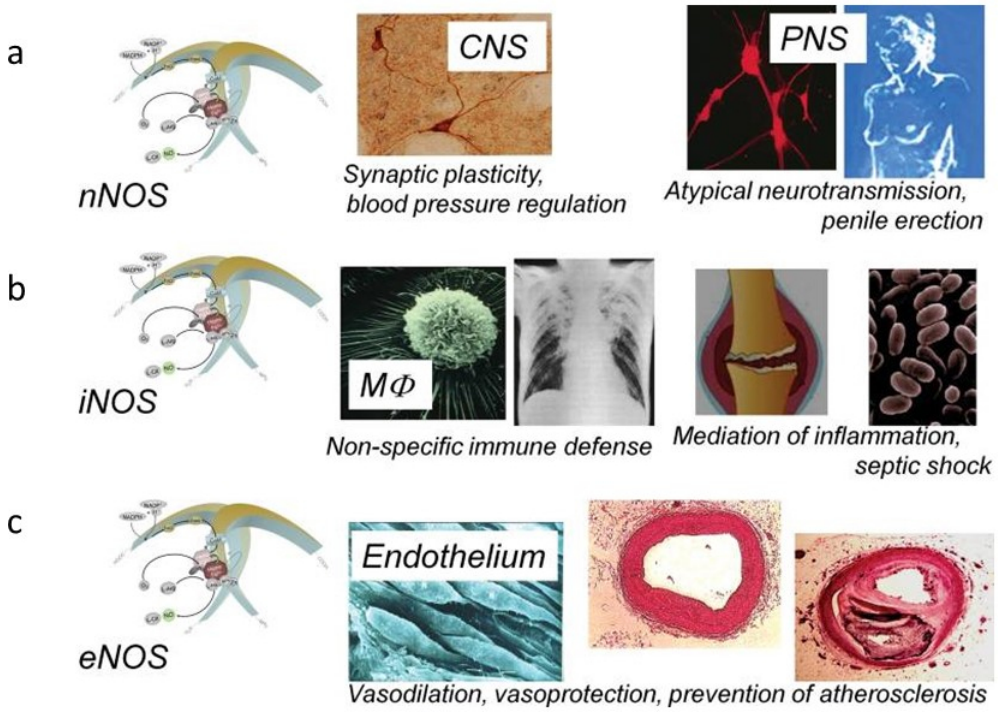

Figure 1.12: Important functions of the different NOS isoforms. (a) Neuronal nitric oxide synthase is expressed in neuronal cells in the central nervous system (CNS) and in the peripheral nervous system (PNS). In the CNS, on the one hand, it is involved in synaptic plasticity, which is important in the learning process and the memory formation. On the other hand, it takes part in central blood pressure regulation. In the PNS, nNOS produced NO is an atypical neurotransmitter mediating relaxation of gut peristaltic, penile erection and vasodilation.
(b) Inducible NOS can be expressed in many different cell types. Its presence was first proven in macrophages (M). In marcophages it plays an important role in fighting intracellular bacteria such as Mycobacterium tuberculosis [130, 118] or the parasite Leishmania [176, 200]. In contrast, the iNOS also acts as a mediator of inflammation, and is a major factor contributing to vasodilation (and therefore drop in blood pressure) in septic shock [148, 204].
(c) Endothelial NOS-derived NO is a strong vasodilator and important in vasoprotection. eNOS produces NO inhibits platelet aggregation and adhesion to the vessel wall. This also counteracts smooth muscle cell migration. Modified from Forstermann et al. 2012 [52].

In addition to L-Arginine, NOSs uses flavin adenine dinucleotide (FAD), flavin mononucleotide (FMN) and 5,6,7,8-tetrahydro-L-biopterin (BH4) as co-factors [24]. NOSs are composed of two monomers, each consisting of one reductase domain and one oxygenase domain, forming a homodimer (Fig. 1.13). In the reductase domain, electrons are transferred from NADPH to FAD and FMN. The electrons then get transferred to haem in the oxygenase domain. In the presence of the above cofactors electrons are used to reduce

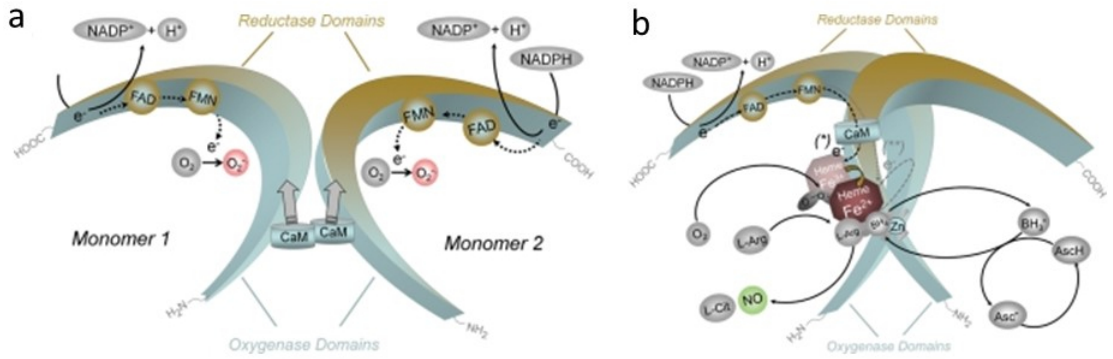

Figure 1.13: Structure and catalytic mechanisms of functional NOS. (a) The NOS enzymes consist of two monomers, each having an isolated reductase domain that can bind calmodulin (to enhance electron transfer) [1] and an oxygenase domain. The reductase domain can transfer electrons from reduced nicotinamide-adenine-dinucleotide phosphate (NADPH), to flavin-adenine-dinucleotide (FAD) and flavin-mononucleotide (FMN). In the process molecular oxygen gets reduced to superoxide (O_2^-) [178, 97, 100]. Only in the eNOS and nNOS elevated Ca^{2+} concentration is necessary to enhance calmodulin binding.
(b) NOS monomers are unable to bind the cofactor (BH4) or the substrate l-arginine and cannot catalyze NO production [97, 113]. Only in the presence of haem, NOS can form a functional dimer [97, 113]. In presence of the substrate l-arginine (l-Arg) and cofactor (6R-)5,6,7,8-tetrahydrobiopterin (BH4), intact NOS dimers couple their haem. It is important in the transfer of electrons. From l-Arg and oxygen nitric oxide is formed with l-citrulline (l-Cit) as the byproduct. In the process ferric haem (Fe^{3+}) receives an electron (*) and can bind oxygen and form a ferrous-dioxy (Fe^{2+}) species. This one can receive a second electron (**) from the cofactor. All NOS isoforms contain a zinc ion (Zn) at the dimer interface. Modified from Forstermann et al. 2012 [52].

oxygen and oxidize L-arginine into nitric oxide and L-citrulline [178]. All three isoenzymes bind calmodulin which facilitates the transfer of electrons from NADPH to haem. Binding of calmodulin depends on the intracellular CA^{2+} level in both eNOS and nNOS, whereas in the iNOS it is not sensitive to calcium [21, 70]. Since the endothelium is critically involved in the pathophysiology of SAH and possibly in the formation of microvasospasms, the role of eNOS may play a prominent role.

1.4.2 Physiological function of endothelial NO-Synthase

Under physiological conditions NO plays an important role in regulating resting perfusion of the brain. It furthermore is essential for blood pressure regulation [37]. Nitric oxide is a strong vasodilator in the cerebral microcirculation in response to shear stress, metabolic demand, and changes of carbon dioxide partial pressure [144]. It influences the diameter of arterioles and capillaries by targeting smooth muscle cells and pericytes, respectively. In arteries, NO diffuses from the endothelium into smooth muscle cell. There it binds to and activates soluble guanylyl cyclase (sGC), which in turn transforms guanosine-monophosphate (GMP) into cyclic guanosine-monophosphate (cGMP). The second messenger cGMP activates protein kinases that stimulate the relaxation of smooth muscle cells through calcium dependent pathways thereby causing vasodilation [64]. In capillaries, NO diffuses from the

endothelium into pericytes. There it maintains the phenotype of pericytes and inhibits their transformation into contractile smooth-muscle cells, which may induce microvascular constriction and release of cytokines [108]. Studies suggest that cGMP also plays a role in transformation of pericytes to their α-SMA phenotype.

1.4.2.1 Further functions

NO produced by eNOS is a strong inhibitor of platelet aggregation and adhesion to the blood vessel wall [4]. In addition, it has anti-inflammatory functions, for example by inhibiting endothelial cell apoptosis and modulating leucocyte adhesion [32]. A study in 2004 emphasizes the importance of eNOS for neovascularization in mice [3]. NO is involved in the release of many excitatory neurotransmitters [143, 147]. Its neuroprotective function [67], as well as an anticonvulsive function [197] have been recognized (Fig. 1.14). In addition, as previously indicated, nitric oxide is essential for blood brain barrier integrity [19].

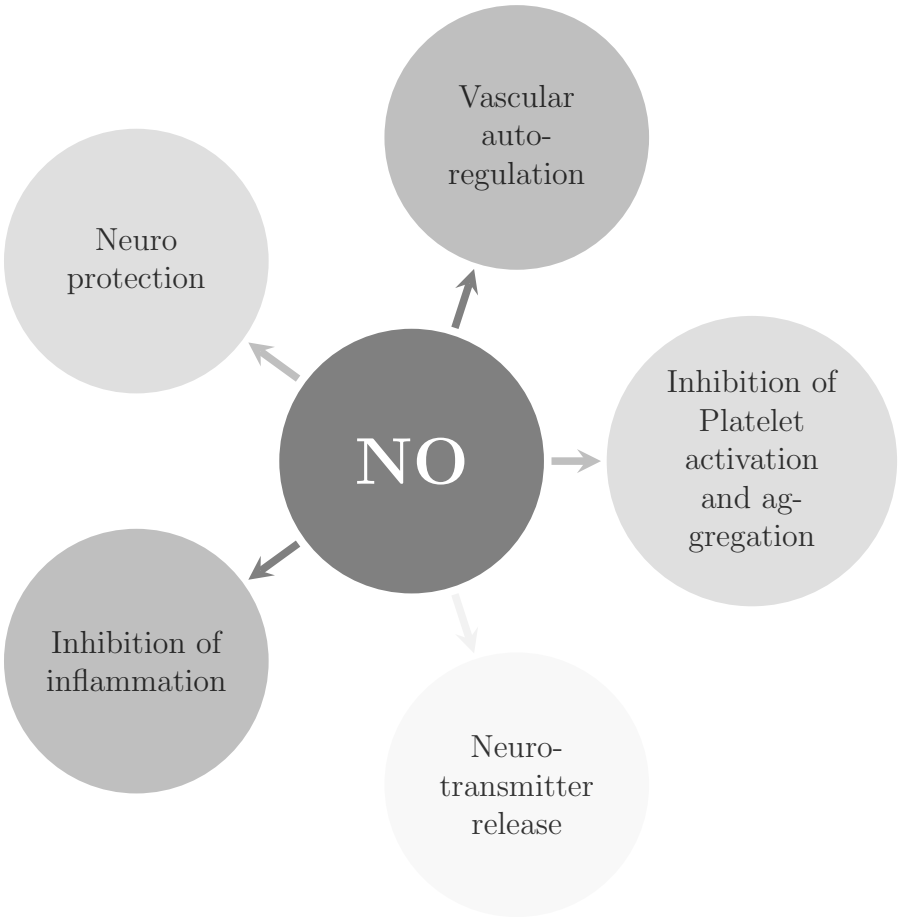

Figure 1.14: Function of cerebral NO. eNOS produced NO has many important functions in the human brain. First, the vascular autoregulation. NO is a strong vasodilator and inhibits arterial constriction. Second, nitric oxide inhibits platelet activation and aggregation, and therefore reducing artheriogenisis. Third, NO has proven to have neuroprotective function. Fourth, eNOS produced NO plays an important role in inhibition of inflammation and fifth, it is involved in many neurotransmitter pathways.

1.4.3 Nitric oxide in subarachnoid hemorrhage

It has been suggested that NO is lacking early after SAH [164, 166, 169]. A triphasic change with acute decrease after SAH, followed by recovery and increase within 24 hours has been observed in animal models of SAH [164]. The depletion of nitric oxide is associated with EBI [177] and delayed macrovasospasms/DCI in humans [38, 92] and in animal model of SAH [2, 41, 145, 164, 166, 169, 180]. Prevention and complete reversal of macrovasospasms could be obtained by counteracting NO depletion by intracarotid infusion of nitric oxide donors in a primate model [145], further indicating the importance of NO in macrovascular changes after SAH. The exact mechanisms behind the early depletion in nitric oxide remain unclear. Two possibilities have been further investigated in the last decade: NO scavenging by hemoglobin and lack/or dysfunction of eNOS. During subarachnoid bleeding hemoglobin comes in contact with endothelial cells. On the one hand hemoglobin may lead to NO scavenging [69, 154], on the other hand it may inhibit the eNOS and cGMP pathway [144]. Previous studies indicated that NO depletion early after SAH was mainly caused by NO scavenging by hemoglobin, vascular neutrophils, or free radicals, as overall NOS activity remained unchanged in the first 90 minutes after SAH. Lately it has been clarified that only nNOS and iNOS are not involved in the acute alterations of cerebral NO levels after SAH [165]. More recent studies confirmed that eNOS expression and activity are indeed lacking after SAH [108, 139, 144]. It has been shown in SAH patients that cerebral autoregulation and CO_2 reactivity are impaired up to one week after hemorrhage [30]. As previously mentioned (see Section 1.3.1.2), animal studies indicated that early after SAH CO_2 reactivity is severely decreased [9, 54, 83, 88]. As the autoregulation is assumed to be mediated mainly by NO produced by eNOS, a lack of the latter would therefore lead to this impairment. A clinical study in 2004 correlated concentration of asymmetric dimethylarginine (ADMA), which is an endogenous inhibitor of nitric oxide synthase, to worse outcome after SAH [107]. This again indicated the importance of eNOS in the pathophysiology after SAH. Most of the research on eNOS and SAH, however, was performed using immunohistological methods [139]. Clear in vivo evidence is missing yet.

1.4.4 Patients with endothelial nitric oxide synthase polymorphisms

Mutations in the eNOS gene are correlated to bad outcome after SAH. Multiple studies indicated that the presence of the T786C polymorphism of eNOS is associated with an increased risk for macrovasospasms after SAH [93, 98, 174]. The T786C polymorphism is a loss-of-function mutation and thus results in a dysfunction in the enzyme and reduced endothelial NO production.

1.5 Hypothesis and aim of study

Based on the findings described above we hypothesize that lack of NO may represent a major step in the pathophysiology of SAH. In order to investigate whether this hypothesis

is valid, we aimed to induce SAH in animals with a complete loss of eNOS function, i.e. eNOS knock-out mice (Fig. 1.15). This strategy was chosen because specific pharmacological inhibitors of eNOS are not available. A second motivation for our study was a publication from 2013 showing that eNOS knockout reduces secondary complications after subarachnoid hemorrhage [156]. Since these findings, generated in a clinically not particularly relevant mouse model of SAH, were widely and controversially discussed in the SAH community, we aimed to investigate eNOS knockout mice using the filament perforation model of SAH, the currently clinically most relevant SAH model, which does not only mimic the presence of blood in the subarachnoid space as the model used by Sabri and colleagues, but in addition also the initial bleeding and the phase of global cerebral ischemia.

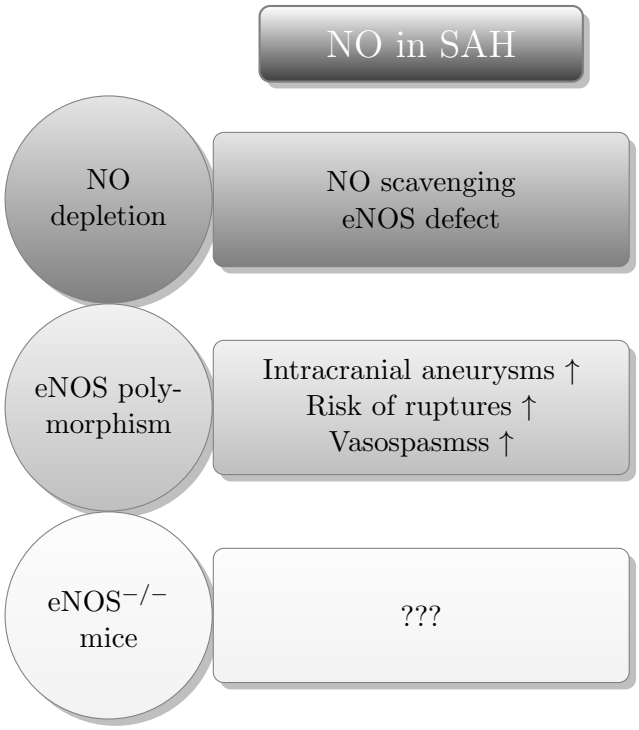

Figure 1.15: Importance of nitric oxide in subarachnoid hemorrhage. NO depletion after SAH has been widely shown. It is caused by both NO scavenging by hemoglobin and a defect in the endothelial nitic oxide synthase. In patients with eNOS polymorphisms, a higher risk of intracranial aneurysms has been observed. They have an elevated risk of rupture and after subarachnoid hemorrhage present an increased risk of vasospasms. eNOS knockout mice have been used to investigate the eNOS NO pathway. But the exact importance of the enzyme had to be investigated.

2 Materials and Methods

2.1 General

2.1.1 Ethical statement

All experiments were conducted between October 2015 and June 2017 in the Institute of Stroke and Dementia Research, University of Munich. All procedures performed on animals, group size calculation, and all statistical methods used to analyze in vivo data were reviewed and approved by the Government of Upper Bavaria (protocol # Az. 136 - 11). The results of the study are presented in accordance with the ARRIVE guidelines [94].

2.1.2 Study design

Sample size calculations were performed using SigmaStat (SigmaStat 3.0, Jandel Scientific, Erkrath, Germany) with the following parameters: alpha error = 0.05, beta error = 0.2, calculated standard deviation ranged from 15% - 20% (depending on the parameter investigated), and biologically relevant difference = 30%. Mice were given random numbers by another researcher and the investigator was therefore blinded to the genotype of the mouse during both surgery and analysis of the data.

2.1.3 Experimental animals

The eNOS gene, consisting of 52106 base pairs, twenty-eight axons and encoding the eNOS protein of 1203 amino acids [129], is located on the chromosome 7q36 in humans [120, 128]. Multiple mouse strains for eNOS deficiency have been developed, many with a combined targeted mutation in another gene, such as the BKSCg-Lepr^{db} NOS3^{tm1Unc}/RhrsJ, a model suited for studying diabetic nephropathy. The mouse strain currently used, B6.129P2-NOS3^{m1Unc}/J [80], is a purely eNOS deficient. These mice are suitable for studying hypertension, cardiovascular defects, insulin resistance, hyperlipidemia and lung development. They are also used in models for stroke. Other suitable eNOS knockout strains are Nos3$^{em1(IMPC)Mbp}$, and Nos3$^{tm282188(L1L2_Bact_P)}$ [48] but they are rarely used due to their limited availability. eNOS knockout was shown to lead to elevated blood pressure [76] and to play an important role in remodeling of blood vessels, since eNOS depletion promotes abnormal vessel remodeling and leads to pathological changes in vessel wall morphology in mice upon arterial wall injury [152]. eNOS deficient animals show more severe tissue

damage and worse functional outcome than wild type controls [75, 77, 109]. In models of global ischemia eNOS depletion worsens outcome as well [137].

eNOS transgenic animals were purchased from Jackson Laboratories (stock # 002684). In this mouse line, which was developed by Dr. Smithies of the University of North Carolina [172], a neomycin cassette replaced 129 base pairs of exon twelve of the eNOS gene, which disrupts the calmodulin binding site of the protein and introduces a premature stop codon into the transcripts [172]. These transgenic mice have been crossbred back to C57Bl/6 for over ten generations at the Jackson Laboratories. The purchased homozygous knockout animals were crossbred in our animal facility with C57Bl/6N from Charles River (Charles River, Kisslegg, Germany) to obtain heterozygous eNOS deficient mice. For this study, male and female mice with an average age of 8 weeks and a mean bodyweight of 22.5 g were used.

Husbandry Mice were housed in maximal groups of five in standard cages (207 x 140 x 265 mm, Macrolon II, Ehret Life Science Solutions, Emmendingen, Germany) under a 12-hour day/12-hour night cycle with free access to water and food. Health screens and hygiene management checks were performed in accordance with the Federation of European Laboratory Animal Science Associations guidelines and recommendations [45].

2.2 Experimental subarachnoid hemorrhage

2.2.1 Anesthesia and monitoring

Anesthesia was induced as previously described [185]. Mice were placed in a chamber flooded with 5% isoflurane (Abbot GmbH & Co. KG; Wiesbaden, Germany) until loss of consciousness and pain reflexes. They then received an intraperitoneal injection of 0.05 mg/kg bodyweight fentanyl, (Eurovet Animal Health BV, Bladel, Netherlands), 0.5 mg/kg bodyweight medetomidine, (Eurovet Animal Health BV, Bladel, Netherlands), and 5.0 mg/kg bodyweight midazolam (B.Braun Melsungen AG, Melsungen, Germany,). To maintain anesthesia and analgesia mice received an intraperitoneal injection with half of the initial dose every hour. Mice were then orotracheally intubated with a tube made from a 20G venous catheter, placed under the operation microscope (Carl Zeiss AG; Oberkochen, Germany), and mechanically ventilated (Minivent 845, Hugo Sachs, March-Hungstetten, Germany) under continuous monitoring of end-tidal CO_2 partial pressure by microcapnography (Model 340, Hugo Sachs, Germany). The ventilation frequency was adapted to maintain an end-expiratory pCO_2 at 30 mmHg. Eyes and mucous membranes were protected from exsiccation with eye ointment (Bepanthen Creme, Bayer Vital, Leverkusen, Germany). Core body temperature was kept at 37 ℃ by a feedback-controlled heating pad (FHC Bowdoinham, Bowdoin, ME, USA) and a sensor at the hind paw (SpO2-MSE, Kent Scientific Corporation, Torrington, CT, USA) was used to continuously measure oxygen saturation and heart rate. Depending on the experiment, mean arterial blood pressure was either monitored non-invasively before and up to 15 minutes after induction of SAH by a tail-cuff monitor (Kent Scientific, Torrington, CT, USA) at five-minute intervals, or

invasively via a catheter placed in the left femoral artery. For catheter placement, mice were placed in supine position and the left hind paws were slightly extended and fixed with tape. The catheter (outer diameter: 0.61 mm, inner diameter: 0.28 mm; Smiths Medical, Keene, USA) was cut to approximately 30 cm, and its end then thinned over a lighter and cut angularly. The catheter end is connected to a one ml syringe via a 30G needle (0.3 x 0.13 mm) and is flushed with heparin (Rathiopharm GmbH, Ulm, Germany) and then with saline. A 2 cm incision was then made along the thigh of the mouse. The femoral nerve, artery and vein were dissected with extra care to not injuring the nerve. A preparatory 5-0 silk suture (Pearsalls Limited 10C103000, England) was placed around the femoral artery and the distal part of the artery was ligated. A microsurgical vessel clip (Peter Lazig GmbH, Tuttlingen, Germany) was then placed proximally. The femoral artery lumen was opened and a saline filled catheter was then inserted into the artery and fixed with the previously placed silk filament. Then the clip was removed from the vessel and the catheter connected to the blood pressure measurement system (Perfusor secura; B.Braun Melsungen AG, Melsungen, Germany). The skin was closed with monofilaments (Ethibond 5-0, Ethicon, Norderstedt, Germany). Before and during intravital microscopy, blood pressure was also always monitored invasively. All physiological parameters were recorded using Lab Chart 8.0 (AD Instruments Pty Ltd, New South Wales, Australia).

2.2.2 Measurement of intracranial pressure and cerebral blood flow

Intracranial pressure (ICP) was measured continuously by an intraparenchymal probe (Codman ICP Express, DePuy Synthes, Umkirch, Germany) placed in the contralateral or ipsilateral epidural space, depending on the subseries as previously described [15, 44]. Intracranial pressure was measured starting 15 minutes before until 15 minutes or 90 minutes after induction of subarachnoid hemorrhage and is given in mmHg. Cerebral blood flow (CBF) was measured via Laser-Doppler-Flowmetry (Perimed, Järfälla, Sweden) as previously described [15, 44]; The fiberglass probe was fixed perpendicularly to the skull after partially removing the temporal muscle in order to measure the ipsilateral or contralateral territory of the middle cerebral artery. Cerebral blood flow was recorded starting 15 minutes before until 15 minutes or 90 minutes after induction of subarachnoid hemorrhage. Values are given as percent of pre-hemorrhage (=baseline) blood flow (Fig. 2.1).

2.2.3 Tail bleeding time

Bleeding time was determined as previously described [54, 184]. A 1 mm part of the distal end of the tail was amputated in deep anesthesia. The tail was promptly placed perpendicularly in temperature 37°C physiological saline. The arterial bleeding time was then timed manually.

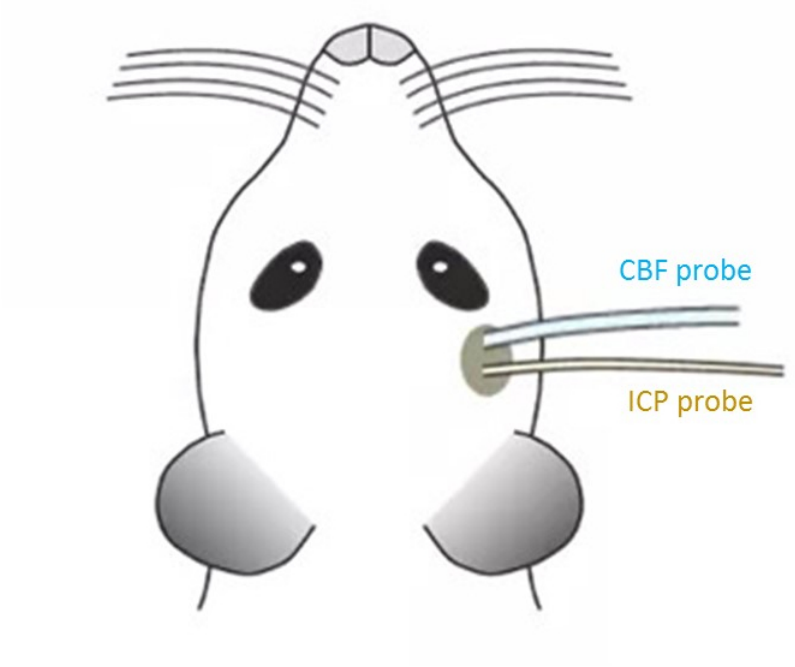

Figure 2.1: Placement of ICP and CBF probe. Two probes were applied to the mouse skull. The intracranial pressure probe was inserted through a small hole under the skull and fixed with cement. The probe measuring the cerebral blood flow was glued to the skull under the temporal muscle. Both probes were placed on the same side and contralateral to the subarachnoid bleeding. Modified from Schuller et al. 2013 [161].

2.2.4 The MCA perforation model

Subarachnoid hemorrhage was induced by filament perforation as previously described [44, 55, 161, 184]. The animal was placed in a supine position after ICP and CBF probe placement. Depending on the experimental group either femoral artery catheterization or a tail cuff was used for blood pressure measurements. A 2 cm skin incision was made on the left side of the neck. Then the common carotid artery as well as the carotid bifurcation were carefully dissected sparing the vagus nerve. The superior thyroid artery was then ligated at its origin from the ECA and severed. Two silk sutures were placed around the caudal part of the ECA to later secure the inserted filament, then the cranial part of the ECA was ligated. After carefully placing a vessel clip both on the cranial part of the ECA and the ICA just after the carotid bifurcation a 1 mm short incision was made on the cranial part of the ECA. A 12 mm long prolene filament (Prolene 5-0, Ethicon, Norderstedt, Germany) was then inserted into the external carotid artery facing the bifurcation and secured with the two ligatures. The clips were then removed. The filament was pushed into the ICA and then advanced intravascularly towards the circle of Willis (Fig. 2.2) until a sharp increase in intracranial pressure (more than 58 mmHg) and a drop in cerebral perfusion (below 25% of baseline) indicated vessel perforation.

If these criteria were not met the mice were excluded from analysis. The filament was quickly retracted and the artery stump ligated. The skin incision was closed with sutures (Ethibond 5-0, Ethicon, Norderstedt, Germany) and tissue adhesive (3 M Animal Care

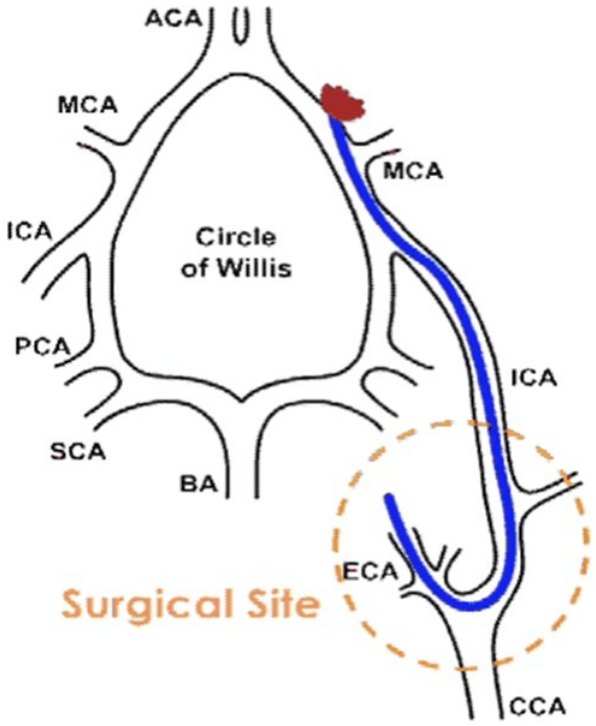

Figure 2.2: Induction of subarachnoid hemorrhage. A filament was inserted through the external carotid artery (ECA) and pushed forward into the internal carotid artery (ICA) until it perforates the circle of Willis at the level of the middle cerebral artery (MCA). From there, the blood disperses into the subarachnoid space. Modified from Schuller et al. 2013 [161].

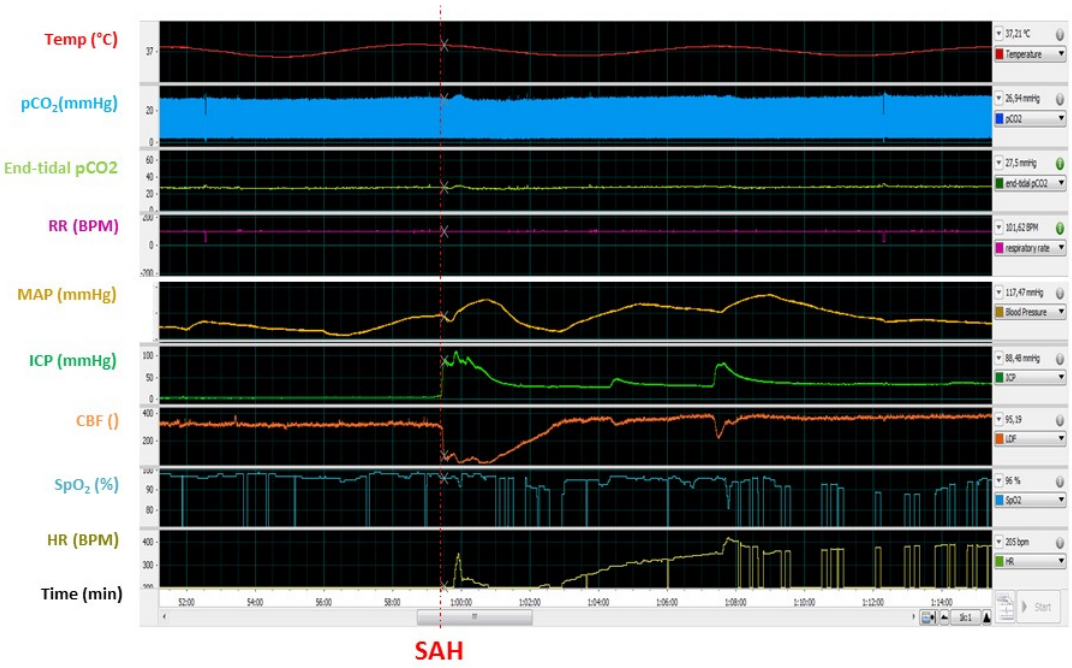

Figure 2.3: Physiological parameters before and after subarachnoid hemorrhage. This image is a display of the different physiological parameters as seen life during surgery. The top panel depicts the temperature, followed by the pCO_2 and the end-tidal pCO_2. Underneath the mean arterial blood pressure is displayed. On the graph of the intracranial pressure the sharp increase during onset of subarachnoid bleeding can be seen. Simultaneously the cerebral blood flow drops. On the bottom are located the oxygenation and the heart rate. The values are shown from 10 minutes before SAH to 15 minutes after SAH.

Products, St. Paul, USA). During SAH induction physiological parameters (temperature, pCO_2, end tidal pCO_2, respiratory rate, pulse, blood pressure, oxygen saturation, ICP, CBF and heart rate) were recorded digitally (Fig. 2.3).

For imaging experiments, mice were monitored for 15 minutes after SAH, then all probes were removed, and the animals were injected with a 2.5 mg/kg bodyweight Atipamezol (Laboratorios SYVA, Leon, Spain), 0.5 mg/kg bodyweight Flumazenil (Synthon BV, Nijmegen, Netherlands), and 1.2 mg/kg bodyweight Naloxon (B.Braun Melsungen AG, Melsungen Germany) to antagonize the anesthesia. Animals were then placed in an incubator at 27.4℃ and 30% air humidity (MediHEATMT, Peco Services Ltd. Brough, Cumbia, UK) for 2 hours. Mice which did not receive imaging after SAH were monitored for 90 minutes and then sacrificed.

2.3 Intravital microscopy

2.3.1 Technical background

Fluorescence microscopy was first described by Sir George G. Stokes in 1852. A large variety of fluorescent molecules, called fluorochromes or fluorophores that emit light of a

certain wavelength when illuminated, have been discovered since. If a fluorescent molecule is hit by a photon of the correct wavelength, it is excited, i.e. it absorbs the energy of the photon and lifts one of its electrons to a higher energy level. Since this higher energy level is unstable, the electron falls back to its initial energy level thereby emitting a photon of a longer wavelength. The emitted light disperses spherically in all directions independently of the direction of excitation [61]. Conventional one-photon fluorescence microscopy is not optimal for cerebral imaging in vivo. Brain tissue is very sensitive to photo toxicity and absorbs and scatters too much excitation and emission light [81]. This phenomenon worsens with increasing depth leading to images of low contrast. In 1990 Denk et al. solved this problem by building a two-photon microscope based on the "non-linear optical effect of two-photon excitation" first described by Maria Göppert-Mayer in 1931 [29, 62]. The idea is that a fluorophore hit almost simultaneously by two photons emits only one photon with twice the energy, i.e. half the wavelength of the excitation photons. Two-photon-excitation microscopy has many advantages over one-photon-excitation microscopy. As only the molecule absorbing two photons at the same time emits light, the image of the focal point has a high contrast to the surrounding tissue both in horizontal and vertical dimension (Fig. 2.4) [16].

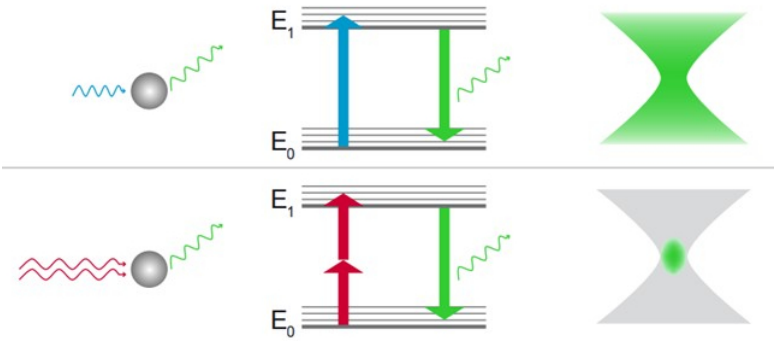

Figure 2.4: Jabłoński-Diagram: Comparison of one- and two-photon-excitation. On the one hand, in one-photon-excitation-microscopy one photon of short wavelength light excites a fluorescence molecule. The electrons receive more energy and move to a higher state. As this state is unstable they soon fall down to the initial level and in the process produce energy in the form of emitted light and heat. The emission of the focal point is not very precise, many surrounding molecules get also hit by one photon and emit light. In the two photon-excitation-microscopy on the other hand the needed energy to excite a fluorescent molecule is produced by two photons of each half the needed wavelength. Only when both hit the molecule at approximately the same time this one gets excited. As the surrounding molecules may be hit by one photon, but not two, the energy is not high enough to excite them. Hence, the emission of focal point is more precise. Modifed from Burgold, 2013 [16].

This leads to a high intrinsic three-dimensional resolution of the sample. The most common used laser wavelength is in the range of 650 to 1000 nm. Light of this range can penetrate deeper into the tissue than light of double the range, which would be needed in one-photon-excitation-microscopy. Penetration depths of up to 1 µm have been described for two-photon-excitation-microscopy; in most set-ups, 200 to 700 nm depth can be realistically obtained. In addition, the laser has less energy than lasers of shorter wavelengths used in one-photon microscopy and leads to less tissue damage. The brain can therefore

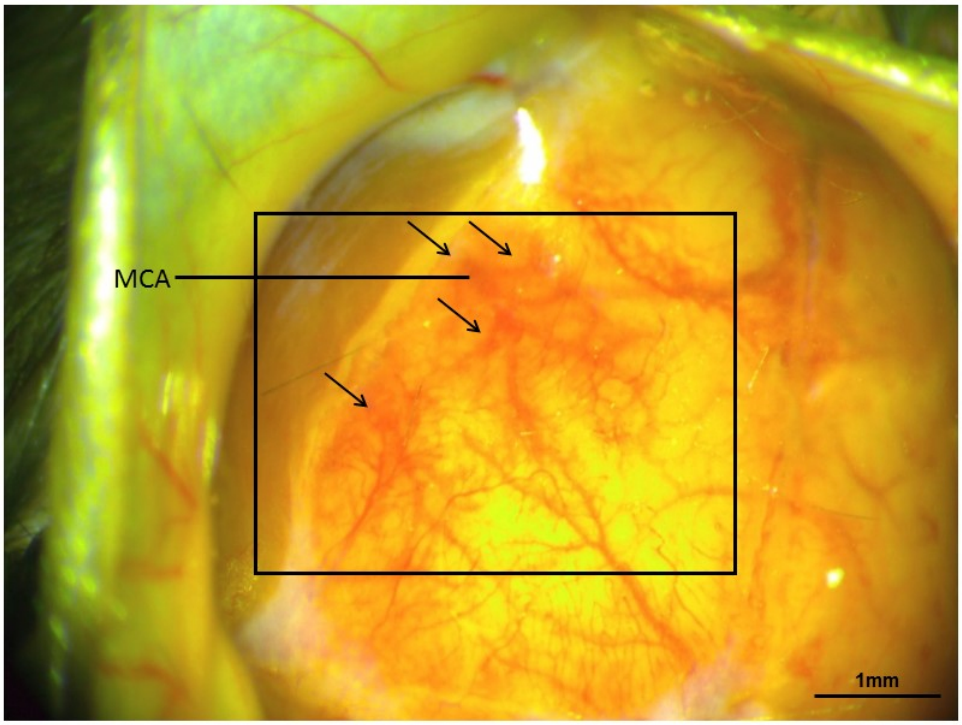

Figure 2.5: Picture of the intact skull over the territory of the middle carotid artery (MCA) after subarachnoid hemorrhage. Before preparation of the cranial window, at about 2.5 hours after SAH leaked blood is visible through the skull. The areas highlighted by arrows are, where blood is visible around the vessels or in the parenchyma.

be imaged for a longer time than in conventional fluorescent microscopy with less phototoxic damage [29, 126]. With this setup it is possible to perform precise three-dimensional imaging of a thin layer of the living brain.

2.3.2 In vivo imaging

For intravital microscopy, mice received a femoral arterial catheter, were placed in prone position, and were fixed in a mouse head holder (Model 921-E, Kopf Instruments, Tujunga, USA). The head was slightly rotated to the right, so the temporal bone was plane. A 3 cm longitudinal incision was made. The skin was elevated by sutures (Ethibond 5-0, Ethicon, Norderstedt, Germany) to form a skin pocket (see Fig. 2.5). The laser Doppler probe was placed as described above (see Sect. 2.2.2). The galea aponeurotica was removed, the skull exposed. A cranial window (1.5 mm x 2 mm; Fig. 2.6) was drilled over the left middle cerebral artery territory with a precision drill (Rewatronik Products; Wald Michelbach, Germany) and a diamond drilling head (diameter 0.5, Aesculap GD 8730 R, B. Braun Melsungen AG, Melsungen, Germany) under continuous cooling with saline in order to avoid heat damage. The craniotomy was lifted exposing the intact dura which was immediately covered with saline in order to avoid dehydration.

The mouse was then carefully placed under the microscope (Zeiss LSM 7, Zeiss, Jena, Germany) equipped with a Li:Ti laser (Chameleon, Coherent, Vision 1, Santa Clara, CA, USA) and a 20x water immersion objective (Plan Apochromat, NA 1.0, Zeiss, Germany).

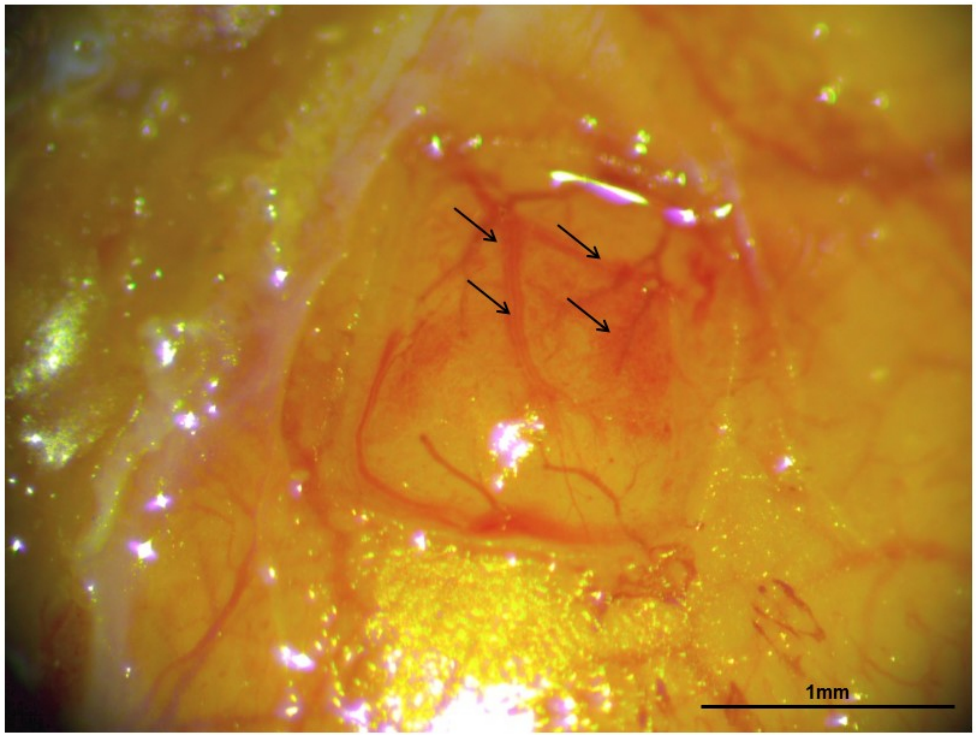

Figure 2.6: Picture of open cranial window (with intact dura) over the MCA territory. After craniotomy, the areas where blood has been leaking into the parenchyma are even clearer. Subarachnoid blood can slow be seen surrounding the biggest artery in the window. The arrows indicate especially obvious points.

Fluoreszeinisothiocyanate (FITC) dextran (0.5% in saline, Merck, Darmstadt, Germany), a plasma marker, was injected to visualize blood vessels. The size of the cranial window allowed proper imaging of a maximum of 1200 x 1200 µm (Fig. 2.7 of imaging of the entire cranial window).

For time reasons four connected, overlapping regions of interest with a size of 425 x 425 µm were imaged. Three-dimensional image stacks (3 µm step distance) were obtained up to a targeted minimum depth of 400 µm using an imaging software (ZEN 2.3 SP1, Carl Zeiss Microscopy GmbH, Jena, Germany). These four stacks were later stitched together to form one big image stack of 800 x 800 µm (Fig. 2.8). Imaging was done every 10 minutes for a time period of 90 minutes.

2.4 Experimental groups (Tab. 2.1)

To validate the surgical techniques and the model, a standardization series of subarachnoid hemorrhage with nine mice in a row was performed. To assess the impact of eNOS deficiency in the acute phase, i.e. up to 90 min after SAH, physiological parameters (temperature, pCO_2, ICP, CBF, HR, MAP, Oxygen saturation) were evaluated in homozygous ($eNOS^{-/-}$), heterozygous ($eNOS^{-/+}$), and wild type mice (Fig. 2.9).

Ninety minutes after SAH the mice received an overdose of the drugs used for anesthesia (see 2.2.1) and were perfused with paraformaldehyde (PFA). The brain was then

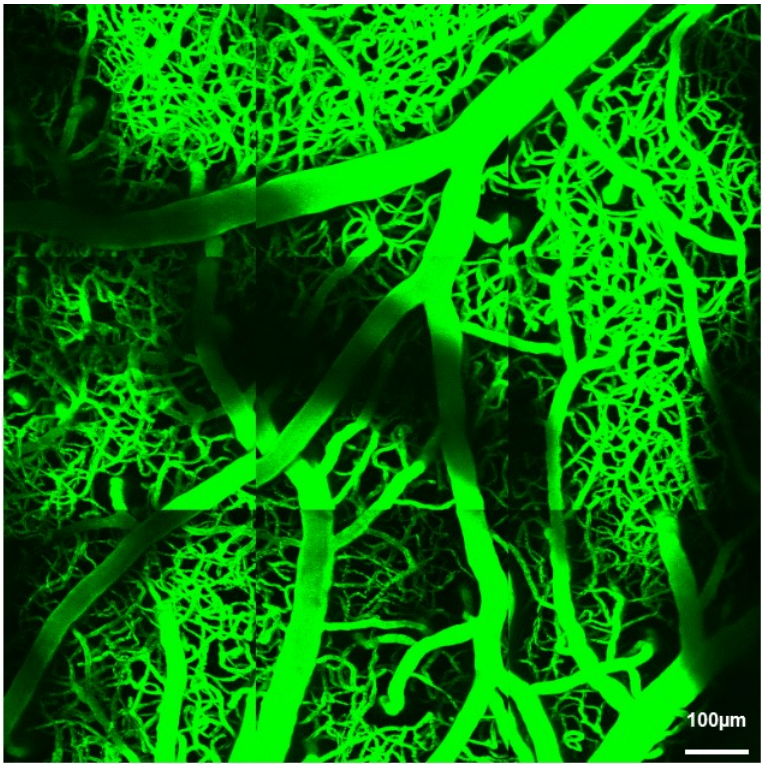

Figure 2.7: Mapping of the entire cranial window. Maximum size of imaging obtainable in this cranial window.

Mouse strain	Total	SAH at least 15 min	SAH 90 min	Imaging	Imaging after SAH
WT	40	32	16	8	8
$eNOS^{-/-}$	38	30	22	8	8
$eNOS^{-/+}$	8	8	8	0	0

Table 2.1: Summary of experimental animals numbers. In total 40 WT, 38 eNOS homozygous knockouts and 8 heterozygous knockouts were used in this study. 32 WT, 30 $eNOS^{-/-}$ and 8 $eNOS^{-/+}$ mice received SAH and were at least monitored for 15 minutes afterwards. A total of 16 wildtyps, 30 homozygous and 8 heterozygous knockouts were observed for a duration of 90 minutes after SAH. Only $eNOS^{-/-}$ and wildtype mice were imaged via two-photon-excitation microscopy. For both the naïve imaging, as well as the imaging after SAH 8 mice were operated from each group.

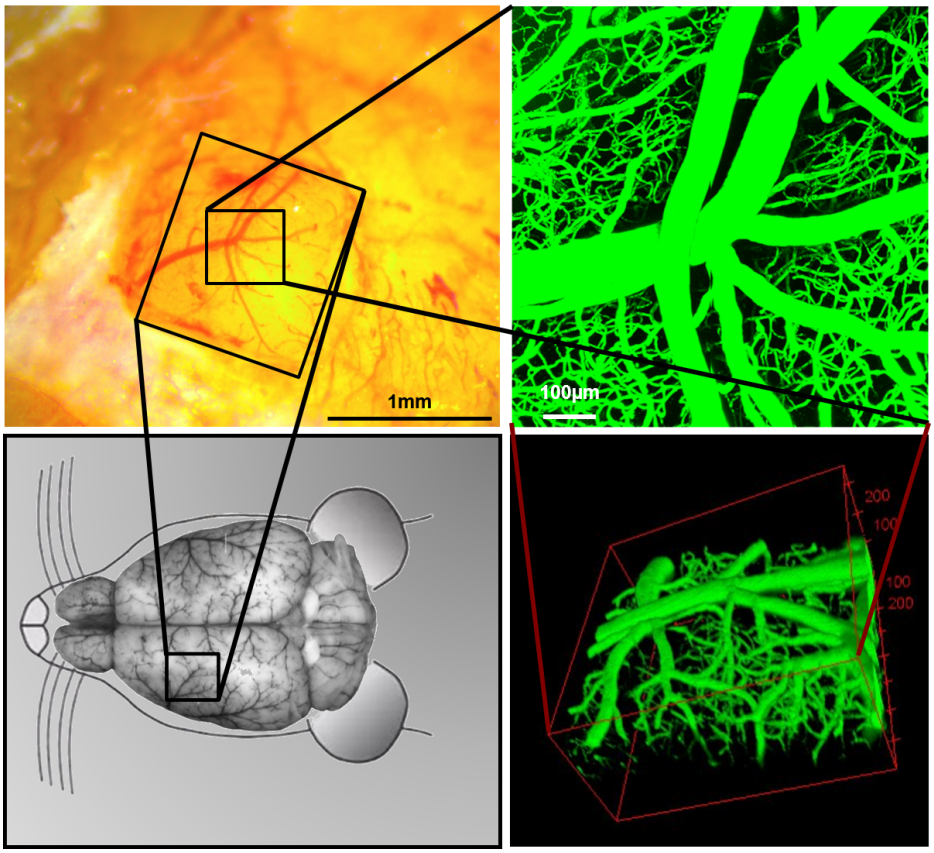

Figure 2.8: Illustration of cranial window location and two-photon-excitation-microscopy size. (a) Picture of a mouse brain. The location of the cranial window is shown over the territory of the left middle cerebral artery (MCA). (b) Picture of the open cranial window (big square). The four connected regions of interest as shown by the small square. (c) Superposition of all one hundred slices of the four regions of interest from (b) received by two-photon-excitation-microscopy. (d) Three-D model of the two-photon-excitation-microscopy slices from (c).

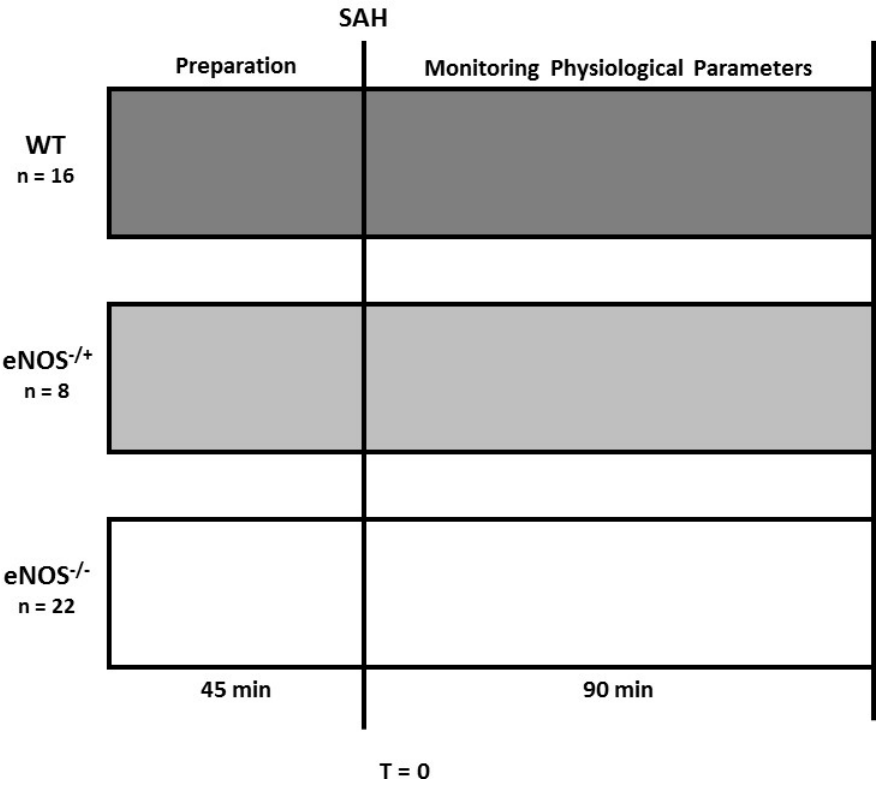

Figure 2.9: Experiment I. A total of 16 wildtype (WT) animals, 8 heterozygous ($eNOS^{-/+}$) mice and 22 homozygous ($eNOS^{-/-}$) mice received subarachnoid hemorrhage after a preparation of around 45 minutes. The physiological parameters were then monitored for a duration of 90 minutes after which the animals where perfused with paraformaldehyde and sacrificed.

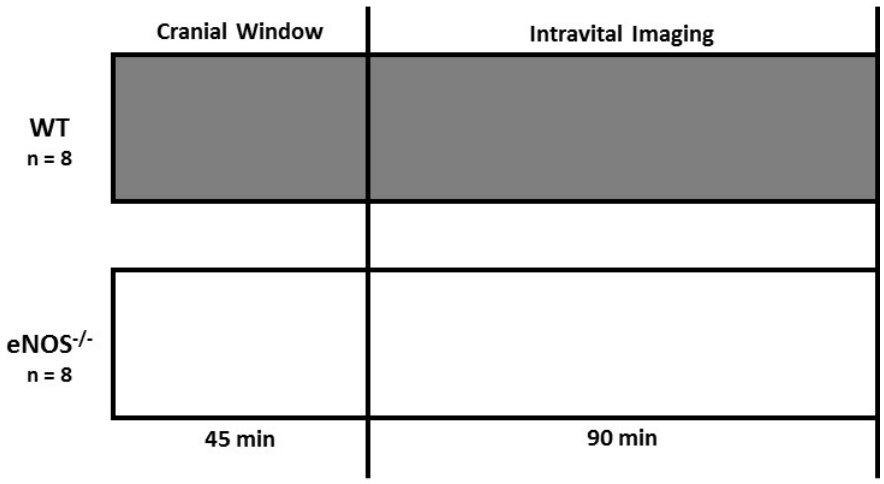

Figure 2.10: Experiment II. A total of 8 wildtype (WT) animals, 8 homozygous ($eNOS^{-/-}$) received a open cranial window with intact dura and were placed unter the two-photon-excitation-microscope. They were imaged for a duration of 90 minutes after which they were sacrificed.

extracted and placed in PFA for preservation. In a second experimental series the cerebral microcirculation was assessed: First, two-photon-excitation microscopy was performed (for 90 minutes every 10 minutes) in naïve homozygous eNOS knockout and wild type after cranial window preparation (Fig. 2.10).

Next, the microcirculatory changes in mice after SAH were assessed. Two hours after SAH induction, mice were re-anesthetized and the cerebral microcirculation imaged by in vivo microscopy (Fig. 2.11).

2.5 Analysis

Intracranial pressure and cerebral blood flow Data from Lab Chart was extracted using Lab Chart viewer 8.0, (ADInstruments Pty Ltd, New South Wales, Australia) at a frequency of 1 Hz, exported to Microsoft Excel and averaged over a period of 20 second.

2.5.1 Re-bleedings

Spontaneous rebleedings after subarachnoid hemorrhage were defined by a sharp increase of intracranial pressure of more than 10 mmHg within 10 seconds. Such an increase was automatically detected by using an Excel macro and manually crosschecked.

2.5.2 Determination of bleeding severity

After perfusion and brain extraction a high-resolution image of the skull base was obtained using a stereomicroscope (Leica M205, Zoom: 10.6 x, resolution: max. 525lp/mm; Meyer Instruments, Houston, USA). The background was extracted with GIMP (The GIMP team, GIMP 2.10.6, `https://www.gimp.org`, 1997-2019)[181]. The amount of blood was

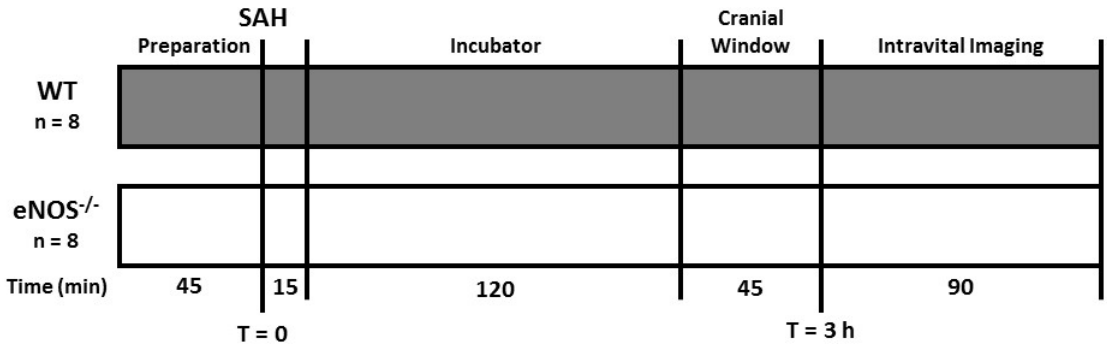

Figure 2.11: Experiment III. A total of 8 wildtype (WT) animals, 8 homozygous ($eNOS^{-/-}$) mice received subarachnoid hemorrhage after a preparation of around 45 minutes. The physiological parameters were then monitored for a duration of 15 minutes after which the animals where given drugs antagonizing the anesthesia. They were placed in an incubator for 2 hours. After that, they were put back under anesthesia and received an open cranial window with intact dura and placed under the two-photon-exciation-microscope. They were imaged for 90 minutes and afterwards they were perfused with paraformaldehyde and sacrificed.

determined by counting red pixels. The area is then expressed as percentage of the total skull base area (Fig. 2.12).

2.5.3 Analysis of two-photon-excitation microscopy

All data was analyzed using ImageJ (Wayne Rasband, National Institutes of Health, USA) [153, 160]. Microvascular constriction and the number of microvasospasms were evaluated as previously described [55, 114]. To determine average vessel diameter each vessel was carefully examined within the different slices of the three-dimensional stack and the widest diameter in all three plains located and measured. One measurement was taken at least every 50 µm along the bigger arteries and up to every 15 µm in capillaries. The shortest diameter within the spasm was then compared to a mean of the two closest non-spastic areas. The severity of the spasms (s) is given as percent constriction of vessel diameter (a) compared to non-constricted vessel segments (b,c) (Fig. 2.13).

$$s = \frac{a}{(\frac{b+c}{2})}$$

Spasms were rated as present when the vessel diameter of the spastic area was less than 85% of the diameter of non-constricted segments of the same vessel. All measurements were related to the mean vessel diameter on two baseline images taken 10 min apart.

For the determination of the totally perfused vessel volume all green pixels in each Z-stack were summed up and those above an intensity-adapted threshold were counted. The perfused volume was then calculated as the percentage of green pixels in relation to all pixels.

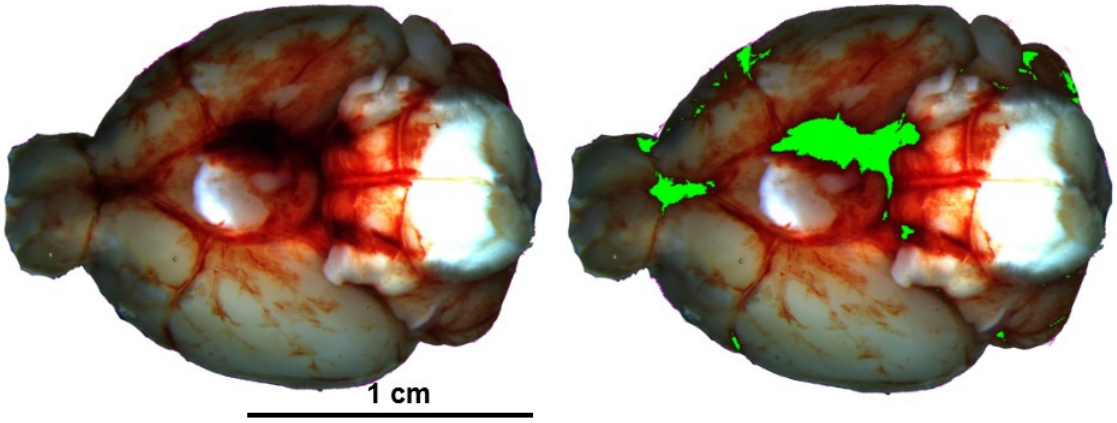

Figure 2.12: Blood clot coverage at the base of the brain. Picture of mouse brain after SAH. The area of dark blood (red colored pixels over a certain threshold) was highlighted in green. To determine the blood clot coverage at the brain base the number of green pixels was then divided by the total number of colored pixels of the brain base.

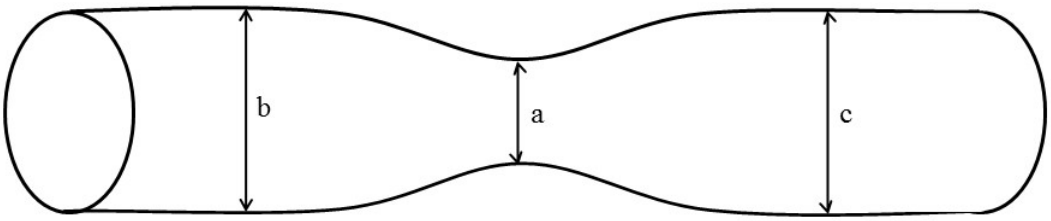

Figure 2.13: Calculation of vasospasm. A spastic area of the arterial blood vessels was calculated as the following. The diameter at the constricted part was divided by the mean of two measurements of the surrounding non-constricted areas. Constriction of spasm: $s = \frac{a}{(\frac{b+c}{2})}$. A constricted area was considered as spastic with a constriction of less then 85% of the diameter of the surrounding non-constricted area.

2.6 Perfusion and brain extraction

At the end of each experiment all mice were deeply anesthetized. Naïve animals were sacrificed by cervical dislocation whereas mice after SAH were perfused with 4% Paraformaldehyde (Morphisto GmbH, Frankfurt am Main, Germany). The brain was extracted and photographed in order to prove SAH.

2.7 Statistical analysis

All calculations were done using a standard statistical software package (SigmaStat 3.0, Jandel Scientific, Erkrath, Germany). Data is presented as mean ± standard deviation if not stated otherwise. Comparisons between groups were performed using the Mann-Whitney Rank Sum Test. Three groups were compared with Kruskall-Wallis ANOVA on ranks test. In cases in which a statistically significant difference was detected between groups, Dunnet analysis was performed post-hoc. Statistical difference was assumed at $p<0.05$.

3 Results

3.1 Standardization

After surgical training, the MCA perforation model was performed in nine mice to validate the model. SAH resulted in a sharp increase in intracranial pressure to 78.8 ± 21.0 mmHg, followed by a rapid decrease plateauing around 22 ± 6 mmHg after few minutes (Fig. 3.1). At the same time, cerebral blood flow quickly dropped to around 39.2 ± 23.3% of baseline values. It recovered within 5 minutes and then very slowly started decreasing again (Fig. 3.2). Mortality in this series was 22% after 24 hours. The results of the standardization series are comparable to previous series in our laboratory [44].

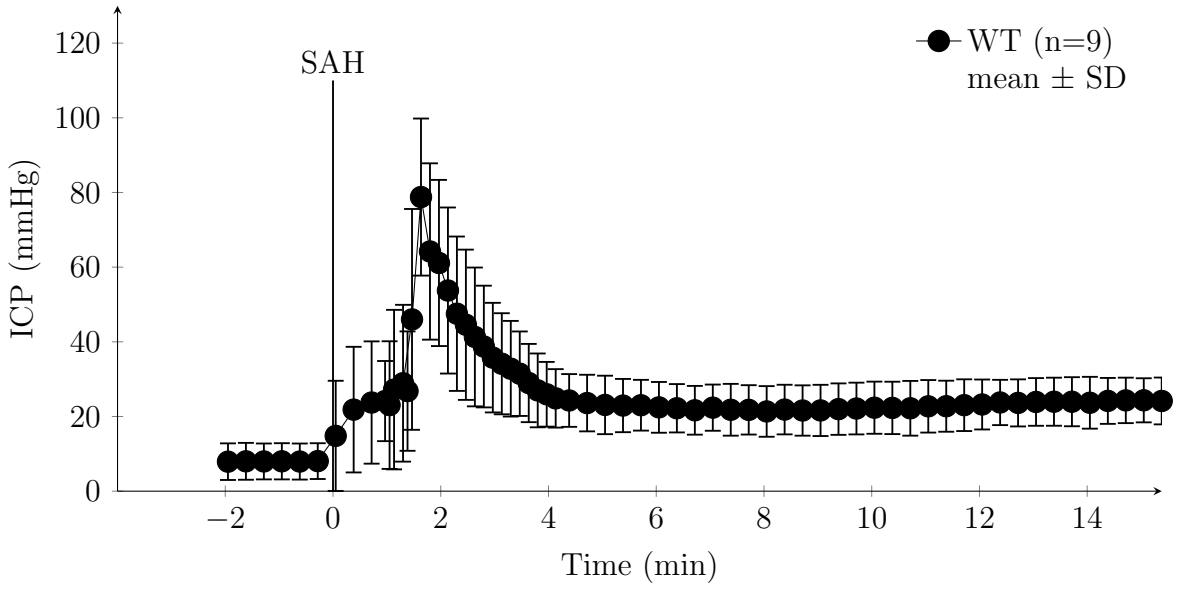

Figure 3.1: Standardization Intracranial pressure in wildtype animals. Nine mice received SAH by perforation at the level of the circle of Willis. The intracranial pressure is very low before protrusion of the filament. It is not zero as the ICP probe is inserted under the skull and leads to slightly elevated pressure. At protrusion of the filament (time=0) the ICP increases rapidly to 78.8 ± 21.0 mmHg. It drops within a few minutes and saturates at a level of around 22 ± 6 mmHg. The values are shown in mean plus minus standarddeviation.

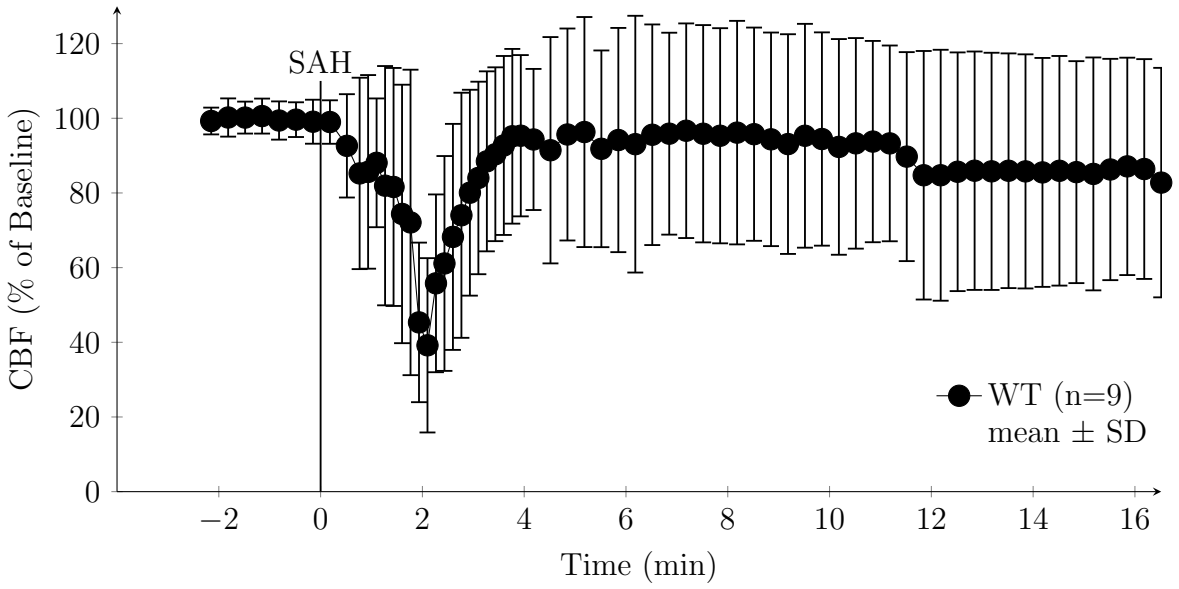

Figure 3.2: Cerebral blood flow standardization in wildtype animals. As the subarachnoid bleeding is induced by protrusion of the filament the cerebral blood flow sharply decreases to 39.2 ± 23.3% of its initial values. Within a few minutes it recovers to baseline and from there slowly decreases over time. Values are shown in percent of initial value.

3.2 Results in eNOS deficient mice

3.2.1 Intracranial pressure and cerebral blood flow

After induction of SAH, wild type mice showed a sharp increase in intracranial pressure to 55.4 ± 11.7 mmHg followed by a recovery to 22 ± 4 mmHg within a few minutes. Only homozygous animals display a significantly higher increase in ICP ($p<0.001$ vs. wild type) to 88.2 ± 25.7 mmHg. In heterozygous mice there was no significant difference to either of the two other groups as they displayed a mean of 84.7 ± 28.1 mmHg (Fig. 3.3). In $eNOS^{-/-}$ mice, values then decrease to 30-40 ± 10-20 mmHg, significantly higher as compared to wild type mice ($p<0.008$ vs. wild type). Heterozygous mice reached levels of 25.9 ± 7.6 mmHg 10 minutes after SAH.

As shown above, CBF dropped quickly to 42.5 ± 26.9% of pre-hemorrhage baseline followed by a fast recovery in wild type mice (Fig. 3.4). CBF later dropped continuously to 88.4 ± 13.7% in wild type mice at 13 minutes after SAH. In eNOS transgenic animals CBF dropped to lower levels than in wild type mice. ($p<0.001$ vs.) The effect was more pronounced in homozygous (20.3 ± 9.0%) than in heterozygous animals (21.8 ± 7.4%). The drop in CBF in $eNOS^{-/-}$ mice was significantly lower than in wild type mice ($p=0.001$ vs WT). No statistical difference was found between heterozygous mice and either of the two other groups. In homozygous knockout animals the continuous drop after fast recovery in CBF attained lower levels than in wild type animals. At 13 minutes after SAH it reached 74.4 ± 51.5% in homozygous and 86.2 ± 17.0% in heterozygous animals.

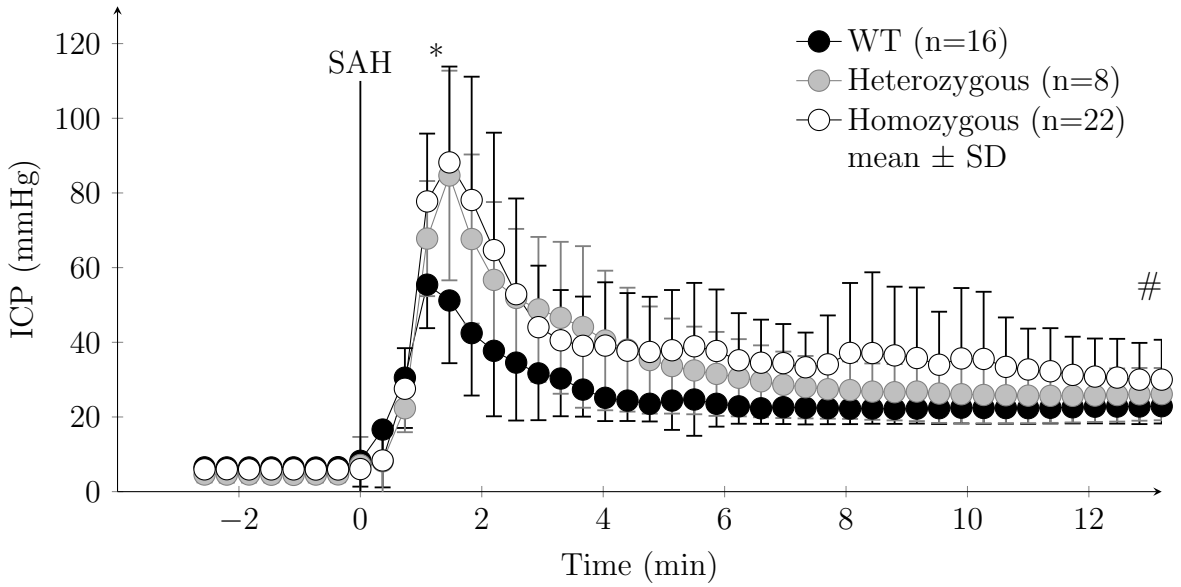

Figure 3.3: Intracranial pressure after subarachnoid hemorrhage in WT, eNOS$^{-/+}$ and eNOS$^{-/-}$. The intracranial pressure is very low before protrusion of the filament. It is not zero as the ICP probe is inserted under the skull and leads to slightly elevated pressure. At protrusion of the filament (time=0) the ICP increases within seconds to levels of around 55.4 ± 11.7 mmHg for the wildtype mice, and 88.2 ± 25.7 mmHg for the eNOS deficient mice. In the wildtype group, it drops within few minutes and saturates at a level of around 22 ± 4 mmHg. The eNOS KO mice need more time to recover the intracranial pressure and it stays at significantly higher levels compared to the wildtype group ($p<0.001$ vs WT control). The irregular line of ICP after SAH in the eNOS depleted mice is due to multiple rebleeding with again increases in ICP in many animals. The ICP 12 minutes after SAH is still significantely elevated in the eNOS knockout mice compared to the wildtype controls ($p<0.008$ vs WT control). The heterozygous animals position themselves between the homozygous knockouts and the wildtype animals. The values are shown in mean plus minus standard deviation.

3.2.2 Hematoma area (Fig. 3.5)

In wild type animals, the blood clot covered 3.1 ± 1.8% of the caudal brain surface. In homozygous eNOS knockout animals, the size of the clot was significantly larger 7.1 ± 2.6% ($p=0.001$ vs WT control).

3.2.3 Mean arterial blood pressure

Mean arterial blood pressure was within physiological limits in all groups and did not change significantly over time (Fig. 3.6); there was no difference between groups, but homozygous knockout animals presented with a slightly higher blood pressure. Directly after SAH, a small increase was observed in all animals as a reaction to the ICP increase (Cushing reflex).

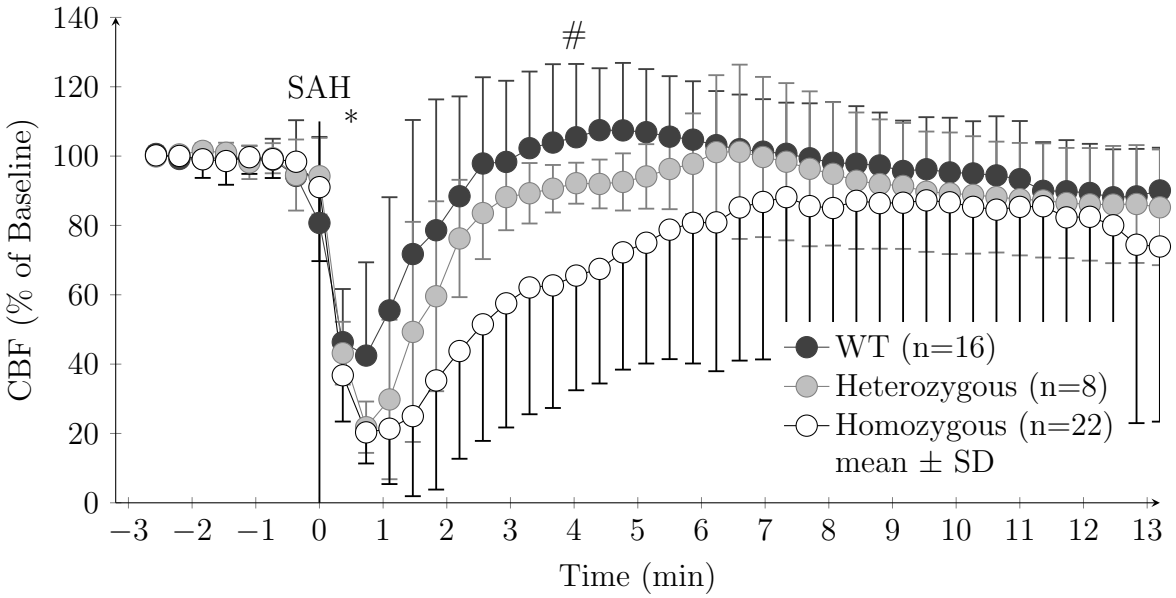

Figure 3.4: Cerebral blood flow after subarachnoid hemorrhage in WT, eNOS$^{-/+}$ and eNOS$^{-/-}$. At onset of SAH the cerebral blood flow sharply decreases in all three groups. In wildtype animals it reaches 42.5 ± 26.9% of initial values, whereas the homozygous knockout animals reach a significantly lower level of 20.3 ± 9.0% of initial values ($p<0.001$ vs WT control). The homozygous eNOS deficient animals need more time (around 3 more minutes) to recover cerebral blood flow. During this time they stay at a significantly lower level of CBF ($p<0.007$ va WT control). They do not reach baseline and the CBF decreases faster than in the wildtype animals. Heterozygous mice show values between those of wildtype and homozygous mice and show no significant difference to either of the other two groups. All values are shown in mean plus minus standard deviation.

3.2.4 Re-Bleedings

Wild type animals infrequently experienced re-bleedings after experimental SAH. Re-bleedings resulted in increases of ICP with concomitant drops in CBF that occurred after the initial event (Fig. 3.7). In this study, homozygous eNOS deficient mice had a significantly higher number (3.1 ± 2.4 per animal) of re-bleedings that their WT control mice (1.1 ±1.3 per animal; p=0.004 vs WT) (Fig. 3.8 & Tab. 3.1). Only half of the wild type animals, but 62.5% of the heterozygous and 91% of the homozygous eNOS transgenic mice experienced one or more spontaneous re-bleedings. Thirteen percent of wild type and heterozygous animals showed more than two supplementary hemorrhages after SAH; this rate increased to 23% in homozygous mice. One eighth of the wild type, none of the eNOS$^{-/+}$ and 18% of the eNOS$^{-/-}$ mice bled three times. Finally, in the wild type animals only 6.25% showed at least four spontaneous rebleedings within the first 90 minutes after SAH, whereas this number was doubled in the heterozygous (12.5%) and increased up to 32% in the homozygous eNOS transgenic mice.

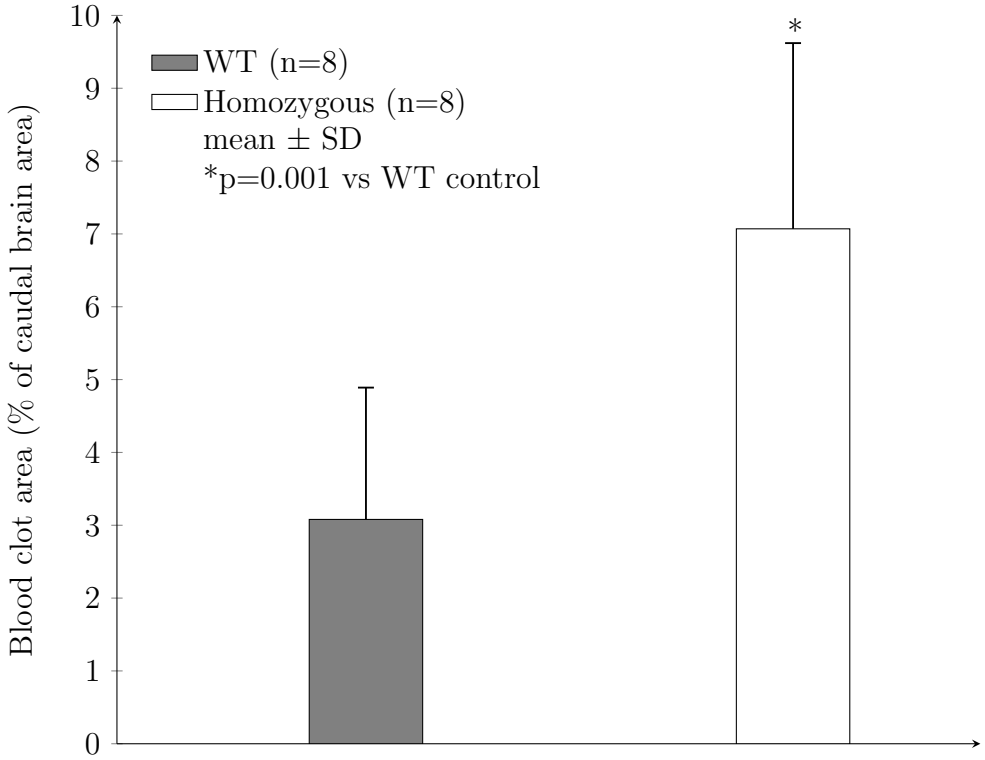

Figure 3.5: Blood clot coverage at the brain base. The area of the brain base that is covered by the blood clot is compared between wildtype animals and homozygous knockout animals. Where the wildtype mice show a coverage of a mean of 3.1 ± 1.8% of the brain base area, the knockouts show a significantly higher coverage of 7.1 ± 2.6% ($p<0.001$ vs WT control). The values are shown in mean plus minus standard deviation.

3.2.5 Mortality

Mortality within the first 3 hours after SAH varied significantly between genotypes (Fig. 3.9). While no wild type animal died within the first 3 hours after SAH, 2 out of 8 (25%) of the heterozygous and 12 out of 25 (48%) of the homozygous knockout animals did not survive.

3.2.6 Bleeding time

In order to look for a cause of the increased hematoma area and the high mortality in eNOS transgenic mice, we assessed primary homeostasis by testing the tail bleeding time (Fig. 3.10). While in control animals bleeding stopped after 1.3 ± 0.2 minutes, bleeding time in eNOS knockouts was significantly prolonged to 3.4 ± 2.9 minutes ($p=0.006$ vs WT control).

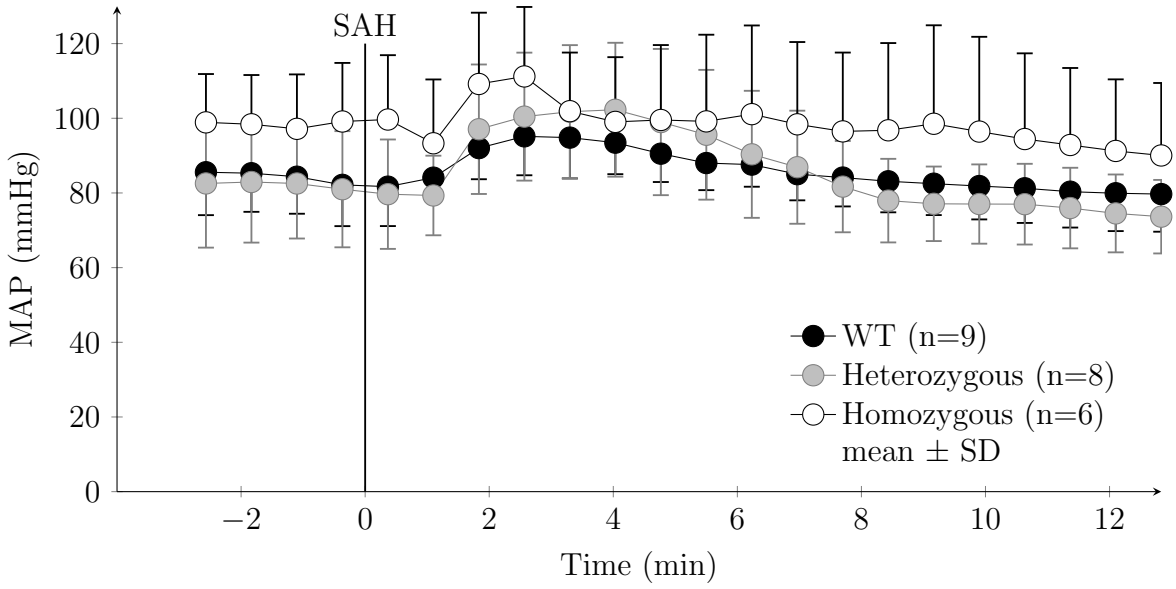

Figure 3.6: Medial arterial blood pressure (MAP) in all three groups. All three groups were continuously monitored. The eNOS$^{-/-}$ show a slightly higher MAP than die wildtype mice (85.5 ± 11.5 mmHg compared to 98.9 ± 13.0 mmHg). But as there is a high standard deviation there is no statistical significant difference between the groups. An onset of SAH the blood pressure drops in all three groups. It then increases above baseline values due to the Cushing reflex. The Cushing reflex is a reflex to increase blood pressure when intracranial pressure increases to maintain cerebral perfusion. The values then reach initial values where they stay. The values are shown in mean plus minus standard deviation.

3.3 Microcirculatory changes

3.3.1 Microcirculation

After cranial window preparation, SAH-induced changes (perivascular blood) were found to be more pronounced in eNOS transgenic animals (Fig. 3.11). eNOS deficient mice displayed a difference in vessel density already before SAH; after the hemorrhage, the changes (reduced vessel density, constrictions) were even more pronounced (Fig. 3.12. In homozygous knockouts, the microcirculation appeared less well structured as in healthy wild type animals. The arteries seemed thinner and vastly interconnected, but showed less branching. After subarachnoid hemorrhage the perfusion of capillaries in the parenchyma appeared impaired in wild type mice. The artery looked constricted compared to the naïve wild type animals. In eNOS deficient animals, the microcirculation was even more severely impaired; a large number of arteries was constricted and the entire capillary bed was not perfused.

When quantified (Fig. 3.13), the perfused vascular volume in naïve mice was significantly smaller (p=0.009 vs WT control) in eNOS homozygous animals at 34 ± 3% of entire imaged area compared to wild type animals at 38 ± 4% of imaged area. After SAH the difference became even more pronounced (p=0.001 vs WT control) with a perfused vascular volume of 35 ± 1% of entire area in WT mice and 30 ± 3% of imaged area in eNOS knockout animals. In eNOS$^{-/-}$ mice perfused vessel volume was not only smaller than in WT SAH

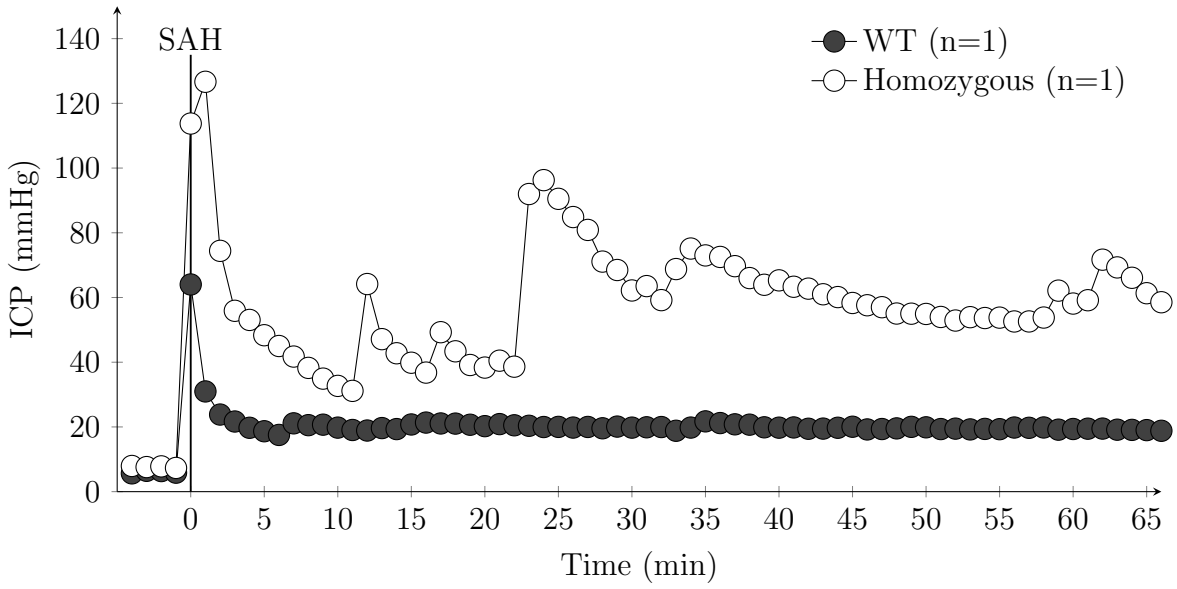

Figure 3.7: Exemplary ICP traces for one WT and one eNOS$^{-/-}$ mouse.

animals but also significantly reduced compared to healthy eNOS$^{-/-}$ mice (p=0.02 vs naïve eNOS$^{-/-}$). One healthy wild type mouse needed to be excluded from this analysis as it showed a very big vein within the imaged area not comparable to the other mice. Another mouse had to be excluded due to technical issues with cranial window preparation.

3.3.2 Microvasospasms

A total of 355 arterial vessel segments with a total length of approximately 62 000 µm were analyzed (90 vessel segments in healthy wild type animals, 85 in wild type animals after SAH, 89 in naïve eNOS$^{-/-}$ mice, and 91 in eNOS$^{-/-}$ mice after SAH). In naïve wild type animals, 0.3 ± 0.2 spasms per vessel segment were detected (Fig. 3.14); 3 hours after SAH, this number significantly increased to 1.0 ± 0.6 spasms per vessel segment (p=0.006 vs naïve WT). eNOS$^{-/-}$ animals showed significantly higher numbers of spasms before SAH (0.9 ± 0.3, p=0.005 vs WT control) and a tendency of increased number of spasms after SAH (1.4 ± 0.4, n.s.). Of note, the incidence of microvasospasms in naïve eNOS transgenic mice was almost as high as in wild type animals after SAH. The same pattern was found for the total number of spasms per animal (Fig. 3.15). Spasms were predominantly located in smaller vessels with a diameter of 20–30 µm (Fig. 3.16 and 3.17). In wild type mice subjected to SAH 87.5% of spasms were located in vessels smaller than 30 µm, while in eNOS deficient mice this rate was 94.7%.

3.4 Summary of results

The present results show that SAH induces a significantly more severe phenotype in eNOS deficient mice than in wild type controls. SAH is more severe since clot size is larger in knockout mice and ICP increases and CBF decreases are more pronounced. Furthermore,

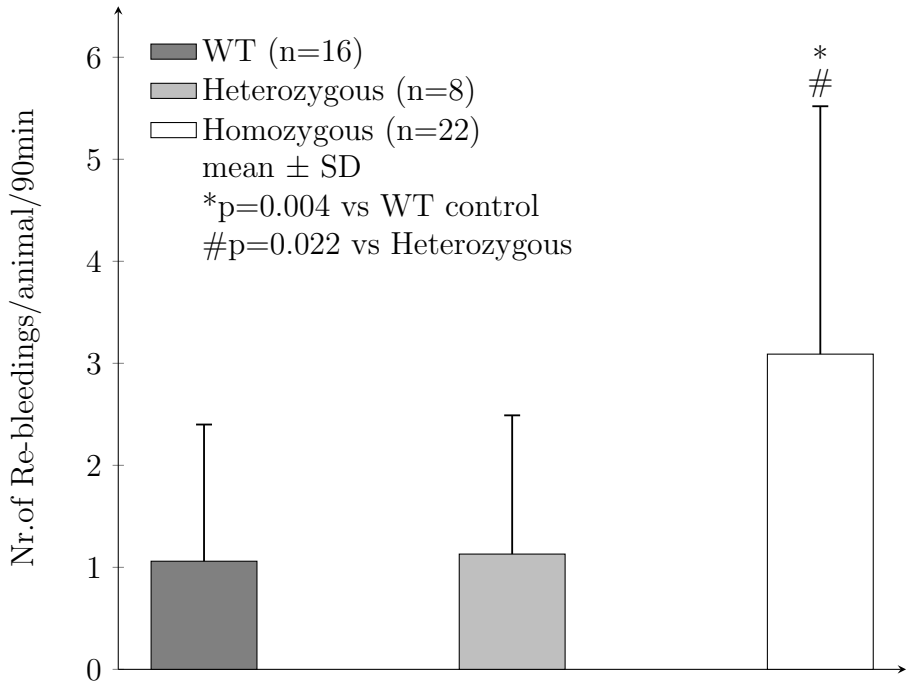

Figure 3.8: Number of rebleedings per animal in the first 90 minutes after subarachnoid hemorrhage.

NOS KO animals experience significantly more re-bleedings. Subsequently, mortality is significantly higher in eNOS$^{-/-}$ animals. Regarding the cerebral microcirculation, post-hemorrhagic dysfunction is more pronounced in eNOS transgenic animals, since these animals had significantly less perfused vessel volume indicating a reduction of microcirculatory perfusion and a higher number of microvasospasms (Fig. 3.18).

% of WT (n=16)	% of eNOS$^{-/+}$ (n=8)	% of eNOS$^{-/-}$ (n=8)	Nr. of rebleedings
50	62.5	91	≥1
31	25	73	>1
12.5	12.5	23	2
12.5	0	18	3
6.25	12.5	32	≥4

Table 3.1: Exact number of rebleedings in WT, eNOS$^{-/+}$and eNOS$^{-/-}$ animals within the first 90 minutes of subarachnoid hemorrhage. Number of rebleedings in all three experimental groups shown in % of mice suffering from a certain number of rebleedings.

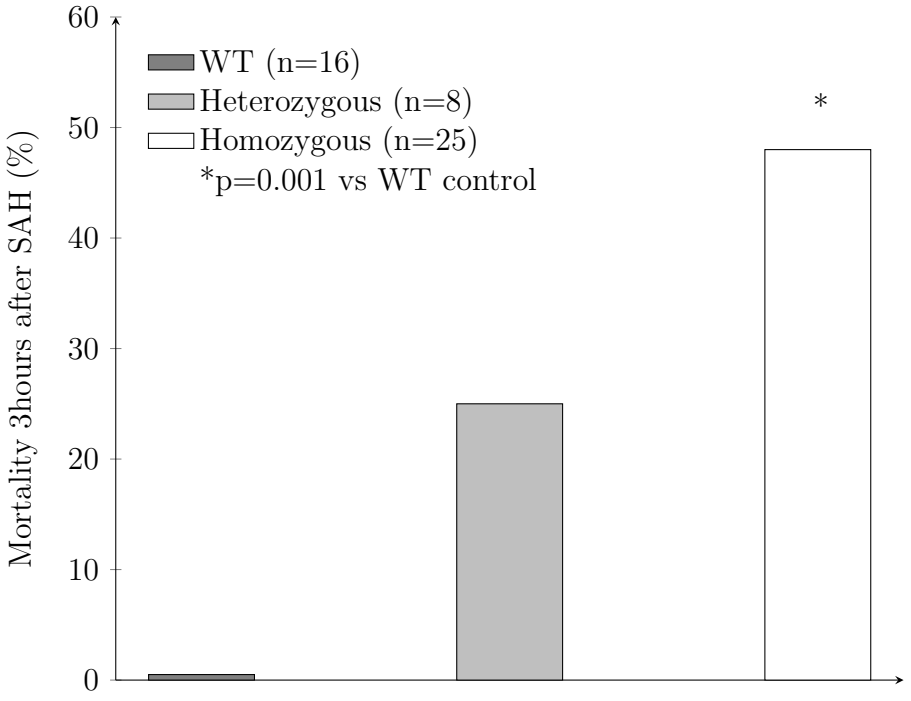

Figure 3.9: Mortality within the first 3 hours after subarachnoid hemorrhage in all three groups. The mortality within the first 3 hours after SAH. Mortality was 0% in the wildtype mice, 25% in the heterozygous and 48% in the homozygous mice. eNOS$^{-/-}$ animals show a significantly higher mortality than wild type mice (p=0.001 vs WT control).

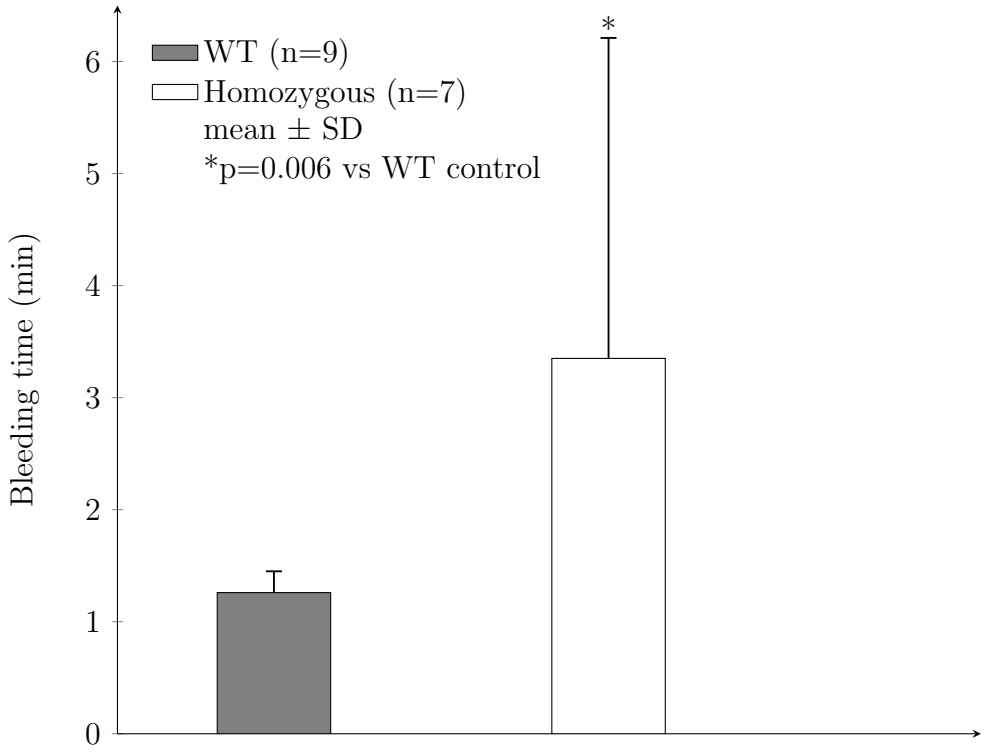

Figure 3.10: Arterial and venous bleeding time in Wildtype and eNOS$^{-/-}$ animals. Time until bleeding stop was measured in minutes after amputation of the distal 1 mm of the mouse tail. In wildtype animals bleeding stops after 1.3 ± 0.2 minutes. In eNOS deficient mice the bleeding stopped after a significantly longer time of a mean of 3.4 ± 2.9 minutes (p=0.006 vs WT control). Some mice bled for more then 6 minutes. The values are shown in mean plus minus standard deviation.

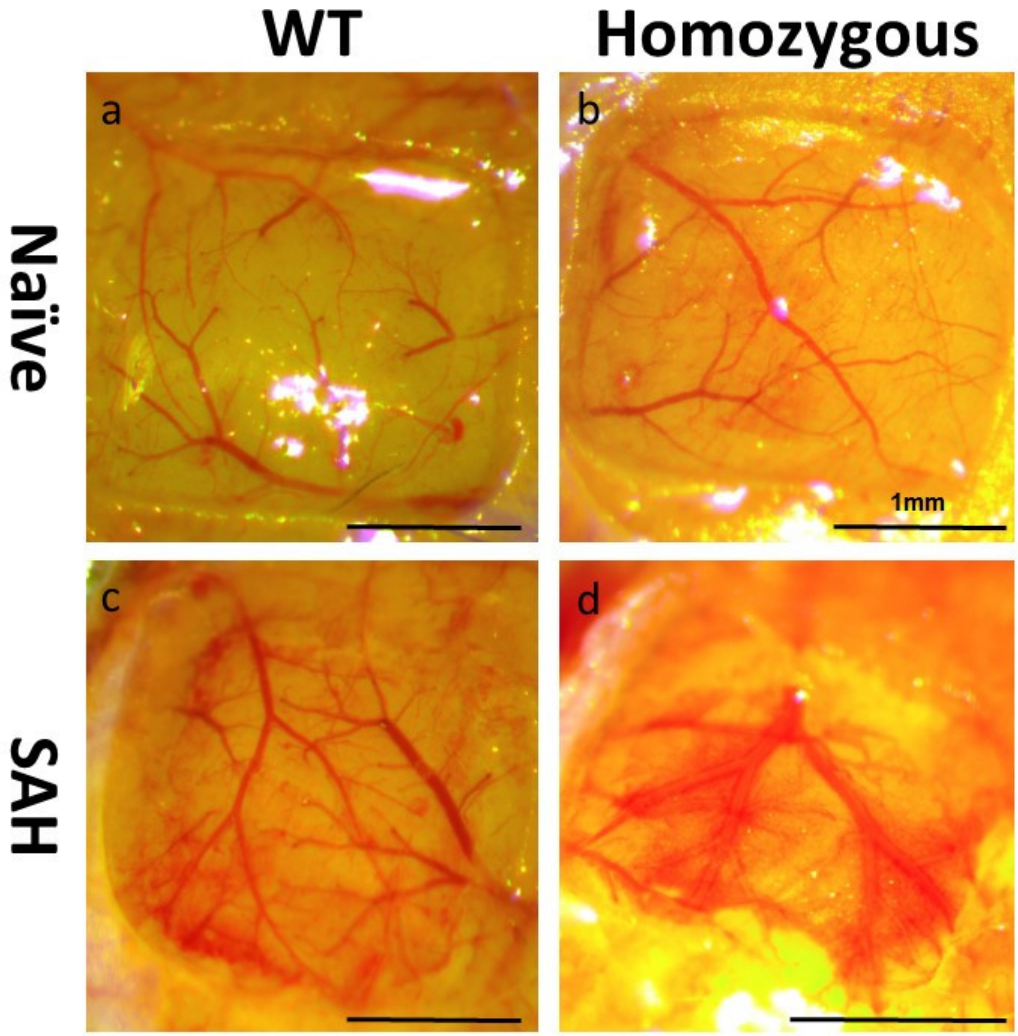

Figure 3.11: Cranial window comparison between wildtype and eNOS$^{-/-}$ mice. (a) Display of a cranial window in healthy wildtype animals. The window is clear and vessels are nicely visible. No blood is seen around the arteries. (b) Depiction of a cranial window in homozygous knockout. They presente with more difficulties during craniotomy. Tiny bleedings from vessels between dura and skull occur more frequently. (c) Presentation of a cranial window after SAH in wildtype mice. The blood around the vessels can clearly be seen. There is more small hemorrhage from dural vessels. (d) Illustration of a cranial window after SAH in eNOS deficient animals. They are difficult to image. Those few who survive the first 3 hours after subarachnoid bleed, show significant amounts of blood around the vessels and large amount of hemorrhage in the parenchyma. The small bleedings from severed vessels during separation of skull and dura occurred the most frequently of all four groups.

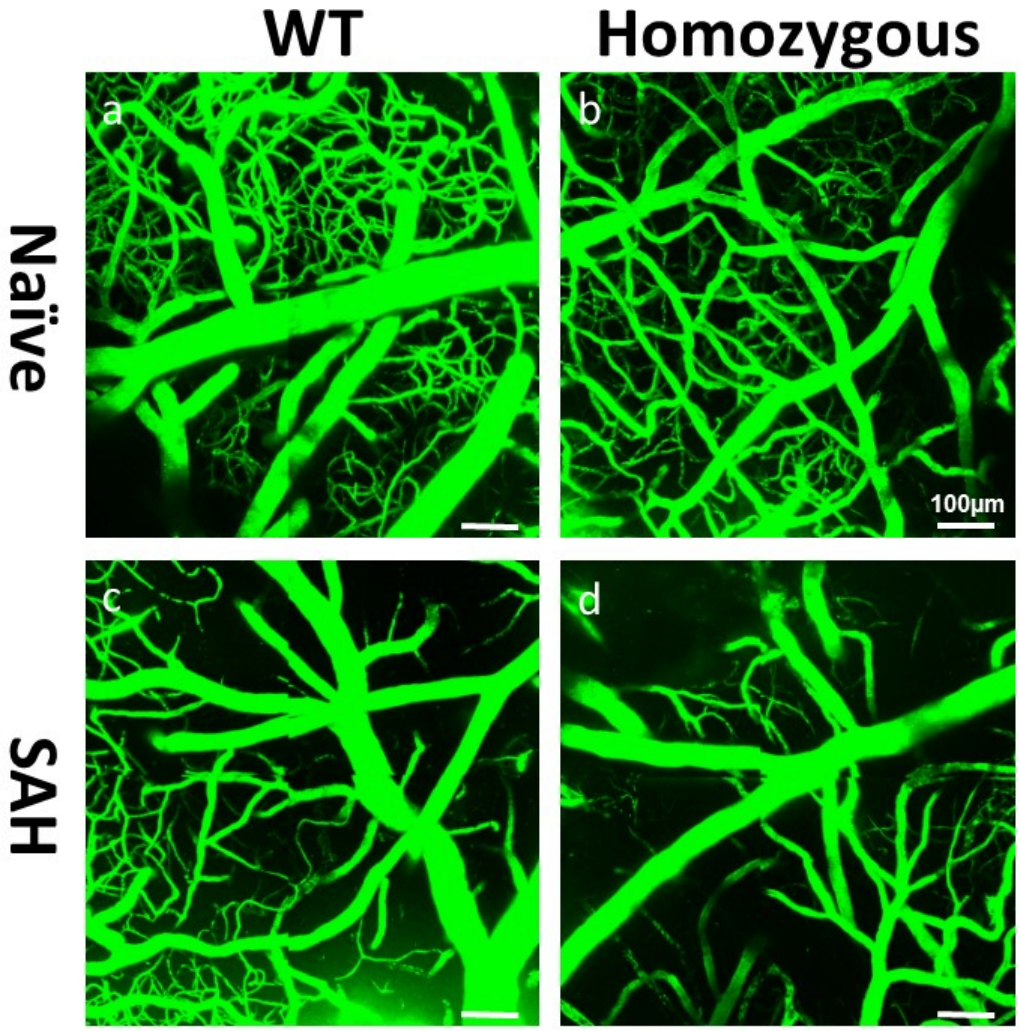

Figure 3.12: Comparison of maximum-intensity stack superposition of four regions of interest in wildtype and eNOS knockout animal without and after SAH. (a) Display of imaging of 4 regions of interest in healthy wildtype animals. There is one big artery, dividing into smaller arteries and arterioles. The microcirculation of the capillary level is highly perfused and interconnected. Vessel diameter ranges from big to very small and all in between. (b) Depiction of imaging of 4 regions of interest in homozygous knockout. The microcirculation seems to be not as well structured as in the healthy wildtype animals. The arteries are thin and there is not the same level of diameter increase at the bifurcations as in the wildtype mice. Arterioles are vastly interconnected but show less branching and the capillary level is to as distinct as in the wildtype. There are pearl-string-like spasms along the vessels. (c) Presentation of imaging of 4 regions of interest after SAH in wildtype mice. The perfusion of the capillaries in the parenchyma seems impaired. The artery looks constricted compared to the naïve wildtype and also compared to the big vein, that is coming into the image from the right lower corner. There are vasospasms visible in the small blood vessels. (d) Illustration of imaging of 4 regions of interest after SAH in eNOS deficient animals. Homozygous knockout animals after SAH present a strongly impaired microcirculation. Here arteries are constricted and have pear-string-like micro vasospasms. The entire capillary level is not visibly perfused. There is an active bleeding in the top left corner, which casts a shadow over this area.

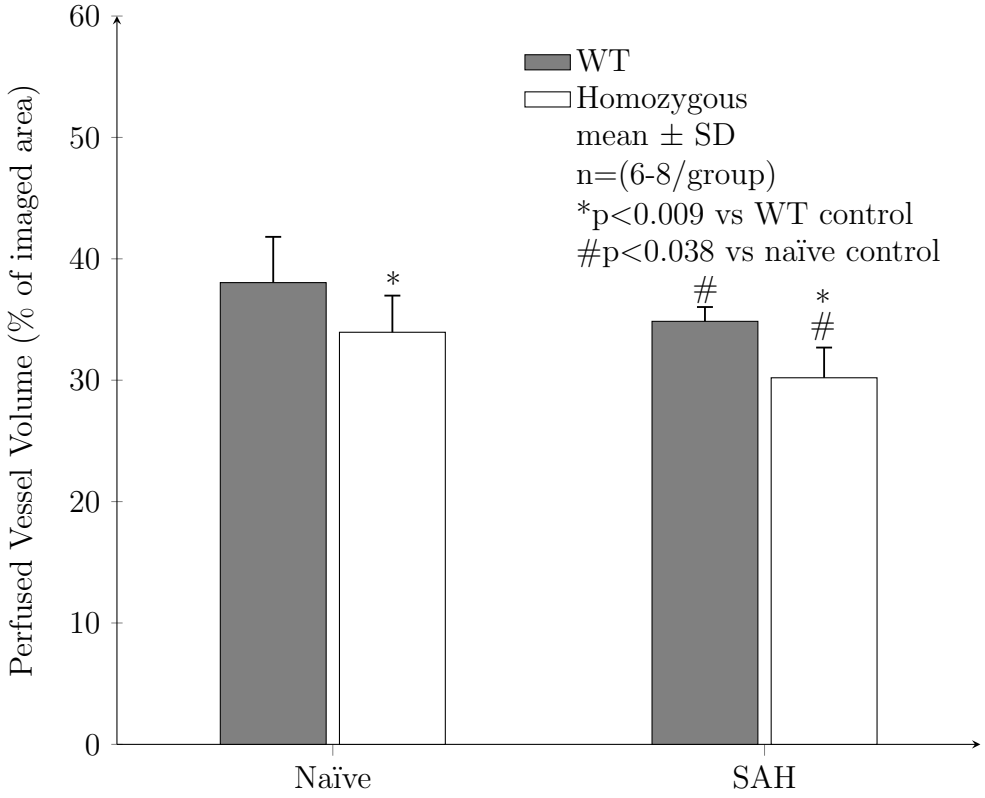

Figure 3.13: Perfused vessel volume in WT and eNOS$^{-/-}$ animals. Display of perfused vessel volume in the four regions of interest. The number of fluorescent pixels in the three-D-reconstructed image from the two-photon-excitation-microscopy was counted and then divided by the total number of pixels in the area. This led to a representation of the perfused vessel volume in percent of all pixels in the image. In naïve wildtype animals the perfused volume takes 38 ± 4% of the area. eNOS$^{-/-}$ mice present significantly less perfused vessel volume of 34 ± 3% (p<0.009 vs WT control). On the right side of the graph, there is a depiction of perfused vessel volume in both mouse lines after subarachnoid hemorrhage. Compared to healthy wildtype animals the wildtype animal after SAH show a reduced percentage of perfused vessel volume of 35 ± 1% (p<0.038 vs naïve control). The lest perfused vessel volume depicted the eNOS$^{-/-}$ knockouts. They showed a perfused vessel volume of 30 ± 3% of the entire image. This was significantly reduced compared to both the wildtype animals after SAH and the naïve eNOS deficient mice (p<009 vs WT control and p<0.038 vs naïve control).

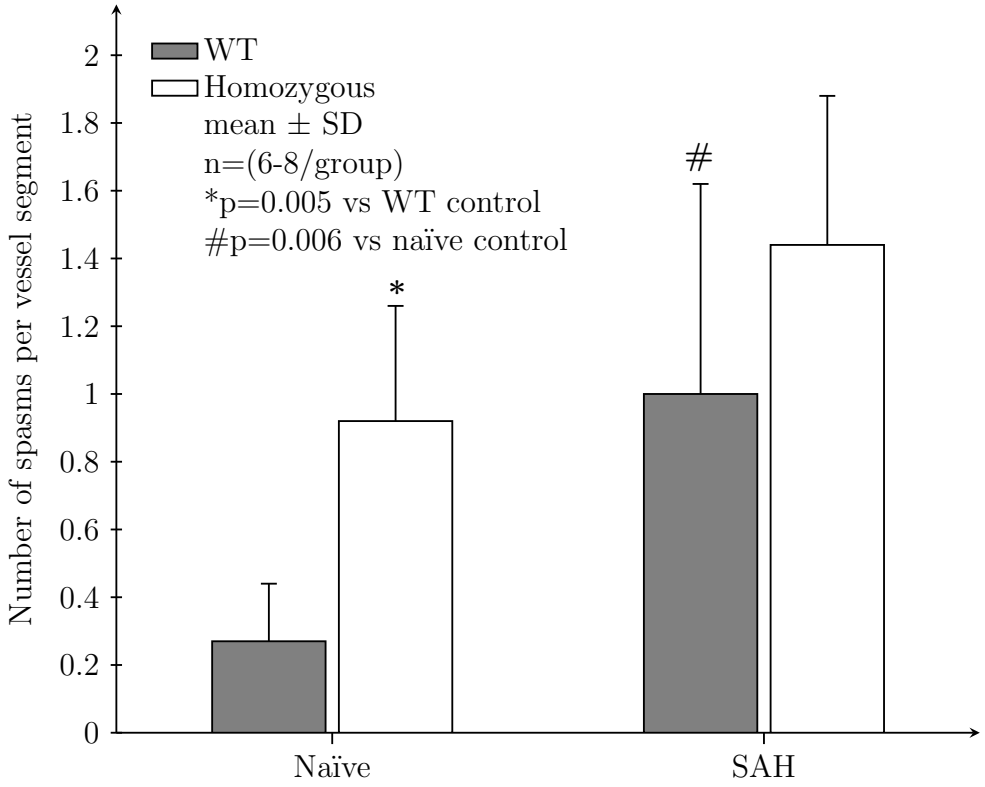

Figure 3.14: Numbers of spasms per vessel segment in WT and eNOS$^{-/-}$ animals. Healthy wildtype animals had a mean of 0.3 ± 0.2 spasms per vessel segment. Compared to in wildtype animals, in eNOS$^{-/-}$ the number of spasms was significantly elevated (p=0.005 vs WT control) to a mean of 0.9 ± 0.3 spasms per vessel segment, very comparable to wildtype animals after SAH, whom present with a mean of 1.0 ± 0.6 spasms per vessel segment. This number is again significantly increased compared to the naïve control, which present with 0.3 ± 0.2 spasms per mouse (p=0.006 vs naïve control). Not surprisingly, eNOS knockout mice after SAH show the most vasospasms. They obtain a mean of 1.4 spasms per vessel segment.

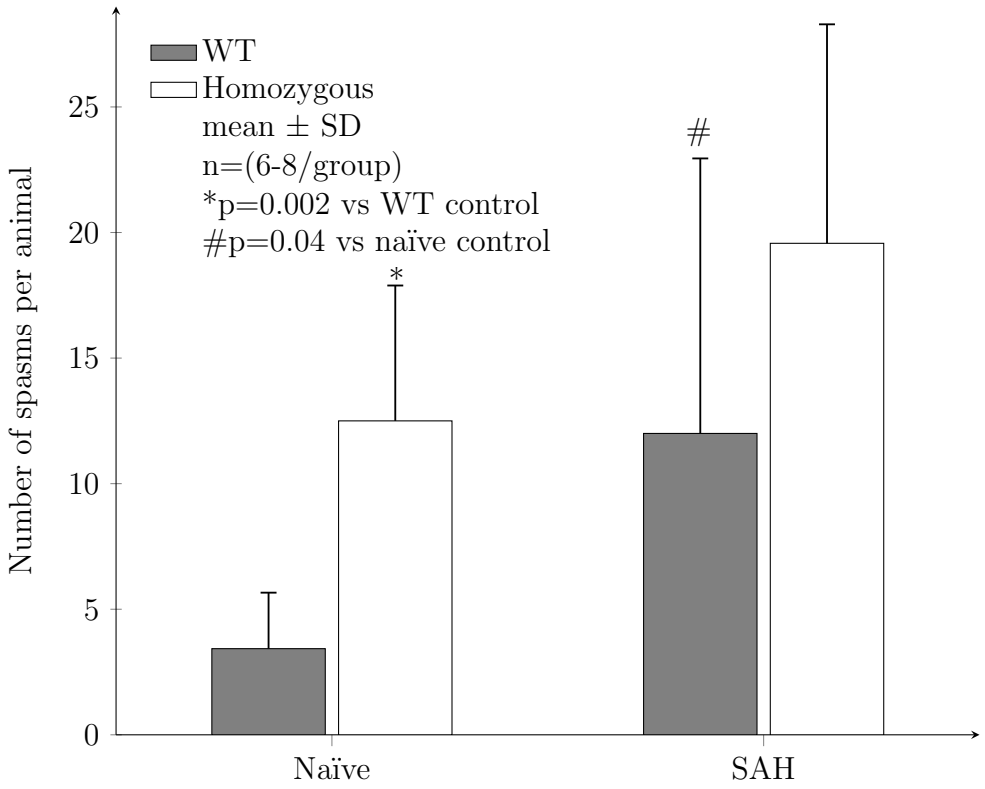

Figure 3.15: Numbers of spasms per animal in WT and eNOS$^{-/-}$ animals. Display of the number of spasms per animal. The number of spasms in eNOS$^{-/-}$ was significantly elevated compared to wildtype animals (p=0.002 vs WT control) to a mean of 12.5 ± 5.4. Again, approximately as many as Wildtype animals after SAH, whom display a mean of 12.0 ± 11.0 spasms per animal. Compared to the naïve control the number of microvasospasms is again significantly higher(p=0.04 vs naïve control). eNOS knockout mice after SAH present the most vasospasms. They obtain a mean of 19.6 ± 8.7 spasms per animal.

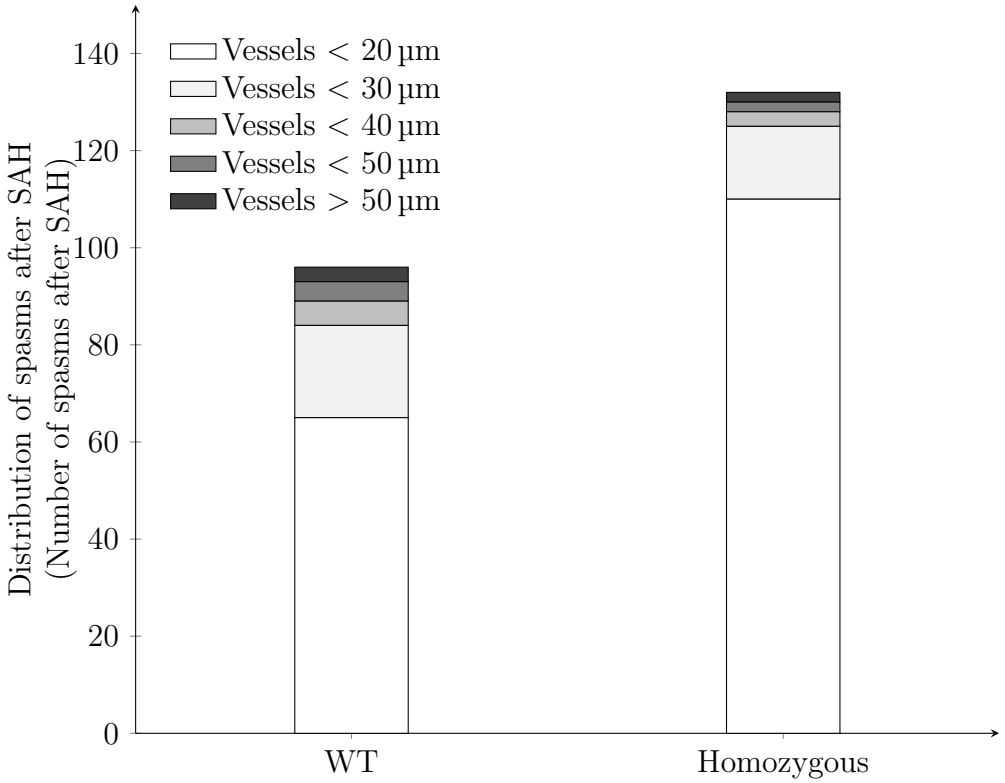

Figure 3.16: Distribution of spasms after subarachnoid hemorrhage in WT and eNOS$^{-/-}$ mice. In all wildtype animals after SAH I found a total of around 100 spasms, of which 65 were in vessels smaller than 20 µm and another 19 in the category between 20 µm and 30 µm of diameter. In the group of eNOS$^{-/-}$ mice after SAH I counted a total of 132 spasms. 125 were located in vessels smaller than 30 µm.

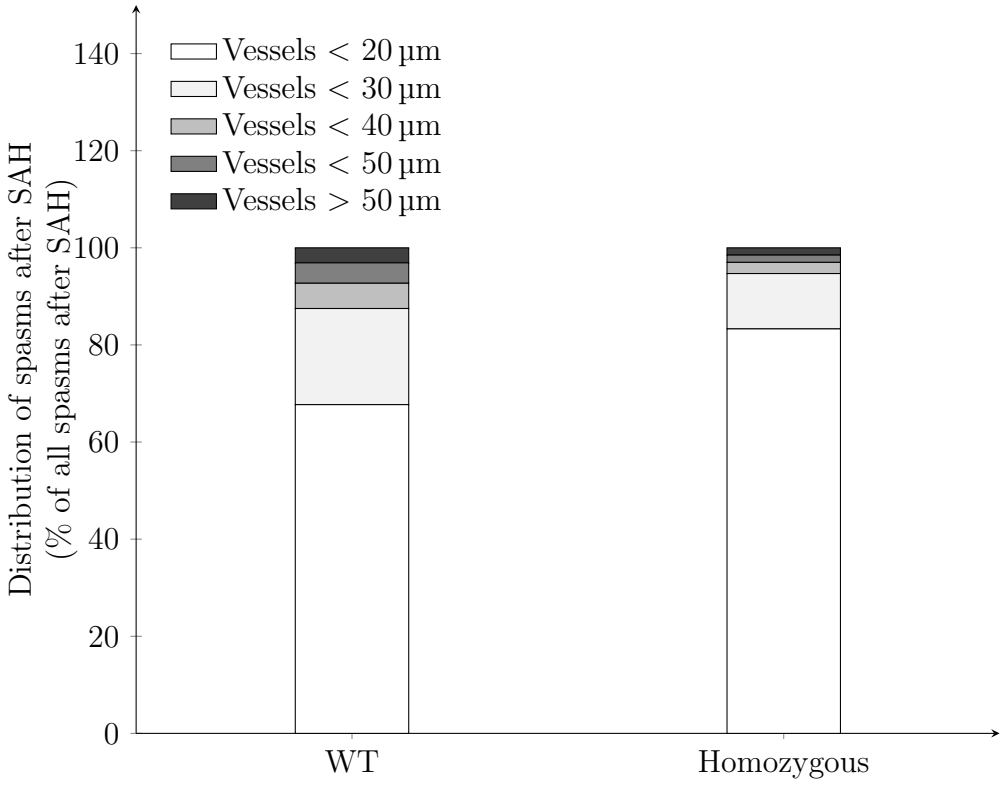

Figure 3.17: Percental distribution of spasms after subarachnoid hemorrhage in WT and eNOS$^{-/-}$ mice. Most of the spams were located in the smallest vessels. In the wildtype animals 78.5% of spasms showed in arterioles smaller than 30% in the wildtype animals and in the knockouts almost 94.7% presented in this vessel category.

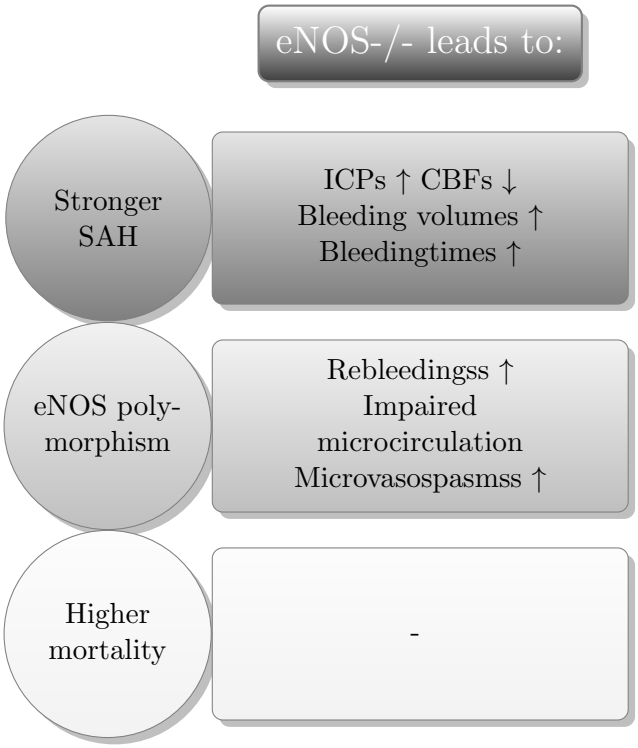

Figure 3.18: Summary of results. eNOS deficient mice had a stronger subarachnoid bleeding, indicated by higher intracranial pressure, lower cerebral blood flow, increased bleeding volume and longer bleeding time. They presented more complications, which were an elevated number of rebleedings, an impaired microcirculation and an elevated number of micro vasospasms. Hence, they had a higher mortality.

4 Discussion

4.1 Model

Due to the unpredictable nature of aneurysm ruptures in SAH [188], the analyzable information retained from patients only begins once they are admitted to the hospital and monitored. Therefore, the observations are already delayed unless spontaneous re-bleeding occurs under monitoring. However, recurrent hemorrhage does not accurately represent the initial bleed, as there are certainly effects of lingering blood from the initial impact. In order to investigate ultra-early as well as complex pathophysiological changes, e.g. after subarachnoid hemorrhage, animal models are indispensable. Thanks to genetically modified animals in vivo experiments allow detailed insights into causal relationships between molecular pathways and functional as well as histopathological outcome. In order to deliver clinically relevant information an animal model for subarachnoid hemorrhage needs to fulfill the following criteria: It needs to be as close to the human presentation as possible. Hence, it must simulate the rupture of a cerebral aneurysm and show both the bleeding magnitude and dispersion of blood observed in patients. The mortality of the model must be comparable to humans so as to allow correct interpretation of its variations. Lastly, it needs to be highly standardized. The first model of SAH was published by Barry et al. in 1979 [10]. In their model, they perforated the basilar artery in rats through a midline craniotomy. To induce artery rupture, the tip of a microelectrode was advanced through the dura mater and arachnoid mater into the basilar artery lumen. Since then more than 60 models in 7 different species have been developed to investigate subarachnoid hemorrhage. Only a few are reliable and consistent [119]. The two most commonly used models of SAH are the circle-of-Willis-perforation model [161] and the cisternal injection model [17, 110]. In the cisternal injection model, autologous blood (and saline as a control) is injected directly into the cistern, without any vessel injury. The easiest injection site is the cisterna magna; however, most SAHs in patients occur in the anterior circulation; therefore, the model was adapted to an injection in the perichiamsatic area [157, 186]. Animals exposed to the injection model are suitable to study delayed vasospasms but not for the investigation of early brain injury and delayed ischemia [125] since the model has some major disadvantages: 1. there is no endothelial injury to simulate the rupture of an aneurysm, 2. the injection needle perforates the brain parenchyma, so the differentiation between cerebral damage caused by the needle and the damage caused by the injected blood is difficult, and 3. the cisternal injection model has a very low bleeding-induced mortality of only 0-15%, which does not fully represent clinical SAH. Further, some injection models use already hemolysed blood, a procedure not fully representing actual SAH [142]. For the current study the middle cerebral artery perforation model was used. As in

this model SAH is initiated by perforation of a blood vessel, it simulates the rupture of a cerebral aneurysm well. The site of perforation corresponds to the location of aneurysmal SAH in humans. The acute changes in physiological parameters like intracranial pressure and cerebral blood flow correspond to those observed in patients. In addition, this model has a mortality of 30% to 50%. Thus, among all available SAH animal models the middle cerebral artery perforation model resembles the clinical situation most adequately. A commonly discussed limitation of the perforation model is that the amount of bleeding and hemorrhage severity cannot be controlled, leading to a relatively large standard deviation of outcome parameters. At the same time, the contribution of the initial global ischemia cannot be differentiated from the effect of blood in the subarachnoid space since controls addressing the effect of ICP are not possible. A minor disadvantage of this model is that it is technically quite challenging. This problem can be overcome by intensive surgical training; however, this process is time consuming and not every researcher may reach the same skill level. Since the aim of this study was to investigate early changes in both microcirculation and physiological parameters after SAH in the most significant SAH model, the circle-of-Willis-perforation model seems to be the best suited one.

4.1.1 Anesthesia

To be certain that the observed changes after experimental SAH solely derive from hemorrhage, it is necessary to ascertain that the used anesthesia confounds the experiment as little as possible. Most importantly, the used anesthesia should not affect systemic blood pressure and cerebral blood flow. Regarding isoflurane, an anesthetic agent commonly used as in animal models of SAH, one must consider that it causes peripheral vasodilation and subsequent hypotension and impairs cerebral autoregulation [74, 198]. Anesthesia with chloral hydrate affects both, the cardiovascular and pulmonary system, leading to decreased blood pressure [46]. Thus, in this study anesthesia was induced with a triple combination of fentanyl, medetomidine and midazolam. This combination has been reported to have a very small impact on autoregulation and systemic blood pressure [185]. Therefore, it seems best suited for the current study.

4.1.2 Intravital microscopy

The murine model is well-suited for intravital microscopy of the cerebral microcirculation because mice - in contrast to rats - have a transparent dura mater. Even when a two-photon-excitation-microscope is used the maximal imaging depth in rat brain is only 70 µm, while in mice 500 µm can easily be achieved [132]. Therefore, a murine SAH model in combination with a cranial window and intact dura mater was chosen for the current study.

4.2 Experimental animals

The most commonly used experimental animals are rodents. There are many reasons for their preference. They are easy to breed and simple to care for. There is also the possibility of creating genetically modified mice. Many findings on subarachnoid hemorrhage and its immediate effects have been done in mice and therefore choosing a mouse model facilitates comparison between new and old data. A disadvantage of a murine model is that, as mice are very small, the surgery becomes more technically challenging and needs assistance like the use of operative microscopes. In contrary to humans, the rodent brain is not gyrencephalic. This has to be considered in interpreting and translating findings from mouse to human. In different hemorrhage models the distribution of blood after SAH varies. In the mouse model, blood distributes mainly along blood vessels while in humans the blood distributes predominantly along the brain sulci. This may not be a major disadvantage, since blood vessels suppling the brain are located within sulci. Hence, the cerebral vascular pathologies after SAH may be to some extent comparable in mice and humans [161]. Pharmacological inhibitors of eNOS are available, e.g. L-N^G-Nitroarginine (L-NNA) or Asymmetric dimethylarginine (ADMA), however, their specificity is under debate [108]. As this study was designed as a proof of concept, a complete inactivity of the eNOS enzyme was targeted in order to obtain no eNOS produced NO. In transgenic mice, a complete lack of the enzyme can be obtained by deletion or disruption of the gene. There are available NOSIII deficient mice, which are easy to obtain and breed, e.g. the B6.129P2-NOS3^{m1Unc}/J mouse line used in the current study. Results cannot be translated directly from knockout animals to humans, but they are a valuable tool to investigate the importance of pathophysiological molecular pathways. One must consider though, that the eNOS enzyme is already absent during the development of the eNOS knockout mice. Therefore, it is only partly reliable as a mimic of acute enzyme defects. In eNOS depleted animals, compensatory mechanisms may be present. Hence, ultimate proof may only be provided by inducible eNOS knockout mice, which are, however, not available yet.

4.3 Importance of eNOS after SAH

The current study reveals a significant difference between eNOS knockout and non-transgenic/wild type control animals. The transgenic mice have more severe subarachnoid bleeding indicating a vital role of eNOS in the pathophysiology of SAH. In the mice with functional eNOS, the increase in ICP is less severe than in those with heterozygous or homozygous eNOS knockout. As high intracranial pressure is associated with large bleeding volumes our results in eNOS knockout mice indicate that loss of endothelial NO leads to more severe hemorrhage. In accordance with this hypothesis eNOS knockout had larger clots at the skull base after SAH. Hence, eNOS may be important for stopping arterial bleeding. This assumption is supported by the prolonged tail bleeding time in eNOS deficient mice observed in the current study. Published data on bleeding times in eNOS knockout mice are not equivocal. In a study by Freedmann et al. in 1999 eNOS knockout mice demonstrated a reduced venous bleeding time [53]. In this study blood clotting

was determined after a single puncture in the dorsal tail vein with a 23-gauge needle. Another study in 2003 reported eNOS knockout animals to have a longer tail bleeding times [121]. Since the venous puncture method is not comparable to the Ivy bleeding time used by Matsushita and by us, our results are well in line with the current literature. The underlying mechanisms for this phenotype is hard to explain since NO dilates vessels and has well-known anti-adhesive effects [124]. Hence, lack of NO should cause vasoconstriction and increased platelet adhesion and is therefore expected to shorten rather than prolong arterial bleeding. The only possible explanation may be that eNOS depletion promotes abnormal vessel remodeling and leads to pathological changes in the morphology of vessel walls, thus resulting in prolonged bleeding [152]. An alternative explanation for longer tail bleeding times and more severe SAH in eNOS deficient mice could be the previously observed hypertension observed in these mice, a finding corroborated in the current study. Hypertension is a main risk for SAH in humans and can cause more severe bleeding. eNOS deficient mice of older age have been shown to be indeed hypertensive [76], however, this was shown in different knockout mouse strains than the one used in the current study [122] [175]. In the current study, the eNOS depleted mice had a slightly increased medial arterial blood pressure. But as there was no statistical difference between groups, this may be an insufficient sole explanation for stronger subarachnoid hemorrhage in these animals.

4.3.1 Microcirculation

As previously indicated, nitric oxide is a strong vasodilator in the cerebral microcirculation in response to shear stress, metabolic demand, and changes of carbon dioxide partial pressure [144]. Lack of NO after SAH is caused both by NO scavenging by hemoglobin [165], as well as by a defect in the endothelial nitric oxide synthase, the main source of vascular NO in the brain [108, 139, 144]. eNOS produced NO inhibits vasoconstriction and promotes vasodilation. This could be confirmed in the present study by showing impaired microcirculatory blood flow by two-photon microscopy. $eNOS^{-/-}$ mice have less parenchymal capillaries and the perfused vessel volume is significantly decreased as compared to wild type animals. This could be seen both in arterioles as well as in capillaries further indicating the importance of eNOS in arterial constriction mediated by the cGMP pathway, and in capillaries mediated by pericyte modification [64] [108]. The observed number of microvasospasms early after SAH indicate an importance of eNOS in the inhibition of such arterial narrowing. The number of spams in naïve eNOS mutant mice corresponded to that of wild type mice after SAH and further increases after SAH. As indicated earlier, eNOS might play an important role in neovascularization [3]. This could explain the observed microcirculatory defect in vessel density and structure as eNOS is already lacking when the microcirculation is formed. As a consequence, it is difficult to differentiate between microcirculatory impairment due to SAH or eNOS knockout. A way around this dilemma is to compare the microcirculation of naïve eNOS transgenic mice with the same mouse line after SAH. The observed impairment (reduced perfused vessel volume, increased number of microvasospasms) increased significantly after SAH. Therefore, we conclude that both mechanisms play a role for the observed phenotype: the microcirculation of eNOS

knockout mice is already impaired before SAH, but worsens thereafter due to lack of NO. Considering the phenotypes described so far in eNOS deficient mice after SAH, it is not surprising that these mice have an increased mortality after hemorrhage. These findings are well in line with the worse outcome of SAH patients with loss-of-function mutations in the eNOS gene. Quantitatively it is important to consider, that while 50% of the homozygous transgenic eNOS mice died within three hours after SAH, mortality in heterozygous knockout mice was only 25%. This indicates, that even a small amount on functional eNOS has protective effects after SAH.

4.4 Conclusion and outlook

Genetic elimination of eNOS leads to worse outcome after SAH. eNOS knockout mice show stronger bleedings with higher intracranial pressure and larger clots at the base of the skull. This could indicate an important role of eNOS in counteracting vessel injury and bleeding. At the same time the autoregulation is more severely impaired in the knockout animals than in the wild type control group. Cerebral blood flow decreases more and compensatory mechanisms are insufficient to counteract this reaction. CBF remains reduced for a longer period of time than in the control group and drops faster after the initial recovery. This confirms the importance of eNOS for the regulation of basal cerebral blood flow and systemic blood pressure. eNOS knockout mice show more re-bleedings and prolonged tail bleeding times further supporting the role of eNOS for hemostasis after vessel injury. Regarding the cerebral microcirculation, eNOS deficiency causes a reduced capillary density and a more severe rarefication of cerebral capillaries after SAH. Hence, we conclude that eNOS and endothelial NO play an important protective role after SAH. Therefore, restoring or enhancing endothelial NO production and/or function acutely after SAH may represent a promising future therapeutic strategy. Inhaled NO, as suggested by our laboratory [184], or directly targeting downstream NO signaling may be viable options.

Appendices

Abbreviations

CBF	Cerebral Blood Flow
CCA	Common Carotid Artery
CO_2	Carbon Dioxide
DCI	Delayed Cerebral Ischemia
EBI	Early Brain Injury
ECA	External Carotid Artery
eNOS	endothelial Nitric Oxide Synthase
GSC	Glasgow Coma Scale
ICA	Internal Carotid Artery
ICP	Intra-Cranial Pressure
MCA	Medial Carotid Artery
MVS	Micro-Vaso-Spams
NO	Nitric Oxide
SAH	Subarachnoid Hemorrhage
WT	Wildtype

List of Figures

List of Tables

Bibliography

[1] Abu-Soud, H. M. and Stuehr, D. J. (1993). Nitric oxide synthases reveal a role for calmodulin in controlling electron transfer. *Proceedings of the National Academy of Sciences*, 90(22):10769–10772.

[2] Afshar, J. K., Pluta, R. M., Boock, R. J., Thompson, B. G., and Oldfield, E. H. (1995). Effect of intracarotid nitric oxide on primate cerebral vasospasm after subarachnoid hemorrhage. *J Neurosurg*, 83(1):118–22.

[3] Aicher, A., Heeschen, C., Mildner-Rihm, C., Urbich, C., Ihling, C., Technau-Ihling, K., Zeiher, A. M., and Dimmeler, S. (2003). Essential role of endothelial nitric oxide synthase for mobilization of stem and progenitor cells. *Nat Med*, 9(11):1370–6.

[4] Alheid, U., Frolich, J. C., and Forstermann, U. (1987). Endothelium-derived relaxing factor from cultured human endothelial cells inhibits aggregation of human platelets. *Thromb Res*, 47(5):561–71.

[5] Ames, A., Wright, R. L., Kowada, M., Thurston, J. M., and Majno, G. (1968). Cerebral ischemia. ii. the no-reflow phenomenon. *Am J Path*, 52(2):437–53.

[6] Anson, J. A., Lawton, M. T., and Spetzler, R. F. (1996). Characteristics and surgical treatment of dolichoectatic and fusiform aneurysms. *J Neurosurg*, 84(2):185–93.

[7] Arbeitsgemeinschaft der Wissenschaftlichen Medizinischen Fachgesellschaften (AWMF)-Ständige Kommission Leitlinien. (2012). AWMF-Regelwerk "Subarachnoidalblutung" 1.Auflage September 2012 (Verlängert August 2015). `https://www.dgn.org/leitlinien/2318-ll-26-2012-subarachnoidalsblutung-sab` [Accessed 23.11.2018].

[8] Arutiunov, A. I., Baron, M. A., and Majorova, N. A. (1974). The role of mechanical factors in the pathogenesis of short-term and prolonged spasm of the cerebral arteries. *J Neurosurg*, 40(4):459–72.

[9] Balbi, M., Koide, M., Schwarzmaier, S. M., Wellman, G. C., and Plesnila, N. (2017). Acute changes in neurovascular reactivity after subarachnoid hemorrhage in vivo. *J Cereb Blood Flow Metab*, 37(1):178–187.

[10] Barry, K. J., Gogjian, M. A., and Stein, B. M. (1979). Small animal model for investigation of subarachnoid hemorrhage and cerebral vasospasm. *Stroke*, 10(5):538–41.

[11] Bederson, J. B., Germano, I. M., and Guarino, L. (1995). Cortical blood flow and cerebral perfusion pressure in a new noncraniotomy model of subarachnoid hemorrhage in the rat. *Stroke*, 26(6):1086–91; discussion 1091–2.

[12] Benninger, F., Raphaeli, G., and Steiner, I. (2015). Subarachnoid hemorrhage mimicking myocardial infarction. *J Clin Neurosci*, 22(12):1981–2.

[13] Britz, G. W., Meno, J. R., Park, I. S., Abel, T. J., Chowdhary, A., Nguyen, T. S., Winn, H. R., and Ngai, A. C. (2007). Time-dependent alterations in functional and pharmacological arteriolar reactivity after subarachnoid hemorrhage. *Stroke*, 38(4):1329–35.

[14] Budohoski, K. P., Guilfoyle, M., Helmy, A., Huuskonen, T., Czosnyka, M., Kirollos, R., Menon, D. K., Pickard, J. D., and Kirkpatrick, P. J. (2014). The pathophysiology and treatment of delayed cerebral ischaemia following subarachnoid haemorrhage. *J Neurol Neurosurg Psychiatry*, 85(12):1343–53.

[15] Buhler, D., Schuller, K., and Plesnila, N. (2014). Protocol for the induction of subarachnoid hemorrhage in mice by perforation of the circle of willis with an endovascular filament. *Transl Stroke Res*, 5(6):653–9.

[16] Burgold, S. (2013). Charakterisierung der in vivo Wachstumskinetik amyloider Plaques und der synaptischen Pathologie mit Evaluierung eines immuntherapeutischen Ansatzes in einem Alzheimer-Mausmodell. (Dissertation), Faculty of Biology, LMU Munich.

[17] Calisaneller, T. e. a. (2009). Blood injection subarachnoid hemorrhage mouse model. *In: Chen J., Xu Z.C., Xu XM., Zhang J.H. (eds) Animal Models of Acute Neurological Injuries. Humana Press*, pages 287–292.

[18] Chen, S., Luo, J., Reis, C., Manaenko, A., and Zhang, J. (2017). Hydrocephalus after subarachnoid hemorrhage: Pathophysiology, diagnosis, and treatment. *Biomed Res Int*,

(2017):8584753.

[19] Chi, O. Z., Wei, H. M., Sinha, A. K., and Weiss, H. R. (1994). Effects of inhibition of nitric oxide synthase on blood-brain barrier transport in focal cerebral ischemia. *Pharmacology*, 48(6):367–73.

[20] Chicoine, M. R. (2003). Microsurgery and clipping: the gold standard for the treatment of intracranial aneurysms. *J Neurosurg Anesthesiol*, 15(1):61–3.

[21] Cho, H. J., Xie, Q. W., Calaycay, J., Mumford, R. A., Swiderek, K. M., Lee, T. D., and Nathan, C. (1992). Calmodulin is a subunit of nitric oxide synthase from macrophages. *J Exp Med*, 176(2):599–604.

[22] Choi, K. S., Won, Y. D., Yi, H. J., Lim, T. H., Lee, Y. J., and Chun, H. J. (2013). Therapeutic and prognostic implications of subarachnoid hemorrhage in patients who suffered cardiopulmonary arrest and underwent cardiopulmonary resuscitation during an emergency room stay. *Clin Neurol Neurosurg*, 115(10):2088–93.

[23] Clower, B. R., Yoshioka, J., Honma, Y., and Smith, R. R. (1988). Pathological changes in cerebral arteries following experimental subarachnoid hemorrhage: role of blood platelets. *Anat Rec*, 220(2):161–70.

[24] Crane, B. R., Arvai, A. S., Ghosh, D. K., Wu, C., Getzoff, E. D., Stuehr, D. J., and Tainer, J. A. (1998). Structure of nitric oxide synthase oxygenase dimer with pterin and substrate. *Science*, 279(5359):2121–6.

[25] Crowley, R. W., Medel, R., Dumont, A. S., Ilodigwe, D., Kassell, N. F., Mayer, S. A., Ruefenacht, D., Schmiedek, P., Weidauer, S., Pasqualin, A., and Macdonald, R. L. (2011). Angiographic vasospasm is strongly correlated with cerebral infarction after subarachnoid hemorrhage. *Stroke*, 42(4):919–23.

[26] de Rooij, N. K., Linn, F. H., van der Plas, J. A., Algra, A., and Rinkel, G. J. (2007). Incidence of subarachnoid haemorrhage: a systematic review with emphasis on region, age, gender and time trends. *J Neurol Neurosurg Psychiatry*, 78(12):1365–72.

[27] Debdi, M., Seylaz, J., and Sercombe, R. (1992). Early changes in rabbit cerebral artery reactivity after subarachnoid hemorrhage. *Stroke*, 23(8):1154–62.

[28] Degen, L. A., Dorhout Mees, S. M., Algra, A., and Rinkel, G. J. (2011). Interobserver variability of grading scales for aneurysmal subarachnoid hemorrhage. *Stroke*, 42(6):1546–9.

[29] Denk, W., Strickler, J. H., and Webb, W. W. (1990). Two-photon laser scanning fluorescence microscopy. *Science*, 248(4951):73–6.

[30] Dernbach, P. D., Little, J. R., Jones, S. C., and Ebrahim, Z. Y. (1988). Altered cerebral autoregulation and co2 reactivity after aneurysmal subarachnoid hemorrhage. *Neurosurgery*, 22(5):822–6.

[31] Deutsch, B. C., Neifert, S. N., and Caridi, J. M. (2018). No disparity in outcomes between surgical clipping and endovascular coiling after aneurysmal subarachnoid hemorrhage. *World Neurosurg*, 120:e318–e325.

[32] Dimmeler, S. and Zeiher, A. M. (1999). Nitric oxide-an endothelial cell survival factor. *Cell Death Differ*, 6(10):964–8.

[33] Diringer, M. (2009). Management of aneurysmal subarachnoid hemorrhage. *Crit Care Med*, 37(2):432–40.

[34] Dirnagl, U., Iadecola, C., and Moskowitz, M. A. (1999). Pathobiology of ischaemic stroke: an integrated view. *Trends Neurosci*, 22(9):391–7.

[35] Dodel, R., Winter, Y., Ringel, F., Spottke, A., Gharevi, N., Muller, I., Klockgether, T., Schramm, J., Urbach, H., and Meyer, B. (2010). Cost of illness in subarachnoid hemorrhage: a german longitudinal study. *Stroke*, 41(12):2918–23.

[36] Dority, J. S. and Oldham, J. S. (2016). Subarachnoid hemorrhage: An update. *Anesthesiol Clin*, 34(3):577–600.

[37] Duchemin, S., Boily, M., Sadekova, N., and Girouard, H. (2012). The complex contribution of nos interneurons in the physiology of cerebrovascular regulation. *Front Neural Circuits*, 6:51.

[38] Durmaz, R., Ozkara, E., Kanbak, G., Arslan, O. C., Dokumacioglu, A., Kartkaya, K., and Atasoy, M. A. (2008). Nitric oxide level and adenosine deaminase activity in cerebrospinal fluid of patients with subarachnoid hemorrhage. *Turk Neurosurg*, 18(2):157–64.

[39] Ecker, A. and Riemenschneider, P. A. (1951). Arteriographic demonstration of spasm of the intracranial arteries, with special reference to saccular arterial aneurysms. *J Neurosurg*, 8(6):660–7.

[40] Edlow, J. A. and Caplan, L. R. (2000). Avoiding pitfalls in the diagnosis of subarachnoid hemorrhage. *N Engl J Med*, 342(1):29–36.

[41] Edwards, D. H., Byrne, J. V., and Griffith, T. M. (1992). The effect of chronic subarachnoid hemorrhage on basal endothelium-derived relaxing factor activity in intrathecal cerebral arteries. *J Neurosurg*, 76(5):830–7.

[42] Eisenberg, H. M., Gary, H. E., J., Aldrich, E. F., Saydjari, C., Turner, B., Foulkes, M. A., Jane, J. A., Marmarou, A., Marshall, L. F., and Young, H. F. (1990). Initial ct findings in 753 patients with severe head injury. a report from the nih traumatic coma data bank. *J Neurosurg*, 73(5):688–98.

[43] Feigin, V. L., Rinkel, G. J., Lawes, C. M., Algra, A., Bennett, D. A., van Gijn, J., and Anderson, C. S. (2005). Risk factors for subarachnoid hemorrhage: an updated systematic review of epidemiological studies. *Stroke*, 36(12):2773–80.

[44] Feiler, S., Friedrich, B., Scholler, K., Thal, S. C., and Plesnila, N. (2010). Standardized induction of subarachnoid hemorrhage in mice by intracranial pressure monitoring. *J Neurosci Methods*, 190(2):164–70.

[45] FELASA working group on revision of guidelines for health monitoring of and rabbits and rodents. Mahler Convenor, M. and Berard, M. and Feinstein, R. and Gallagher, A. and Illgen-Wilcke, B. and Pritchett-Corning, K. and Raspa, M. (2014). FELASA recommendations for the health monitoring of mouse, rat, hamster, guinea pig and rabbit colonies in breeding and experimental units. *Lab Anim*, 48(3):178–192.

[46] Field, K. J., White, W. J., and Lang, C. M. (1993). Anaesthetic effects of chloral hydrate, pentobarbitone and urethane in adult male rats. *Lab Anim*, 27(3):258–69.

[47] Filipce, V. and Caparoski, A. (2015). The effects of vasospasm and re-bleeding on the outcome of patients with subarachnoid hemorrhage from ruptured intracranial aneurysm. *Pril (Makedon Akad Nauk Umet Odd Med Nauki)*, 36(3):77–82.

[48] Finger, J., Smith, C., Hayamizu, T., McCright, I., Xu, J., Law, M., Shaw, D., Baldarelli, R., Beal, J., Blodgett, O., Campbell, J., Corbani, L., Lewis, J., Forthofer, K., Frost, P.J.and Giannatto, S., Hutchins, L., Miers, D., Motenko, H., Stone, K., Eppig, J.T.and Kadin, J., Richardson, J., and Ringwald, M. (2017). The mouse Gene Expression Database (GXD): 2017 update. Nucleic Acids Res. 2017 Jan. 4;45 (D1): D730-D736. `https://www.mousephenotype.org/data/genes/MGI:97362s` accessed on 13.11.2018.

[49] Finsterer, J. and Wahbi, K. (2014). Cns-disease affecting the heart: brain-heart disorders. *J Neurol Sci*, 345(1-2):8–14.

[50] Fisher, C. M., Kistler, J. P., and Davis, J. M. (1980). Relation of cerebral vasospasm to subarachnoid hemorrhage visualized by computerized tomographic scanning. *Neurosurgery*, 6(1):1–9.

[51] Fisher, C. M., Roberson, G. H., and Ojemann, R. G. (1977). Cerebral vasospasm with ruptured saccular aneurysm–the clinical manifestations. *Neurosurgery*, 1(3):245–8.

[52] Forstermann, U. and Sessa, W. C. (2012). Nitric oxide synthases: regulation and function. *Eur Heart J*, 33(7):829–37, 837a–837d.

[53] Freedman, J., Sauter, R., Battinelli, E. M., Ault, K., Knowles, C., Huang, P. L., and Loscalzo, J. (1999). Deficient platelet-derived nitric oxide and enhanced hemostasis in mice lacking the nosiii gene. *Circulation research*, 84 12:1416–21.

[54] Friedrich, B., Michalik, R., Oniszczuk, A., Abubaker, K., Kozniewska, E., and Plesnila, N. (2014). Co2 has no therapeutic effect on early microvasospasm after experimental subarachnoid hemorrhage. *J. Cereb. Blood Flow Metab.*, 34(8):e1–6.

[55] Friedrich, B., Muller, F., Feiler, S., Scholler, K., and Plesnila, N. (2012). Experimental subarachnoid hemorrhage causes early and long-lasting microarterial constriction and microthrombosis: an in-vivo microscopy study. *J Cereb Blood Flow Metab*, 32(3):447–55.

[56] Friedrich, V., Flores, R., Muller, A., and Sehba, F. A. (2010). Escape of intraluminal platelets into brain parenchyma after subarachnoid hemorrhage. *Neuroscience*, 165(3):968–75.

[57] Frontera, J. A., Fernandez, A., Schmidt, J. M., Claassen, J., Wartenberg, K. E., Badjatia, N., Connolly, E. S., and Mayer, S. A. (2009). Defining vasospasm after subarachnoid hemorrhage:

what is the most clinically relevant definition? *Stroke*, 40(6):1963–8.

[58] Fuller, G. and Manford, M. (2010). Subarachnoid haemorrhage. In Fuller, G. and Manford, M., editors, *Neurology (Third Edition)*, pages 72 – 73. Churchill Livingstone.

[59] Garry, P. S., Ezra, M., Rowland, M. J., Westbrook, J., and Pattinson, K. T. (2015). The role of the nitric oxide pathway in brain injury and its treatment–from bench to bedside. *Exp Neurol*, 263:235–43.

[60] Gasparotti, R. and Liserre, R. (2005). Intracranial aneurysms. *Eur Radiol*, 15(3):441–7.

[61] Ghiran, I. C. (2011). Introduction to fluorescence microscopy. *Methods Mol Biol*, 689:93–136.

[62] Göppert-Mayer, M. (1931). über elementarakte mit zwei quantensprüngen. *Annalen der Physik*, 401:273–294.

[63] Graff-Radford, N. R., Torner, J., Adams, H. P., J., and Kassell, N. F. (1989). Factors associated with hydrocephalus after subarachnoid hemorrhage. a report of the cooperative aneurysm study. *Arch Neurol*, 46(7):744–52.

[64] Griffiths, M. J. and Evans, T. W. (2005). Inhaled nitric oxide therapy in adults. *N Engl J Med*, 353(25):2683–95.

[65] Guglielmi, G., Vinuela, F., Dion, J., and Duckwiler, G. (1991a). Electrothrombosis of saccular aneurysms via endovascular approach. part 2: Preliminary clinical experience. *J Neurosurg*, 75(1):8–14.

[66] Guglielmi, G., Vinuela, F., Sepetka, I., and Macellari, V. (1991b). Electrothrombosis of saccular aneurysms via endovascular approach. part 1: Electrochemical basis, technique, and experimental results. *J Neurosurg*, 75(1):1–7.

[67] Haberny, K. A., Pou, S., and Eccles, C. U. (1992). Potentiation of quinolinate-induced hippocampal lesions by inhibition of no synthesis. *Neurosci Lett*, 146(2):187–90.

[68] Harders, A. G. and Gilsbach, J. M. (1987). Time course of blood velocity changes related to vasospasm in the circle of willis measured by transcranial doppler ultrasound. *J Neurosurg*, 66(5):718–28.

[69] Helms, C. and Kim-Shapiro, D. B. (2013). Hemoglobin-mediated nitric oxide signaling. *Free Radic Biol Med*, 61:464–72.

[70] Hemmens, B. and Mayer, B. (1998). Enzymology of nitric oxide synthases. *Methods Mol Biol*, 100:1–32.

[71] Herz, D. A., Baez, S., and Shulman, K. (1975). Pial microcirculation in subarachnoid hemorrhage. *Stroke*, 6(4):417–24.

[72] Heuer, G. G., Smith, M. J., Elliott, J. P., Winn, H. R., and LeRoux, P. D. (2004). Relationship between intracranial pressure and other clinical variables in patients with aneurysmal subarachnoid hemorrhage. *J Neurosurg*, 101(3):408–16.

[73] Hirashima, Y., Hamada, H., Kurimoto, M., Origasa, H., and Endo, S. (2005). Decrease in platelet count as an independent risk factor for symptomatic vasospasm following aneurysmal subarachnoid hemorrhage. *J Neurosurg*, 102(5):882–7.

[74] Hockel, K., Trabold, R., Scholler, K., Torok, E., and Plesnila, N. (2012). Impact of anesthesia on pathophysiology and mortality following subarachnoid hemorrhage in rats. *Exp Transl Stroke Med*, 4(1):5.

[75] Huang, P. L. (1999). Neuronal and endothelial nitric oxide synthase gene knockout mice. *Braz J Med Biol Res*, 32(11):1353–9.

[76] Huang, P. L., Huang, Z., Mashimo, H., Bloch, K. D., Moskowitz, M. A., Bevan, J. A., and Fishman, M. C. (1995). Hypertension in mice lacking the gene for endothelial nitric oxide synthase. *Nature*, 377(6546):239–42.

[77] Huang, Z., Huang, P. L., Ma, J., Meng, W., Ayata, C., Fishman, M. C., and Moskowitz, M. A. (1996). Enlarged infarcts in endothelial nitric oxide synthase knockout mice are attenuated by nitro-l-arginine. *J Cereb Blood Flow Metab*, 16(5):981–7.

[78] Hughes, J. D., Bond, K. M., Mekary, R. A., Dewan, M. C., Rattani, A., Baticulon, R., Kato, Y., Azevedo-Filho, H., Morcos, J. J., and Park, K. B. (2018). Estimating the global incidence of aneurysmal subarachnoid hemorrhage: A systematic review for central nervous system vascular lesions and meta-analysis of ruptured aneurysms. *World Neurosurg*, 115:430–447 e7.

[79] Hunt, W. E. and Hess, R. M. (1968). Surgical risk as related to time of intervention in the repair of intracranial aneurysms. *J Neurosurg*, 28(1):14–20.

[80] Jackson Laboratory (2018). Mous strain datasheet 002684. `https://www.jax.org/strain/002684` accessed on 13.11.2018.

[81] Jacques, S. L. (2013). Optical properties of biological tissues: a review. *Phys Med Biol*, 58(11):R37–61.

[82] Jain, S. and Iverson, L. M. (2018). *Glasgow Coma Scale*. Treasure Island (FL).

[83] Jakubowski, J., Bell, B. A., Symon, L., Zawirski, M. B., and Francis, D. M. (1982). A primate model of subarachnoid hemorrhage: change in regional cerebral blood flow, autoregulation carbon dioxide reactivity, and central conduction time. *Stroke*, 13(5):601–11.

[84] Johnston, S. C., Selvin, S., and Gress, D. R. (1998). The burden, trends, and demographics of mortality from subarachnoid hemorrhage. *Neurology*, 50(5):1413–8.

[85] Juvela, S. (2000). Risk factors for multiple intracranial aneurysms. *Stroke*, 31(2):392–7.

[86] Juvela, S., Hillbom, M., Numminen, H., and Koskinen, P. (1993). Cigarette smoking and alcohol consumption as risk factors for aneurysmal subarachnoid hemorrhage. *Stroke*, 24(5):639–46.

[87] Juvela, S., Siironen, J., and Kuhmonen, J. (2005). Hyperglycemia, excess weight, and history of hypertension as risk factors for poor outcome and cerebral infarction after aneurysmal subarachnoid hemorrhage. *J Neurosurg*, 102(6):998–1003.

[88] Kamiya, K., Kuyama, H., and Symon, L. (1983). An experimental study of the acute stage of subarachnoid hemorrhage. *J Neurosurg*, 59(6):917–24.

[89] Kapp, J., Mahaley, M. S., J., and Odom, G. L. (1968). Cerebral arterial spasm. 2. experimental evaluation of mechanical and humoral factors in pathogenesis. *J Neurosurg*, 29(4):339–49.

[90] Kassell, N. F. and Torner, J. C. (1983). Aneurysmal rebleeding: a preliminary report from the cooperative aneurysm study. *Neurosurgery*, 13(5):479–81.

[91] Keedy, A. (2006). An overview of intracranial aneurysms. *Mcgill J Med*, 9(2):141–6.

[92] Khaldi, A., Zauner, A., Reinert, M., Woodward, J. J., and Bullock, M. R. (2001). Measurement of nitric oxide and brain tissue oxygen tension in patients after severe subarachnoid hemorrhage. *Neurosurgery*, 49(1):33–8; discussion 38–40.

[93] Khurana, V. G., Sohni, Y. R., Mangrum, W. I., McClelland, R. L., O'Kane, D. J., Meyer, F. B., and Meissner, I. (2004). Endothelial nitric oxide synthase gene polymorphisms predict susceptibility to aneurysmal subarachnoid hemorrhage and cerebral vasospasm. *J Cereb Blood Flow Metab*, 24(3):291–7.

[94] Kilkenny, C., Browne, W. J., Cuthill, I. C., Emerson, M., and Altman, D. G. (2012). Improving bioscience research reporting: the arrive guidelines for reporting animal research. *Osteoarthritis Cartilage*, 20(4):256–60.

[95] Kim, S. T., Baek, J. W., Lee, W. H., Lee, K. S., Kwon, W. H., Pyo, S., Jeong, H. W., and Jeong, Y. G. (2018). Causes of early rebleeding after coil embolization of ruptured cerebral aneurysms. *Clin Neurol Neurosurg*, 174:108–116.

[96] Kissela, B. M., Sauerbeck, L., Woo, D., Khoury, J., Carrozzella, J., Pancioli, A., Jauch, E., Moomaw, C. J., Shukla, R., Gebel, J., Fontaine, R., and Broderick, J. (2002). Subarachnoid hemorrhage: a preventable disease with a heritable component. *Stroke*, 33(5):1321–6.

[97] Klatt, P., Pfeiffer, S., List, B. M., Lehner, D., Glatter, O., Bächinger, H. P., Werner, E. R., Schmidt, K., and Mayer, B. (1996). Characterization of heme-deficient neuronal nitric-oxide synthase reveals a role for heme in subunit dimerization and binding of the amino acid substrate and tetrahydrobiopterin. *Journal of Biological Chemistry*, 271(13):7336–7342.

[98] Ko, N. U., Rajendran, P., Kim, H., Rutkowski, M., Pawlikowska, L., Kwok, P. Y., Higashida, R. T., Lawton, M. T., Smith, W. S., Zaroff, J. G., and Young, W. L. (2008). Endothelial nitric oxide synthase polymorphism (-786t-¿c) and increased risk of angiographic vasospasm after

aneurysmal subarachnoid hemorrhage. *Stroke*, 39(4):1103–8.

[99] Konczalla, J., Schmitz, J., Kashefiolasl, S., Senft, C., Seifert, V., and Platz, J. (2015). Non-aneurysmal subarachnoid hemorrhage in 173 patients: a prospective study of long-term outcome. *Eur J Neurol*, 22(10):1329–36.

[100] Kotsonis, P., Fröhlich, L. G., Shutenko, Z. V., Horejsi, R., Pfleiderer, W., and Schmidt, H. H. H. W. (2000). Allosteric regulation of neuronal nitric oxide synthase by tetrahydrobiopterin and suppression of auto-damaging superoxide. *Biochemical Journal*, 346(3):767–776.

[101] Kowalski, R. G., Claassen, J., Kreiter, K. T., Bates, J. E., Ostapkovich, N. D., Connolly, E. S., and Mayer, S. A. (2004). Initial misdiagnosis and outcome after subarachnoid hemorrhage. *JAMA*, 291(7):866–9.

[102] Lantigua, H., Ortega-Gutierrez, S., Schmidt, J. M., Lee, K., Badjatia, N., Agarwal, S., Claassen, J., Connolly, E. S., and Mayer, S. A. (2015). Subarachnoid hemorrhage: who dies, and why? *Crit Care*, 19:309.

[103] Lanzino, G., Kassell, N. F., Germanson, T., Truskowski, L., and Alves, W. (1993). Plasma glucose levels and outcome after aneurysmal subarachnoid hemorrhage. *J Neurosurg*, 79(6):885–91.

[104] Larsen, C. C. and Astrup, J. (2013). Rebleeding after aneurysmal subarachnoid hemorrhage: a literature review. *World Neurosurg*, 79(2):307–12.

[105] Lewandowski, P. (2014). Subarachnoid haemorrhage imitating acute coronary syndrome as a cause of out-of-hospital cardiac arrest - case report. *Anaesthesiol Intensive Ther*, 46(4):289–92.

[106] Li, H. and Forstermann, U. (2000). Nitric oxide in the pathogenesis of vascular disease. *J Pathol*, 190(3):244–54.

[107] Li, H., Wu, W., Liu, M., Zhang, X., Zhang, Q. R., Ni, L., and Hang, C. H. (2014). Increased cerebrospinal fluid concentrations of asymmetric dimethylarginine correlate with adverse clinical outcome in subarachnoid hemorrhage patients. *J Clin Neurosci*, 21(8):1404–8.

[108] Li, Q., Chen, Y., Li, B., Luo, C., Zuo, S., Liu, X., Zhang, J. H., Ruan, H., and Feng, H. (2016). Hemoglobin induced no/cgmp suppression deteriorate microcirculation via pericyte phenotype transformation after subarachnoid hemorrhage in rats. *Sci Rep*, 6:22070.

[109] Li, S., Wang, Y., Jiang, Z., Huai, Y., Liao, J. K., Lynch, K. A., Zafonte, R., Wood, L. J., and Wang, Q. M. (2018). Impaired cognitive performance in endothelial nitric oxide synthase knockout mice after ischemic stroke: A pilot study. *Am J Phys Med Rehabil*, 97(7):492–499.

[110] Lin, C. L., Calisaneller, T., Ukita, N., Dumont, A. S., Kassell, N. F., and Lee, K. S. (2003). A murine model of subarachnoid hemorrhage-induced cerebral vasospasm. *J Neurosci Methods*, 123(1):89–97.

[111] Lindgren, A., Vergouwen, M. D., van der Schaaf, I., Algra, A., Wermer, M., Clarke, M. J., and Rinkel, G. J. (2018). Endovascular coiling versus neurosurgical clipping for people with aneurysmal subarachnoid haemorrhage. *Cochrane Database Syst Rev*, 8:CD003085.

[112] Linn, F. H., Rinkel, G. J., Algra, A., and van Gijn, J. (1998). Headache characteristics in subarachnoid haemorrhage and benign thunderclap headache. *J Neurol Neurosurg Psychiatry*, 65(5):791–3.

[113] List, B. M., Klösch, B., Völker, C., Gorren, A. C. F., Sessa, W. C., Werner, E. R., Kukovetz, W. R., Schmidt, K., and Mayer, B. (1997). Characterization of bovine endothelial nitric oxide synthase as a homodimer with down-regulated uncoupled nadph oxidase activity: tetrahydrobiopterin binding kinetics and role of haem in dimerization. *Biochemical Journal*, 323(1):159–165.

[114] Liu, H., Dienel, A., Scholler, K., Schwarzmaier, S. M., Nehrkorn, K., Plesnila, N., and Terpolilli, N. A. (2018). Microvasospasms after experimental subarachnoid hemorrhage do not depend on endothelin a receptors. *Stroke*, 49(3):693–699.

[115] Loan, J. J. M., Wiggins, A. N., and Brennan, P. M. (2018). Medically induced hypertension, hypervolaemia and haemodilution for the treatment and prophylaxis of vasospasm following aneurysmal subarachnoid haemorrhage: systematic review. *Br J Neurosurg*, 32(2):157–164.

[116] Lovelock, C. E., Rinkel, G. J., and Rothwell, P. M. (2010). Time trends in outcome of subarachnoid hemorrhage: Population-based study and systematic review. *Neurology*, 74(19):1494–501.

[117] Macdonald, R. L., Higashida, R. T., Keller, E., Mayer, S. A., Molyneux, A., Raabe, A., Vajkoczy, P., Wanke, I., Bach, D., Frey, A., Nowbakht, P., Roux, S., and Kassell, N. (2012). Randomized trial of clazosentan in patients with aneurysmal subarachnoid hemorrhage undergoing endovascular coiling. *Stroke*, 43(6):1463–9.

[118] MacMicking, J., Xie, Q., and Nathan, C. (1997). Nitric oxide and macrophage function. *Annual Review of Immunology*, 15(1):323–350.

[119] Marbacher, S., Fandino, J., and Kitchen, N. D. (2010). Standard intracranial in vivo animal models of delayed cerebral vasospasm. *Br J Neurosurg*, 24(4):415–34.

[120] Marsden, P. A., Schappert, K. T., Chen, H. S., Flowers, M., Sundell, C. L., Wilcox, J. N., Lamas, S., and Michel, T. (1992). Molecular cloning and characterization of human endothelial nitric oxide synthase. *FEBS Lett*, 307(3):287–93.

[121] Matsushita, K.and Morrell, C. N., Cambien, B., Yang, S. X., Yamakuchi, M., Bao, C., Hara, M. R., Quick, R. A., Cao, W., O'Rourke, B., Lowenstein, J. M., Pevsner, J., Wagner, D. D., and Lowenstein, C. J. (2003). Nitric oxide regulates exocytosis by s-nitrosylation of n-ethylmaleimide-sensitive factor. *Cell*, 115(2):139–50.

[122] Miyamoto, Y., Saito, Y., Kajiyama, N., Yoshimura, M., Shimasaki, Y., Nakayama, M., Kamitani, S., Harada, M., Ishikawa, M., Kuwahara, K., Ogawa, E., Hamanaka, I., Takahashi, N., Kaneshige, T., Teraoka, H., Akamizu, T., Azuma, N., Yoshimasa, Y., Yoshimasa, T., Itoh, H., Masuda, I., Yasue, H., and Nakao, K. (1998). Endothelial nitric oxide synthase gene is positively associated with essential hypertension. *Hypertension*, 32(1):3–8.

[123] Molyneux, A., Kerr, R., Stratton, I., Sandercock, P., Clarke, M., Shrimpton, J., Holman, R., and International Subarachnoid Aneurysm Trial Collaborative, G. (2002). International subarachnoid aneurysm trial (isat) of neurosurgical clipping versus endovascular coiling in 2143 patients with ruptured intracranial aneurysms: a randomised trial. *Lancet*, 360(9342):1267–74.

[124] Moore, C., Tymvios, C., and Emerson, M. (2010). Functional regulation of vascular and platelet activity during thrombosis by nitric oxide and endothelial nitric oxide synthase. *Thromb Haemost*, 104(2):342–9.

[125] Mori, K. (2014). Double cisterna magna blood injection model of experimental subarachnoid hemorrhage in dogs. *Transl Stroke Res*, 5(6):647–52.

[126] Mostany, R., Miquelajauregui, A., Shtrahman, M., and Portera-Cailliau, C. (2015). Two-photon excitation microscopy and its applications in neuroscience. *Methods Mol Biol*, 1251:25–42.

[127] Muller, D. and Muller, O. (2018). [neurointensive care: Aneurysmal subarachnoid hemorrhage - state of the art]. *Anasthesiol Intensivmed Notfallmed Schmerzther*, 53(10):654–667.

[128] Nadaud, S., Bonnardeaux, A., Lathrop, M., and Soubrier, F. (1994). Gene structure, polymorphism and mapping of the human endothelial nitric oxide synthase gene. *Biochem Biophys Res Commun*, 198(3):1027–33.

[129] National center for biology information (2018). NCBI Gene, NOS3 nitric oxide synthase 3 [Homo sapiens (human)]. *https://www.ncbi.nlm.nih.gov/gene/4846*, accessed on 10.11.2018.

[130] Nicholson, S., Bonecini-Almeida, M. d. G., Lapa e Silva, J. R., Nathan, C., Xie, Q. W., Mumford, R., Weidner, J. R., Calaycay, J., Geng, J., Boechat, N., Linhares, C., Rom, W., and Ho, J. L. (1996). Inducible nitric oxide synthase in pulmonary alveolar macrophages from patients with tuberculosis. *Journal of Experimental Medicine*, 183(5):2293–2302.

[131] Nieuwkamp, D. J., de Gans, K., Algra, A., Albrecht, K. W., Boomstra, S., Brouwers, P. J., Groen, R. J., Metzemaekers, J. D., Nijssen, P. C., Roos, Y. B., Tulleken, C. A., Vandertop, W. P., van Gijn, J., Vos, P. E., and Rinkel, G. J. (2005). Timing of aneurysm surgery in subarachnoid haemorrhage–an observational study in the netherlands. *Acta Neurochir (Wien)*, 147(8):815–21.

[132] Niklass, S., Stoyanov, S., Garz, C., Bueche, C. Z., Mencl, S., Reymann, K., Heinze, H. J., Carare, R. O., Kleinschnitz, C., and Schreiber, S. (2014). Intravital imaging in spontaneously hypertensive stroke-prone rats-a pilot study. *Exp Transl Stroke Med*, 6(1):1.

[133] Nornes, H. (1978). Cerebral arterial flow dynamics during aneurysm haemorrhage. *Acta Neurochir (Wien)*, 41(1-3):39–48.

[134] Nornes, H. and Magnaes, B. (1972). Intracranial pressure in patients with ruptured saccular aneurysm. *J Neurosurg*, 36(5):537–47.

[135] Ohkuma, H., Tsurutani, H., and Suzuki, S. (2001). Incidence and significance of early aneurysmal rebleeding before neurosurgical or neurological management. *Stroke*, 32(5):1176–

80.

[136] Oshiro, E. M., Walter, K. A., Piantadosi, S., Witham, T. F., and Tamargo, R. J. (1997). A new subarachnoid hemorrhage grading system based on the glasgow coma scale: a comparison with the hunt and hess and world federation of neurological surgeons scales in a clinical series. *Neurosurgery*, 41(1):140–7.

[137] Panahian, N., Yoshida, T., Huang, P. L., Hedley-Whyte, E. T., Dalkara, T., Fishman, M. C., and Moskowitz, M. A. (1996). Attenuated hippocampal damage after global cerebral ischemia in mice mutant in neuronal nitric oxide synthase. *Neuroscience*, 72(2):343–54.

[138] Papanikolaou, J., Makris, D., Karakitsos, D., Saranteas, T., Karabinis, A., Kostopanagiotou, G., and Zakynthinos, E. (2012). Cardiac and central vascular functional alterations in the acute phase of aneurysmal subarachnoid hemorrhage. *Crit Care Med*, 40(1):223–32.

[139] Park, K. W., Metais, C., Dai, H. B., Comunale, M. E., and Sellke, F. W. (2001). Microvascular endothelial dysfunction and its mechanism in a rat model of subarachnoid hemorrhage. *Anesth Analg*, 92(4):990–6.

[140] Park, Y. K., Yi, H. J., Choi, K. S., Lee, Y. J., Chun, H. J., and Kwon, S. M. (2018). Predictive factors of fever after aneurysmal subarachnoid hemorrhage and its impact on delayed cerebral ischemia and clinical outcomes. *World Neurosurg*, 114:e524–e531.

[141] Pennings, F. A., Bouma, G. J., and Ince, C. (2004). Direct observation of the human cerebral microcirculation during aneurysm surgery reveals increased arteriolar contractility. *Stroke*, 35(6):1284–8.

[142] Peterson, J. W., Roussos, L., Kwun, B. D., Hackett, J. D., Owen, C. J., and Zervas, N. T. (1990). Evidence of the role of hemolysis in experimental cerebral vasospasm. *J Neurosurg*, 72(5):775–81.

[143] Philippu, A. (2016). Nitric oxide: A universal modulator of brain function. *Curr Med Chem*, 23(24):2643–2652.

[144] Pluta, R. M. and Oldfield, E. H. (2007). Analysis of nitric oxide (no) in cerebral vasospasm after aneursymal bleeding. *Rev Recent Clin Trials*, 2(1):59–67.

[145] Pluta, R. M., Oldfield, E. H., and Boock, R. J. (1997). Reversal and prevention of cerebral vasospasm by intracarotid infusions of nitric oxide donors in a primate model of subarachnoid hemorrhage. *J Neurosurg*, 87(5):746–51.

[146] Polmear, A. (2003). Sentinel headaches in aneurysmal subarachnoid haemorrhage: what is the true incidence? a systematic review. *Cephalalgia*, 23(10):935–41.

[147] Prast, H. and Philippu, A. (2001). Nitric oxide as modulator of neuronal function. *Prog Neurobiol*, 64(1):51–68.

[148] Rafiee, P., Ogawa, H., Heidemann, J., Li, M. S., Aslam, M., Lamirand, T. H., Fisher, P. J., Graewin, S. J., Dwinell, M. B., Johnson, C. P., Shaker, R., and Binion, D. G. (2003). Isolation and characterization of human esophageal microvascular endothelial cells: mechanisms of inflammatory activation. *American Journal of Physiology-Gastrointestinal and Liver Physiology*, 285(6):G1277–G1292.

[149] Ravishankar, K. (2016). Looking at "thunderclap headache" differently? circa 2016. *Ann Indian Acad Neurol*, 19(3):295–301.

[150] Rivero-Arias, O., Gray, A., and Wolstenholme, J. (2010). Burden of disease and costs of aneurysmal subarachnoid haemorrhage (asah) in the united kingdom. *Cost Eff Resour Alloc*, 8:6.

[151] Rowland, M. J., Hadjipavlou, G., Kelly, M., Westbrook, J., and Pattinson, K. T. (2012). Delayed cerebral ischaemia after subarachnoid haemorrhage: looking beyond vasospasm. *Br J Anaesth*, 109(3):315–29.

[152] Rudic, R. D., Shesely, E. G., Maeda, N., Smithies, O., Segal, S. S., and Sessa, W. C. (1998). Direct evidence for the importance of endothelium-derived nitric oxide in vascular remodeling. *J Clin Invest*, 101(4):731–6.

[153] Rueden, C. T., Schindelin, J., Hiner, M. C., DeZonia, B. E., Walter, A. E., Arena, E. T., and Eliceiri, K. W. (2017). Imagej2: Imagej for the next generation of scientific image data. *BMC Bioinformatics*, 18(1):529.

[154] Rusak, T., Misztal, T., Piszcz, J., and Tomasiak, M. (2014). Nitric oxide scavenging by cell-free hemoglobin may be a primary factor determining hypertension in polycythemic patients.

Free Radic Res, 48(2):230–8.

[155] Sabri, M., Ai, J., Lakovic, K., D'Abbondanza, J., Ilodigwe, D., and Macdonald, R. L. (2012). Mechanisms of microthrombi formation after experimental subarachnoid hemorrhage. *Neuroscience*, 224:26–37.

[156] Sabri, M., Ai, J., Lass, E., D'Abbondanza, J., and Macdonald, R. L. (2013). Genetic elimination of enos reduces secondary complications of experimental subarachnoid hemorrhage. *J Cereb Blood Flow Metab*, 33(7):1008–14.

[157] Sabri, M., Jeon, H., Ai, J., Tariq, A., Shang, X., Chen, G., and Macdonald, R. L. (2009). Anterior circulation mouse model of subarachnoid hemorrhage. *Brain Res*, 1295:179–85.

[158] Sarker, S. J., Heuschmann, P. U., Burger, I., Wolfe, C. D., Rudd, A. G., Smeeton, N. C., and Toschke, A. M. (2008). Predictors of survival after haemorrhagic stroke in a multi-ethnic population: the south london stroke register (slsr). *J Neurol Neurosurg Psychiatry*, 79(3):260–5.

[159] Schievink, W. I., Torres, V. E., Piepgras, D. G., and Wiebers, D. O. (1992). Saccular intracranial aneurysms in autosomal dominant polycystic kidney disease. *J Am Soc Nephrol*, 3(1):88–95.

[160] Schindelin, J., Arganda-Carreras, I., Frise, E., Kaynig, V., Longair, M., Pietzsch, T., Preibisch, S., Rueden, C., Saalfeld, S., Schmid, B., Tinevez, J. Y., White, D. J., Hartenstein, V., Eliceiri, K., Tomancak, P., and Cardona, A. (2012). Fiji: an open-source platform for biological-image analysis. *Nat Methods*, 9(7):676–82.

[161] Schuller, K., Buhler, D., and Plesnila, N. (2013). A murine model of subarachnoid hemorrhage. *J Vis Exp*, (81):e50845.

[162] Schwartz, C., Aster, H. C., Al-Schameri, R., Muller-Thies-Broussalis, E., Griessenauer, C. J., and Killer-Oberpfalzer, M. (2018). Microsurgical clipping and endovascular treatment of middle cerebral artery aneurysms in an interdisciplinary treatment concept: Comparison of long-term results. *Interv Neuroradiol*, 24(6):608–614.

[163] Sebok, M., Keller, E., van Niftrik, C. H. B., Regli, L., and Germans, M. R. (2018). Management of aneurysmal subarachnoid hemorrhage patients with antiplatelet use before the initial hemorrhage: An international survey. *World Neurosurg*, 120:e408–e413.

[164] Sehba, F. A. and Bederson, J. B. (2011). Nitric oxide in early brain injury after subarachnoid hemorrhage. *Acta Neurochir Suppl*, 110(Pt 1):99–103.

[165] Sehba, F. A., Chereshnev, I., Maayani, S., Friedrich, V., J., and Bederson, J. B. (2004). Nitric oxide synthase in acute alteration of nitric oxide levels after subarachnoid hemorrhage. *Neurosurgery*, 55(3):671–7; discussion 677–8.

[166] Sehba, F. A., Ding, W. H., Chereshnev, I., and Bederson, J. B. (1999). Effects of s-nitrosoglutathione on acute vasoconstriction and glutamate release after subarachnoid hemorrhage. *Stroke*, 30(9):1955–61.

[167] Sehba, F. A., Hou, J., Pluta, R. M., and Zhang, J. H. (2012). The importance of early brain injury after subarachnoid hemorrhage. *Prog Neurobiol*, 97(1):14–37.

[168] Sehba, F. A., Mostafa, G., Friedrich, V., J., and Bederson, J. B. (2005). Acute microvascular platelet aggregation after subarachnoid hemorrhage. *J Neurosurg*, 102(6):1094–100.

[169] Sehba, F. A., Schwartz, A. Y., Chereshnev, I., and Bederson, J. B. (2000). Acute decrease in cerebral nitric oxide levels after subarachnoid hemorrhage. *J Cereb Blood Flow Metab*, 20(3):604–11.

[170] Seibert, B., Tummala, R. P., Chow, R., Faridar, A., Mousavi, S. A., and Divani, A. A. (2011). Intracranial aneurysms: review of current treatment options and outcomes. *Front Neurol*, 2:45.

[171] Sheikhazadi, A. and Gharehdaghi, J. (2009). Survey of sudden death from aneurysmal subarachnoid hemorrhage in cadavers referred to legal medicine organization of tehran, 2001-2005. *Am J Forensic Med Pathol*, 30(4):358–61.

[172] Shesely, E. G., Maeda, N., Kim, H. S., Desai, K. M., Krege, J. H., Laubach, V. E., Sherman, P. A., Sessa, W. C., and Smithies, O. (1996). Elevated blood pressures in mice lacking endothelial nitric oxide synthase. *Proc Natl Acad Sci U S A*, 93(23):13176–81.

[173] Starke, R. M., Connolly, E. S., J., and Participants in the International Multi-Disciplinary Consensus Conference on the Critical Care Management of Subarachnoid, H. (2011). Rebleeding after aneurysmal subarachnoid hemorrhage. *Neurocrit Care*, 15(2):241–6.

[174] Starke, R. M., Kim, G. H., Komotar, R. J., Hickman, Z. L., Black, E. M., Rosales, M. B., Kellner, C. P., Hahn, D. K., Otten, M. L., Edwards, J., Wang, T., Russo, J. J., Mayer, S. A., and Connolly, E. S., J. (2008). Endothelial nitric oxide synthase gene single-nucleotide polymorphism predicts cerebral vasospasm after aneurysmal subarachnoid hemorrhage. *J Cereb Blood Flow Metab*, 28(6):1204–11.

[175] Stauss, H. M., Godecke, A., Mrowka, R., Schrader, J., and Persson, P. B. (1999). Enhanced blood pressure variability in enos knockout mice. *Hypertension*, 33(6):1359–63.

[176] Stenger, S., Thüring, H., Röllinghoff, M., and Bogdan, C. (1994). Tissue expression of inducible nitric oxide synthase is closely associated with resistance to leishmania major. *Journal of Experimental Medicine*, 180(3):783–793.

[177] Stroke Goal Group, Dr Foster Global Comparators Project Dr Foster Ltd in association with the Dr Foster Unit at Imperial College London (2018). Outcome after clipping and coiling for aneurysmal subarachnoid hemorrhage in clinical practice in europe, usa, and australia. *Neurosurgery*.

[178] Stuehr, D., Pou, S., and Rosen, G. M. (2001). Oxygen reduction by nitric-oxide synthases. *J Biol Chem*, 276(18):14533–6.

[179] Sun, B. L., Zheng, C. B., Yang, M. F., Yuan, H., Zhang, S. M., and Wang, L. X. (2009). Dynamic alterations of cerebral pial microcirculation during experimental subarachnoid hemorrhage. *Cell Mol Neurobiol*, 29(2):235–41.

[180] Suzuki, Y., Kajita, Y., Oyama, H., Tanazawa, T., Takayasu, M., Shibuya, M., and Sugita, K. (1994). Dysfunction of nitric oxide in the spastic basilar arteries after subarachnoid hemorrhage. *J Auton Nerv Syst*, 49 Suppl:S83–7.

[181] Team, T. G. (1997 -). Gnu image manipulation program 2.10.6.

[182] Teasdale, G. and Jennett, B. (1974). Assessment of coma and impaired consciousness. a practical scale. *Lancet*, 2(7872):81–4.

[183] Terpolilli, N. A., Brem, C., Buhler, D., and Plesnila, N. (2015). Are we barking up the wrong vessels? cerebral microcirculation after subarachnoid hemorrhage. *Stroke*, 46(10):3014–9.

[184] Terpolilli, N. A., Feiler, S., Dienel, A., Muller, F., Heumos, N., Friedrich, B., Stover, J., Thal, S., Scholler, K., and Plesnila, N. (2016). Nitric oxide inhalation reduces brain damage, prevents mortality, and improves neurological outcome after subarachnoid hemorrhage by resolving early pial microvasospasms. *J Cereb Blood Flow Metab*, 36(12):2096–2107.

[185] Thal, S. C. and Plesnila, N. (2007). Non-invasive intraoperative monitoring of blood pressure and arterial pco2 during surgical anesthesia in mice. *J Neurosci Methods*, 159(2):261–7.

[186] Titova, E., Ostrowski, R. P., Zhang, J. H., and Tang, J. (2009). Experimental models of subarachnoid hemorrhage for studies of cerebral vasospasm. *Neurol Res*, 31(6):568–81.

[187] Togashi, H., Sakuma, I., Yoshioka, M., Kobayashi, T., Yasuda, H., Kitabatake, A., Saito, H., Gross, S. S., and Levi, R. (1992). A central nervous system action of nitric oxide in blood pressure regulation. *J Pharmacol Exp Ther*, 262(1):343–7.

[188] Tsutsumi, K., Ueki, K., Morita, A., and Kirino, T. (2000). Risk of rupture from incidental cerebral aneurysms. *J Neurosurg*, 93(4):550–3.

[189] Uhl, E., Lehmberg, J., Steiger, H. J., and Messmer, K. (2003). Intraoperative detection of early microvasospasm in patients with subarachnoid hemorrhage by using orthogonal polarization spectral imaging. *Neurosurgery*, 52(6):1307–15; disacussion 1315–7.

[190] Vajkoczy, P., Meyer, B., Weidauer, S., Raabe, A., Thome, C., Ringel, F., Breu, V., and Schmiedek, P. (2005). Clazosentan (axv-034343), a selective endothelin a receptor antagonist, in the prevention of cerebral vasospasm following severe aneurysmal subarachnoid hemorrhage: results of a randomized, double-blind, placebo-controlled, multicenter phase iia study. *J Neurosurg*, 103(1):9–17.

[191] van der Wee, N., Rinkel, G. J., Hasan, D., and van Gijn, J. (1995). Detection of subarachnoid haemorrhage on early ct: is lumbar puncture still needed after a negative scan? *J Neurol Neurosurg Psychiatry*, 58(3):357–9.

[192] van Gijn, J. and Rinkel, G. J. (2001). Subarachnoid haemorrhage: diagnosis, causes and management. *Brain*, 124(Pt 2):249–78.

[193] Vergouwen, M. D., Vermeulen, M., Coert, B. A., Stroes, E. S., and Roos, Y. B. (2008). Microthrombosis after aneurysmal subarachnoid hemorrhage: an additional explanation for

delayed cerebral ischemia. *J Cereb Blood Flow Metab*, 28(11):1761–70.

[194] Vergouwen, M. D., Vermeulen, M., van Gijn, J., Rinkel, G. J., Wijdicks, E. F., Muizelaar, J. P., Mendelow, A. D., Juvela, S., Yonas, H., Terbrugge, K. G., Macdonald, R. L., Diringer, M. N., Broderick, J. P., Dreier, J. P., and Roos, Y. B. (2010). Definition of delayed cerebral ischemia after aneurysmal subarachnoid hemorrhage as an outcome event in clinical trials and observational studies: proposal of a multidisciplinary research group. *Stroke*, 41(10):2391–5.

[195] Vermeulen, M. and van Gijn, J. (1990). The diagnosis of subarachnoid haemorrhage. *J Neurol Neurosurg Psychiatry*, 53(5):365–72.

[196] Vermeulen, M. J. and Schull, M. J. (2007). Missed diagnosis of subarachnoid hemorrhage in the emergency department. *Stroke*, 38(4):1216–21.

[197] Wang, Q., Theard, M. A., Pelligrino, D. A., Baughman, V. L., Hoffman, W. E., Albrecht, R. F., Cwik, M., Paulson, O. B., and Lassen, N. A. (1994). Nitric oxide (no) is an endogenous anticonvulsant but not a mediator of the increase in cerebral blood flow accompanying bicuculline-induced seizures in rats. *Brain Res*, 658(1-2):192–8.

[198] Wang, Z., Schuler, B., Vogel, O., Arras, M., and Vogel, J. (2010). What is the optimal anesthetic protocol for measurements of cerebral autoregulation in spontaneously breathing mice? *Exp Brain Res*, 207(3-4):249–58.

[199] Wartenberg, K. E., Schmidt, J. M., Claassen, J., Temes, R. E., Frontera, J. A., Ostapkovich, N., Parra, A., Connolly, E. S., and Mayer, S. A. (2006). Impact of medical complications on outcome after subarachnoid hemorrhage. *Crit Care Med*, 34(3):617–23.

[200] Wei, X.-q., Charles, I. G., Smith, A., Ure, J., Feng, G.-j., Huang, F.-p., Xu, D., Mullers, W., Moncada, S., and Liew, F. Y. (1995). Altered immune responses in mice lacking inducible nitric oxide synthase. *Nature*, 375:408–411.

[201] Weir, B., Grace, M., Hansen, J., and Rothberg, C. (1978). Time course of vasospasm in man. *J Neurosurg*, 48(2):173–8.

[202] Wijdicks, E. F., Vermeulen, M., Murray, G. D., Hijdra, A., and van Gijn, J. (1990). The effects of treating hypertension following aneurysmal subarachnoid hemorrhage. *Clin Neurol Neurosurg*, 92(2):111–7.

[203] Withers, K., Carolan-Rees, G., and Dale, M. (2013). Pipeline embolization device for the treatment of complex intracranial aneurysms: a nice medical technology guidance. *Appl Health Econ Health Policy*, 11(1):5–13. https://doi.org/10.1007/s40258-012-0005-x.

[204] Wong, J. M. and Billiar, T. R. (1995). Regulation and function of inducible nitric oxide synthase during sepsis and acute inflammation. In Ignarro, L. and Murad, F., editors, *Nitric Oxide*, volume 34 of *Advances in Pharmacology*, pages 155 – 170. Academic Press.

[205] World Federation of Neurological Surgeons Committee (1988). Report of world federation of neurological surgeons committee on a universal subarachnoid hemorrhage grading scale. *J Neurosurg*, 68(6):985–6.

[206] Zhou, L. and Zhu, D. Y. (2009). Neuronal nitric oxide synthase: structure, subcellular localization, regulation, and clinical implications. *Nitric Oxide*, 20(4):223–30.

[207] Zoerle, T., Lombardo, A., Colombo, A., Longhi, L., Zanier, E. R., Rampini, P., and Stocchetti, N. (2015). Intracranial pressure after subarachnoid hemorrhage. *Crit Care Med*, 43(1):168–76.

Acknowledgements

Acknowledgements

First, I would like to thank Prof. Plesnila for entrusting me with this topic and for giving me honest and constructive feedback on my working progress so I could always thrive.
Dr. Terpolilli, I would like to thank for tremendous support twenty-four-seven, for teaching me many aspects of the surgeries necessary for this work and for short notice help in all matters surgery or writing.
Further I would like to acknowledge Nicole Heumos, who trained me in the subarachnoid hemorrhage model and Janina Biller for doing genotyping. Big thanks go to my entire research group for interesting discussions about my topic, for giving me new angels to look at my work when I got stuck. For overall support and appreciation.
Great thanks go to my family Sonja, Anja and Inés who helped me a lot with proofreading, and to my mother for supporting me and making this work possible. My family always assisted me in whatever necessary way and I am very lucky to have you all in my life.
But most of all I would like to thank my amazing fiancé Andi for his love and support. For helping in programming magical codes that could save many hours of manual work. For making sure I ate and took a break when I got lost in my data. For always being there for me.

Eidesstattliche Versicherung

Ich, Irina Johanna Lenz, geb. Westermayer, erkläre hiermit an Eides statt, dass ich die vorliegende Dissertation mit dem Thema:

"Importance of Endothelial Nitric Oxide Synthase after Experimental Subarachnoid Hemorrhage in Mice"

selbständig verfasst, mich außer der angegebenen keiner weiteren Hilfsmittel bedient und alle Erkenntnisse, die aus dem Schrifttum ganz oder annähernd übernommen sind, als solche kenntlich gemacht und nach ihrer Herkunft unter Bezeichnung der Fundstelle einzeln nachgewiesen habe.

Ich erkläre des Weiteren, dass die hier vorgelegte Dissertation nicht in gleicher oder in ähnlicher Form bei einer anderen Stelle zur Erlangung eines akademischen Grades eingereicht wurde.

München, 20.02.2020

Irina Johanna Lenz, geb. Westermayer